SLAC-9
UC-28, Particle Accelerators
and High-Voltage Machines
UC-34, Physics
TID-4500

TRANSVERSE RADIATION SHIELDING FOR THE STANFORD TWO-MILE ACCELERATOR

November 1962

by

H. DeStaebler, Jr.
Stanford Linear Accelerator Center

Technical Report
Prepared Under
Contract AT(04-3)-400
for the USAEC
San Francisco Operations Office

Printed in USA. Price $2.25. Available from the Office of Technical Services, Department of Commerce, Washington 25, D.C.

TABLE OF CONTENTS

LIST OF FIGURES

I. INTRODUCTION

A. General Remarks

We are interested in shielding a two-mile-long electron linear accelerator which is similar in many ways to the S-band machines that have been built at Stanford over the past 15 years. The machine is designed for an eventual beam current of 60 μa at 40 Bev, which is 2.4 Mw of beam power. Our goal is to design radiation shielding which is adequate but not excessively expensive.

The accelerator site is in rolling hills, at present relatively unpopulated, on Stanford land west of the campus. The boundary of the project is at least 500 feet from any point which is likely to be struck by the beam, and the resulting decrease in radiation level with distance has the consequence that consideration of the radiation workers just outside the shield, and of the general population potentially at the boundary, yield essentially the same requirements on shielding thickness, because the tolerance levels and expected occupancy are different for these two groups of people.

The accelerator complex is divided into three separate parts which have different radiation problems deriving in part from their different functions. The machine itself is a disk-loaded waveguide about 4 inches in diameter and two miles long which will be located in a housing under 25 ft of earth. (A principal purpose of this report is to review the information that led to the selection of the 25-foot shield.) At the end of the machine, after acceleration is over, there will be a beam-switchyard area where the main electron beam will be deflected by magnets, collimated and energy-analyzed, and directed against targets to make secondary beams or delivered to targets in the various experimental areas. The switchyard area will be covered by 40 feet of earth. (The radiation problems here are similar to those along the machine, and we shall discuss them briefly.) Finally, beyond the switchyard area will be the target areas, where most of the physics experimental equipment will be located and where the experiments will be done. The shielding problems there are much more complicated, and we do not consider them at all in this report. In particular, the μ mesons will be important and may actually dominate target-area shielding in the forward direction, whereas along the machine they are negligible.

From the shielding point of view the machine is a long source of radiation buried in a tunnel with people working above, and the principal question is how thick to make the walls. The switchyard area is similar, except that the probable source strength is greater.

In this report we consider only the design of the main shield for protection against high-energy, penetrating radiation. For example, we do not consider any problems arising from induced radioactivity, or from ducts and passageways through the main shield.

There have been two previous reports on shielding the two-mile accelerator. In the original Proposal, in 1957, all aspects of the shielding were considered by Panofsky who arrived at a shield thickness of 35 feet of earth along the machine.[1] In 1961 the design of shielding along the accelerator (the so-called transverse shielding) was reviewed, and the same thickness (35 ft) was arrived at, although some of the reasons were different.[2] This report is the third, and deals mainly with the transverse shielding. A brief comparison of the conclusions of these three reports appears in Appendix A.

B. Outline of the Calculation

The physical calculation of the shielding thickness involves a number of distinct steps, listed below, each of which affects the radiation level multiplicatively. (We do not consider accelerator operational procedures in detail, although these also affect radiation levels.)

(a) Determination of radiation tolerances.

(b) Estimation of the amount of the average electron beam power that is intercepted by the accelerator.

(c) Development of the electromagnetic cascade.

(d) Production of penetrating particles by the electromagnetic cascade.

(e) Attenuation in the shield.

---

[1] "Proposal for a Two-Mile Linear Electron Accelerator," Stanford University, Stanford, California, April, 1957.

[2] H. DeStaebler, "A Review of Transverse Shielding Requirements for the Stanford Two-Mile Accelerator," M-262, Stanford Linear Accelerator Center, Stanford, California, April, 1961.

NOTE: All references are given on the page where they are cited, and in addition are listed at the end of the report.

(f) Estimation of the biological hazard of the particles coming out of the shield.

(g) Estimation of the biological hazard far from the machine.

(h) Estimation of the errors involved.

In order to choose the shield thickness the result of this calculation is combined with economic and operation considerations, with special attention given to the consequences of making the shield too thin. In this report we concentrate on the physical calculation which is described in the next five chapters.

The essential content of the calculation can be summarized as follows. When an electron of energy E_o is absorbed (e.g., an errant beam electron hits the accelerating structure) the differential photon track length (i.e., the total path length throughout the shower traversed by photons of this energy) is (Approximation A)

$$\frac{d\ell}{dk} = \frac{1}{2}\frac{E_o}{k^2} X_o$$

where k is the photon energy, and X_o is a radiation length.

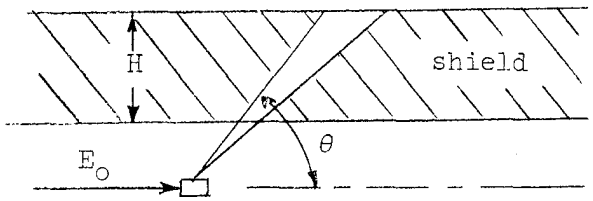

For the transverse shielding the shield is parallel to the beam direction. Since the effective thickness increases at small angles we are primarily interested in the penetrating particles produced at large angles. The photons produce most of these particles, and the neutrons turn out to be the most penetrating component (although at high energies all nucleons and pions are about the same). The nuclear reactions are weak enough so that the soft shower is not perturbed. For example, the giant-resonance reactions

produce about 1/5 neutron per Bev of absorbed electron energy. If each neutron represents 20 Mev, only about 20/5000 = 0.4% of the energy goes into this reaction. If we assume that the photopion cross section is constant at 100 μb/nucleon above 200 Mev, the fraction of the energy absorbed in this way is only

$$f = \frac{1}{E_o} \int_{k_1}^{E_o} \frac{dN}{dk} dk \, \frac{N_o}{A} A\sigma(k) \, k$$

where N_o is Avogadro's number, and A is the atomic weight. Thus

$$f = \frac{N_o \sigma X_o}{2} \ln \frac{E_o}{k_1} \approx \frac{6 \times 10^{23} \times 100 \times 10^{-30} \times 13}{2} \ln \left(\frac{40 \text{ Bev}}{200 \text{ Mev}} \right)$$

or

$$f \approx 0.2\%$$

The angular distributions of the nucleon and pion secondaries leaving the machine are calculated from approximate kinematics. The nuclear cascade in the shield is approximated by a one-dimensional model. The attenuation length for low-energy neutrons is short, and although they are abundant, they are easily absorbed. The absorption length gets longer until the neutron energy reaches about 300 Mev; it increases only slightly above this. High-energy neutrons are rare because there are few high-energy photons. Low-energy neutrons are rapidly absorbed. The neutrons that dominate the shielding calculations have energies around 200-500 Mev, and the relevant cross sections are fairly well known.

The spectrum of particles outside the shield is inferred from shielding measurements, and the biological effect is not calculated from basic principles but is rather estimated empirically.

The yield of secondaries is clearly proportional to the number of beam particles hitting the target. Through Approximation A this yield is proportional to the absorbed electron energy. Therefore it is

proportional to the absorbed beam power. In Section II we make an estimate of the distribution of beam-power absorption in the machine, and conclude that it should be approximately uniform under average operating conditions. This assumption gives rise to a shield of uniform thickness which simplifies construction of the accelerator as well as the shield.

II. RADIATION POLICIES AND HAZARDS

A. Policies

The radiation policies of this project* are similar to those recommended by the U. S. Government but are somewhat more conservative. These policies are described in detail in Appendix B, which is a report written by W.K.H. Panofsky. The following paragraphs are for the most part a summary of the material in Appendix B.

Past experience has shown that the maximum exposures which were considered reasonable have continually decreased with time. In fact, over the past 50 years the recommended maximum exposure for radiation workers has decreased almost exponentially, with a time-constant of about 10 years.[5] So our conservatism, which amounts to about a factor of 3 in tolerance levels, might be thought of as a safety factor, but we prefer to consider it a guess at the official radiation policy in 1966 when the machine is scheduled to turn on.

"Radiation workers" are defined as all persons who work on the site, and the "general population" is everyone else--those with no official connection with the project. The AEC recommends a maximum annual exposure to whole-body penetrating radiation of 5 rem for radiation workers, and of 0.5 rem for the general population. (The unit rem is similar to a roengten and is described more fully in the next section.) The SLAC maximum exposures are 1.5 rem for radiation workers, and 0.1 rem for the general population.

A report by the Federal Radiation Council discusses sources of background radiation, and concludes that the average genetically significant background from natural sources (cosmic rays and natural radioactivity) is about 80 to 170 mrem/year, while from man-made sources (mostly medical X-rays) it is about 80 to 280 mrem/year.[6] The average total background exposure, roughly 200 mrem/year, is referred to as the "doubling dose" because an additional exposure of the same magnitude would roughly double the average radiation exposure. The maximum SLAC exposure for the general population has been set at about half of the doubling dose, which appears to be a suitably conservative choice.

---

*Now called "SLAC" for "Stanford Linear Accelerator Center," and previously known as "Project M."

[5]See a summary in Radiation Hygiene Handbook, Ed. H. Blatz (McGraw-Hill, New York, 1959).

[6]"Background Material for the Development of Radiation Protection Standards," Staff Report No. 1 of the Federal Radiation Council, May 13, 1960, Government Printing Office, Washington 25, D.C.

The FRC report takes the viewpoint that there is no exposure level below which the expected statistical genetic effects are zero, and that therefore every exposure must be justified in terms of the benefits derived in the course of receiving the exposure. There is no "tolerance exposure" with the connotation that exposures below it are completely without ill effect while exposures above it are not permissible. The FRC develops the concept of "guide level" which means, for example, that in the case of radiation workers the benefits derived solely from the fact of their employment are presumed to justify radiation exposures below the guide level. Any exposure above the guide level may be justifiable in terms of increased benefit. (In this report, from habit and from common usage, we still use the term "tolerance" to refer to the levels listed in the table.) However, the FRC report states, "... all exposures should be kept as far below any arbitrarily selected levels as possible," and we tend to consider the SLAC guide levels as nearly absolute upper limits which may be exceeded only under the most exceptional circumstances.

In what follows we evaluate the calculated radiation level at the critical locations, namely, at the surface of the shield for radiation workers, and at the project boundary for the general population. The radiation guides are given in terms of annual exposure, and we convert these to radiation rates (levels) by assuming continuous occupancy for the general population and 40 hr/week for 50 weeks for radiation workers. The ratio of the guide annual exposures is 15, and taking account of occupancy factors the ratio of the average guide levels is 65, which means that the radiation level at the boundary should be at least 65 times lower than the level at the surface of the shield if radiation worker tolerance exists there. For radiation workers the average guide level is 30 mrem/40 hr week = 0.75 mrem/hr, which corresponds to about 5 particles/cm^2-sec (see Fig. 1).

B. Hazards from Penetrating Particles

The rad is a unit of radiation exposure which corresponds to the absorption from a radiation field of 100 ergs of energy in one gram of matter. The unit of radiation exposure for people is called the rem ("roengten equivalent man") and is related to the rad through the relative biological effectiveness (RBE) of the radiation:

$$\text{exposure in rem} = \text{exposure in rad} \times \text{RBE}$$

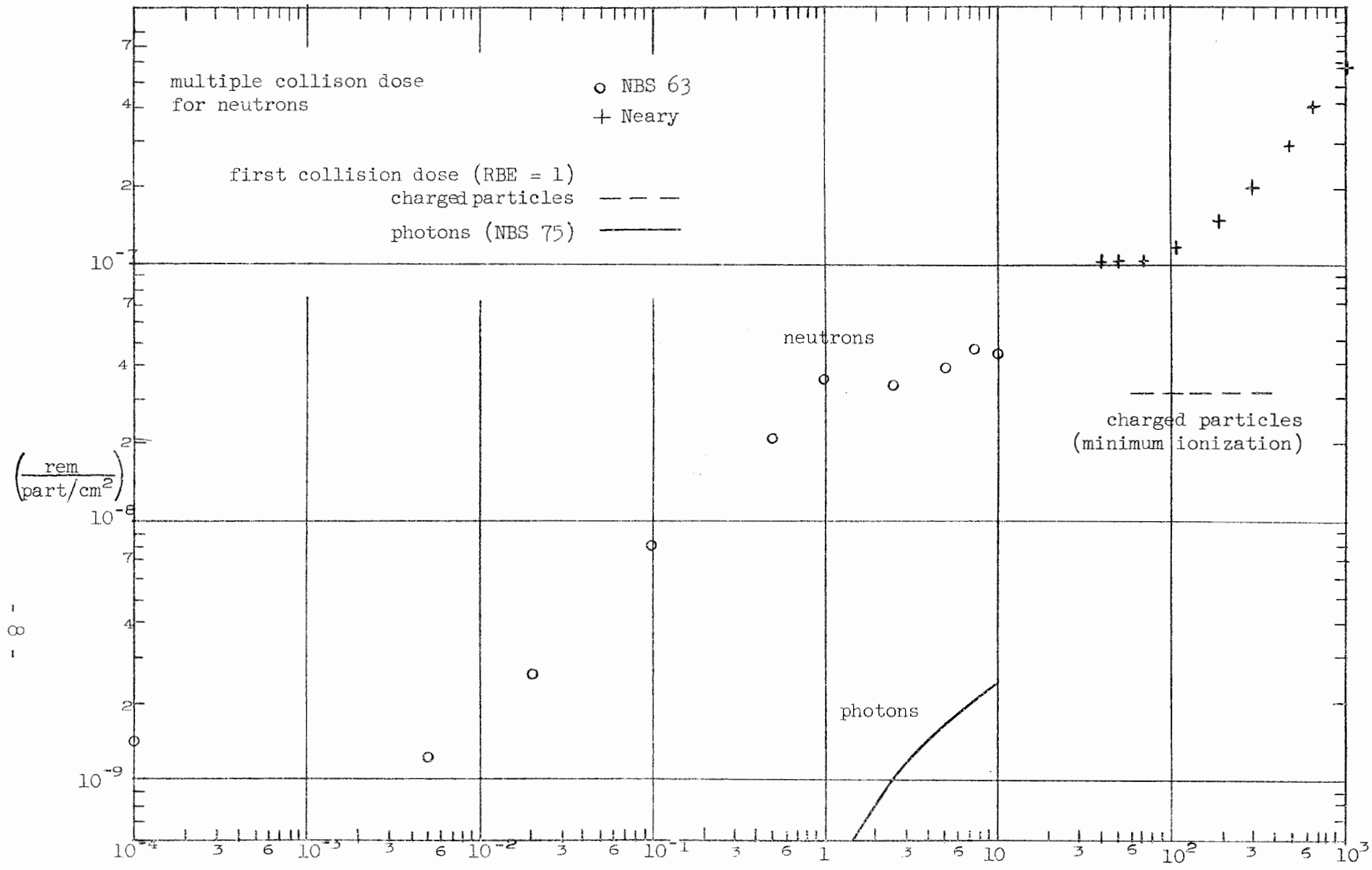

FIG. 1--Exposure from various particles vs energy.

The RBE is a more or less empirically determined quantity and is measured relative to 200-kv X-rays. Generally speaking, the greater the ionization density (equivalently, the greater the linear energy transfer), the greater is the biological effect arising from a given energy loss; hence, the greater the RBE. Basically the RBE indicates the efficiency of a particular radiation field for causing a particular observable biological effect relative to 200-kv X-rays. The RBE depends on the kind of radiation field as well as on the particular effect being observed. The RBE usually varies from 1 to 10, although values as low as 0.85 have been measured for fast electrons, and values as high as 20 have been suggested for heavy ions or recoil fragments. For orientation we list below the values of RBE for neutrons as a function of neutron energy.[3]

Neutron Energy	RBE
Thermal	3
0.1 kev	2
5 kev	2.5
0.1 Mev	8
10 Mev	6.5

In Fig. 1 we show the number of rem resulting from a neutron beam of 1 neutron/cm^2. At 10 Mev and below the points are from Figs. 2B through 12B of the NBS Handbook 63. When low-energy neutrons are incident on a human body there is appreciable absorption of the beam, and thus the dose changes as a function of depth. The points in our Fig. 1 represent the maximum dose at any depth, which usually occurs about 1 cm into the body. The constant dose for neutrons below about 10 kev arises from the effects of the capture gamma rays. In Fig. 1, the points at 40 Mev and above are from preliminary calculations of G. J. Neary.[4] The biological effects of high-energy nuclear particles are complicated and thus difficult to calculate, and we appreciate the fact that Neary has taken it upon himself

---

[3]National Bureau of Standards Handbook 63, "Protection Against Neutron Radiation Up to 30 Mev," November, 1957, Superintendent of Documents, Washington 25, D.C.

[4]G. J. Neary in unpublished reports of the Medical Research Council, Radiobiological Research Unit, AERE, Harwell. It is my understanding that these calculations will be included in a volume of Committee IV of the International Commission on Radiological Protection (probable title, "Protection Against X-Rays above Three Million Volts and Heavy Particles Including Neutrons and Protons") to be published by Pergamon Press probably in 1963.

to write down his thoughts on the subject. The points in Fig. 1 are for neutrons of the stated energies in equilibrium with their secondaries (multiple-collision dose); this is the appropriate situation for a person standing just outside of a thick shield. Neary's high-energy points are uncertain by something like a factor of 2.

For reference, we show in Fig. 1 the first-collision dose for photons and for charged particles, each with an assumed RBE of 1. The photon curve is calculated for standard tissue.[7] For the charged particles we assume an energy loss of 2 Mev/g-cm^{-2}. We then obtain

$$2\left(\frac{\text{Mev}}{\text{g-cm}^{-2}}\right) 1\left(\frac{\text{particle}}{\text{cm}^2}\right) = 3.2 \times 10^{-6} \frac{\text{erg}}{\text{g}} = 3.2 \times 10^{-8} \text{ rad}$$

which is independent of specific gravity.

The composition of the radiation field outside of a thick shield is complicated, and in Section V we discuss the problem of estimating the radiation level from the calculated flux.

---

[7] "Measurement of Absorbed Dose of Neutrons and of Mixtures of Neutrons and Gamma Rays," National Bureau of Standards Handbook 75, February, 1961, Superintendent of Documents, Washington 25, D. C.

III. BEAM LOSS IN THE ACCELERATOR

A. Introduction

All of the SLAC shielding problems arise when high-energy electrons (or other particles) strike matter. If all of the beam electrons were cleanly accelerated without interception to the end of the machine, then there would be no radiation problem along the machine. However, all machines lose some beam during acceleration, and we assume that at times a large fraction of the beam will strike the machine as a result of mis-steering or malfunctioning. We also assume that on the average, even with the accelerator properly adjusted, some small part of the beam will be lost because of such effects as slight imperfections in the injection or steering-magnet optics.

Since the shielding requirements depend directly on the amount of beam loss, it is necessary to make some estimate of this loss. One way to proceed would be to make the shielding thick enough so that if all of the beam were absorbed by the machine continuously at any given point, the shield would be still thick enough to give tolerable radiation levels outside. This is the most conservative approach; however, it is uneconomical, and it is also unnecessary because the accelerator can and will be turned off very rapidly if significant, localized beam interception occurs. Our procedure, then, is to estimate the average operating conditions, and then to design a shield for the accompanying radiation levels. In the next section we describe the way in which the average beam loss has been estimated by making use of measurements from the Mark III accelerator at Stanford.

When the beam strikes something, it is clear that the resulting radiation level is proportional to the number of striking electrons--proportional to the current. It is also proportional to the energy of the electrons because of the physics involved. To see this we note that the primary electrons initiate cascade showers, and as the generations multiply the average energies of the particles decrease as their numbers increase. By simple shower theory (conservation of energy), the number of particles created in an electromagnetic cascade is proportional to the energy of the initiating particle. As long as the energies of the particles producing the radiation field are much smaller than the energies of the

initiating particle, the radiation levels are proportional to the energies of the initiating particles as well as to their number. Thus the radiation level is proportional to the absorbed beam power.

The SLAC accelerator consists of a copper pipe about 4 inches in diameter that contains annular disks which are spaced 1.5 inches apart, are 0.25 inch thick, and have 0.8-inch-diameter holes in the center. (These loading disks are used to reduce the phase velocity of the rf accelerating wave to approximately the velocity of light.) If we assume that the energetic part of the shower is absorbed in 5 radiation lengths, and that the shower develops in the disks, then an electron is absorbed in a distance of about 1.5 ft. Since this distance is small compared to the other distances involved in the shielding, we usually assume that an electron is absorbed in zero distance. If the electron beam is 0.25 inch in diameter, and if it makes an angle of 10^{-3} radian with the axis (a very serious misalignment), then the whole beam will be absorbed over about (1000/4) inches = 22 ft.

B. Calculation of Average Beam Loss Based on Measurements at Mark III

The Mark III accelerator is 310 ft long ($\approx$ 1 Bev maximum energy) and has an internal structure that is very similar to that of the two-mile machine.[8] The injector will also be similar, but we assume that the injection optics of the large machine will be somewhat better than Mark III's, and we include this assumed improvement in the calculation.

The method used here for estimating the average beam loss for the SLAC accelerator is the very simple one of measuring the beam loss on Mark III and extrapolating with a simple model.

1. Analytic

After the electrons have been accelerated for a few wavelengths (λ = 10.5 cm) they are relativistic, and there are no radial forces from the rf fields so the transverse momentum is constant. In Mark III there are some external quadrupole lenses which are sometimes used for focusing, and on the Monster there will probably also be external focusing magnets. However, in the following we neglect these and assume that there are no radial forces.

---

[8]See, for example, Chodorow, Ginzton, Hansen, Kyhl, Neal, Panofsky, et al., Rev. Sci. Instr. 26, 134 (1955).

We first consider an electron which starts from the axis of the accelerator with a radial momentum p_r and an initial momentum p_o (with $p_r \ll p_o$ or, alternatively, a very small injection angle) and which is accelerated in the z direction.

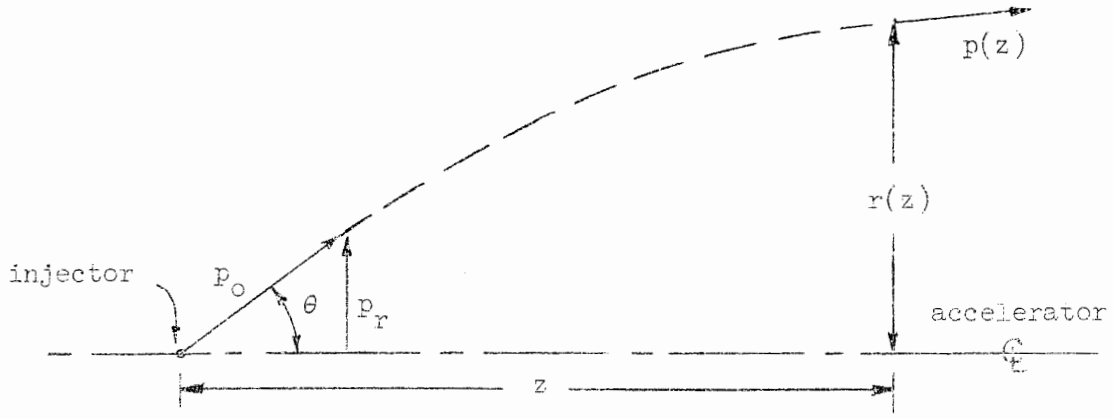

We make the consistent relativistic assumption that the momentum (not the energy) increases linearly with distance,

$$p(z) = p_o + \epsilon z$$

where ϵ is typically 3 Mev/c per foot. The equation of the orbit is

$$\frac{dr}{dz} = \frac{p_r}{p(z)}, \qquad p_r \ll p(z)$$

which integrates immediately to

$$r(z) = r(0) + \frac{p_r}{\epsilon} \ell n \frac{p(z)}{p_o}$$

where in the sketch we assumed $r(0) = 0$. On Mark III the electrons are injected at $T = 80$ kev, for which p_o is

$$cp_o \approx \sqrt{2mc^2T} = 0.29 \text{ Mev}$$

We define a fictitious distance z_o such that

$$p_o = \epsilon z_o$$

$$z_o = \frac{0.29}{3} = 0.1 \text{ ft}$$

Then with $r(0) = 0$ we have

$$r(z) = \frac{p_r}{\epsilon} \ell n(z/z_o)$$

The current at a distance z down the machine consists of all electrons with radial displacements less than the radius of the holes in loading disks, R. We denote by $p_r'(z)$ the radial momentum for which the radial displacement is R at z.

$$p_r'(z) \equiv R\epsilon/\ell n(z/z_o)$$

Now we introduce our arbitrary model by assuming that the injection optics can be specified by a single parameter n,

$$\frac{dN}{d\Omega} \propto \theta^n$$

where $dN/d\Omega$ is the angular distribution of the beam at injection. A value $n = 0$ implies an isotropic, non-focused beam; $n < 0$ implies a focused, directed beam; $n > 0$ implies a diverging beam. Using the

small-angle approximation again we have

$$p_r = \theta p_o$$

$$d\Omega \propto \theta d\theta \propto p_r dp_r$$

$$\frac{dN}{dp_r} = \frac{dN}{d\Omega}\frac{d\Omega}{dp_r} \propto p_r^{n+1}$$

The current at z is

$$I(z) \propto \int_o^{p_r'} \frac{dN}{dp_r}\, dp_r \propto (p_r')^{n+2}$$

$$\propto \left[\ell n \left(z/z_o \right)\right]^{-(n+2)}$$

If the current at the end of the machine $(z = L)$ is I_f, then

$$I(z) = I_f \left[\frac{\ell n \left(L/z_o\right)}{\ell n \left(z/z_o\right)}\right]^{n+2}$$

2. Experimental

On Mark III there are current monitors located at 10 ft, 100 ft, and 310 ft. These monitors are ferrite toroids in which the beam is the primary current winding. The current pulses are photographed on an oscilloscope.

In Fig. 2 we show the calculated variation of I with z for several values of n (for $z_o = 0.1$ ft), and also some experimental points measured at Mark III under tuned-up operation. The errors are only suggestive and apply to all points at the same z. The gun injects a steady current for about 1 μsec. The pre-buncher is a 2856 Mc cavity which bunches the electrons at 10.5 cm intervals before they enter the accelerator. In earlier times no pre-buncher was used, and the bunching occurred in the machine itself. The Monster will be pre-bunched, and $n \approx -1.5$ seems a reasonable value to use.

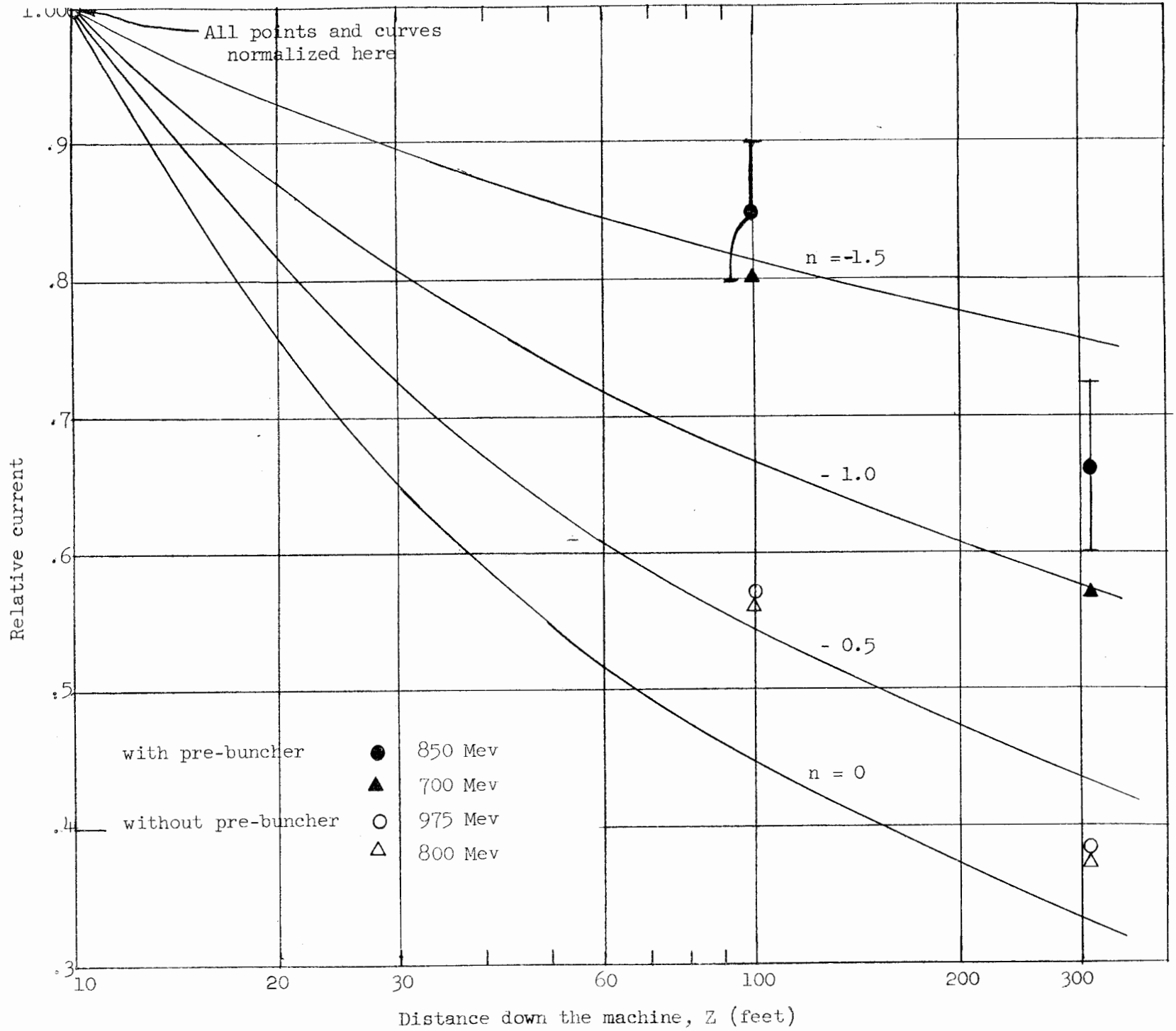

FIG. 2--Current variation along Mark III accelerator.

3. Power Loss

The rate at which power is absorbed is

$$\frac{dP(z)}{dz} = - E(z) \frac{dI}{dz}$$

We have

$$- \frac{dI}{dz} = (n + 2) \frac{I_f}{z} \frac{\left[\ell n \left| L/z_o \right|\right]^{n+2}}{\left[\ell n \left| z/z_o \right|\right]^{n+3}}$$

Since $E(z)/z = \epsilon = \text{const} = E_f/L$, we can write

$$\frac{dP}{dz} = (n + 2) \frac{E_f I_f}{L} \frac{\left[\ell n \left| L/z_o \right|\right]^{n+2}}{\left[\ell n \left| z/z_o \right|\right]^{n+3}}$$

The final beam power is $P_f = E_f I_f$, so the fractional power loss along the machine is

$$\frac{d\left[P/P_f\right]}{d(z/L)} = \frac{(n + 2)}{\ell n \left| L/z_o \right|} \left[\frac{\ell n \left| L/z_o \right|}{\ell n \left| z/z_o \right|} \right]^{n+3}$$

This is shown in Fig. 3a, with $n = - 1.5$, and $z_o = 0.1$ ft for $L = 310$ ft, and $L = 10{,}000$ ft.

The total fractional power loss is

$$P/P_f = \int_{10 \text{ ft}/L}^{1} \frac{d\left[P/P_f\right]}{d(z/L)} d(z/L)$$

We do the integration graphically. There is a logarithmic divergence at $z = 0$ which is integrable. The fractional power loss as a function of n is shown in Fig. 3b for $L = 310$ ft and $L = 10{,}000$ ft with $z_o = 0.1$ ft.

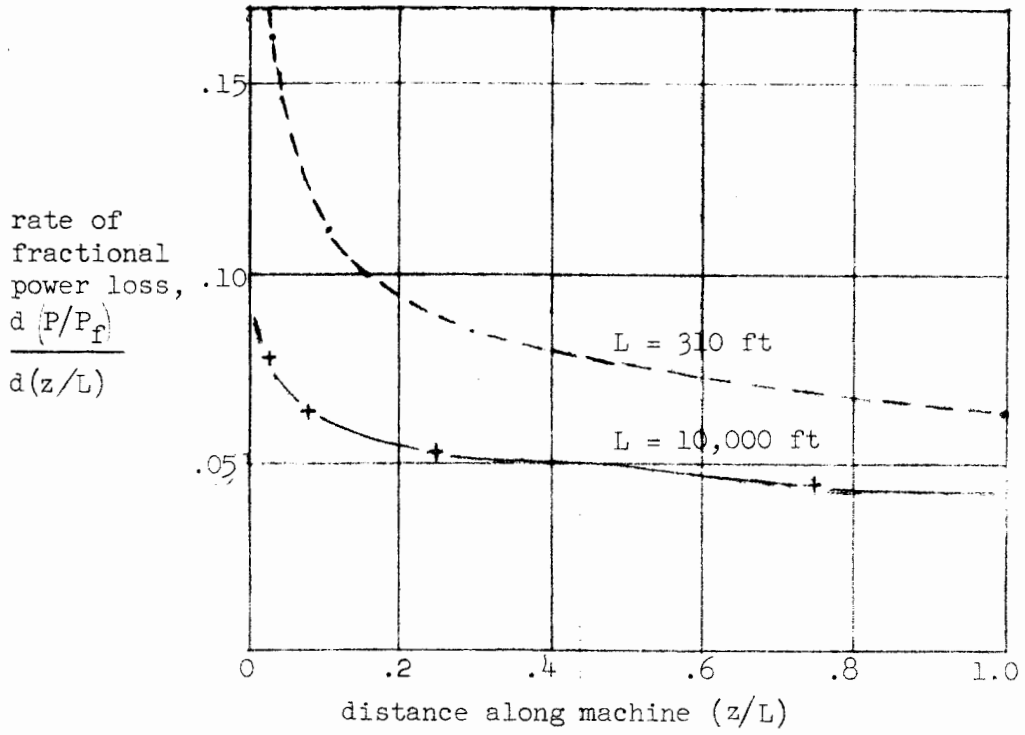

FIG. 3a--Rate of power loss along the machine.

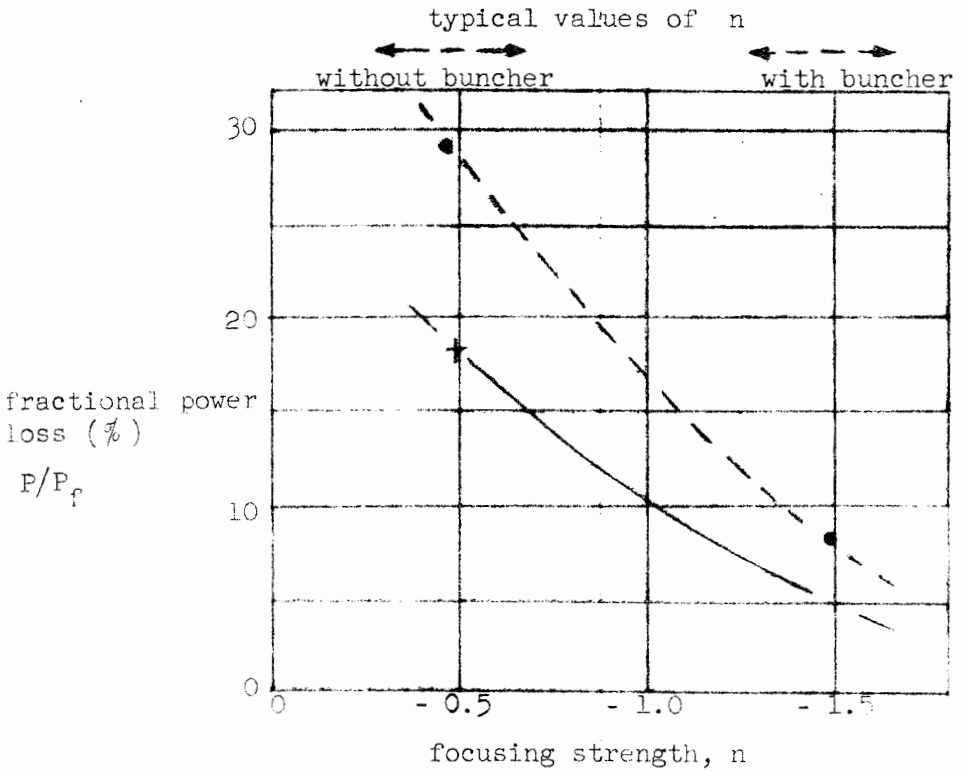

FIG. 3b--Fractional power loss vs

C. Summary

Our goal is to arrive at a reasonable value of average beam power loss to use in shielding calculations. We want to make our best guess at the average operating characteristics, and then at the very end to put in a safety factor which is big enough to insure that the shielding will be adequate.

The experimental data we have introduced are from Mark III under tuned-up operation. From Fig. 3b we estimate that if the beam optics in the two-mile machine were similar to those in Mark III, then the average beam power loss would be about 5% of the final beam power. However, our assumption is that the beam optics will be better, so we arbitrarily take $P/P_f = 3\%$.

So far we have only considered average operating conditions. Occasionally a very large beam loss will occur, for example, from missteering or misalignment. To get a feeling for the magnitude of this problem, we note that if the full current is absorbed at an energy $E_f/2$ for 10 minutes per day then the average power loss is about 0.3% of P_f. This is an example of a serious mistake in accelerator operation, and since it gives an average power loss small compared to our previous number, we judge that 3% is still a reasonable value to use.

Even in an ideal machine there would be some beam loss arising from interactions with the residual gas. We have estimated that, at a pressure of 10^{-5} mm Hg, about 0.4% of the beam power would scatter out.[9]

To summarize, in the following we assume that the total average beam loss along the machine is 3% of a final beam power of 2.4 Mw (e.g., 60 μa at 40 Bev) distributed uniformly along the full length of the machine. We assume rather arbitrarily that this 3% is uncertain by a factor of 3.

Extensive use of collimators along the machine to localize the radiation problems arising from unwanted, errant beam electrons would change the distribution of beam power loss. Unfortunately it is difficult to design collimators and to estimate their efficacy. If they are used, the radiation problems will be easier to handle, and we will incorporate the changes into the shield design.

---

[9]H. DeStaebler, "Scattering of Beam Electrons by the Residual Gas in the Accelerator," M-281, Stanford Linear Accelerator Center, Stanford, California, October, 1961.

Fig. 3a shows that the rate of power loss is greatest near the front end of the machine, and from this one might suppose that the radiation levels there might be higher than that calculated on the assumption of uniform beam loss. However, further consideration suggests general reasons why the sharp rise near $z \approx 0$ in Fig. 3a is not worrisome. First, this sharp rise comes partly from the assumed form of the injection optics, and it may not be present at all in the Monster. Second, electrons below 1 or 2 Bev are not as efficient per unit energy in producing penetrating particles as electrons of a few Bev and higher.

In the beam-switchyard area the average beam loss may be higher than 3%, e.g., when energy slits are used in defining an energy spectrum narrower than the natural energy spread out of the machine ($\approx 0.5\%$). For this reason the shielding will be somewhat thicker in this region.

IV. FLUX OF PARTICLES LEAVING THE MACHINE AND INCIDENT ON THE INSIDE OF THE SHIELD*

In Section A below a number of assumptions are made, with little justification, and only a small effort is given to making them seem plausible. The principal justification lies in the reasonably good (a factor of 2) agreement with experiment that is described in Section B. The reason for deriving a calculational model is that the experiment was done with 925 Mev thin-target bremsstrahlung, whereas we are interested in the yields from a $1/k^2$ spectrum with energies up to 20-40 Bev; thus a model is necessary for extrapolation to the different conditions. Despite these differences the experimental results agree quite closely with the calculations over an important range of energies.

A. Description of Calculation

When an electron of energy E_o is absorbed in the copper of the accelerating structure, the differential photon track length for photons of energy k is

$$\frac{d\ell}{dk} = 0.57 \frac{E_o}{k^2} X_o \qquad (g\text{-}cm^{-2}/Mev)$$

where X_o is a radiation length in copper (13 $g\text{-}cm^{-2}$). This expression is derived under Approximation A of shower theory, in which all interactions are neglected except pair production and bremsstrahlung, each with its high-energy asymptotic cross section.[10] Monte Carlo calculations of shower development in copper carried out at Oak Ridge agree quite well with this expression for the differential track length over most of the range of interesting photon energies.[11] The use of Approximation A is not a significant source of error in the shielding calculation.

---

*I am indebted to Charles H. Moore for programming many of the calculations in Sections IV and V.

[10] B. Rossi, High Energy Particles (Prentice-Hall, 1952), Chap. 5.

[11] C. D. Zerby and H. S. Moran, "Studies of the Longitudinal Development of High-Energy Electron-Photon Cascades in Copper," ORNL-3329, Oak Ridge National Laboratory, Oak Ridge, Tennessee, 1962.

We make approximate calculations of the yields of nuclear particles from the electromagnetic cascade by using the cross sections which have been measured for photons on free nucleons. Because the photon spectrum is weighted as $1/k^2$, and also because absorption in the shielding becomes very great for particle energies below about 200 Mev, the range of secondary-particle energies of greatest significance is around 200-500 Mev. Since neutrons have only nuclear interactions, they have the greatest penetrating power; for thick shields and large angles from the primary beam, such as we consider here, neutrons are the dominant radiation which must be stopped. Charged pions lose an appreciable amount of energy by ionization, and we take them into account more approximately than the neutrons. Neutral pions decay into two photons in about 10^{-16} sec. The photons are rapidly absorbed in the shield, where the electromagnetic absorption length is about five times shorter than the nuclear absorption length. However, it is possible for pions to undergo nuclear interactions which give rise to neutrons, and this is one way we take them into account. We neglect the photoprotons because they lose so much energy by ionization; for example, a 400-Mev proton has a residual range approximately equal to one nuclear mean free path.

Since we put greater emphasis on the photoneutrons, we shall describe the calculations in terms of secondary neutrons. Then we shall indicate how we get the charged-pion spectrum.

Suppose that the cross section per nucleus for a photon of energy k to give rise to a neutron of kinetic energy T at an angle θ is $\delta\sigma/\delta\Omega$.

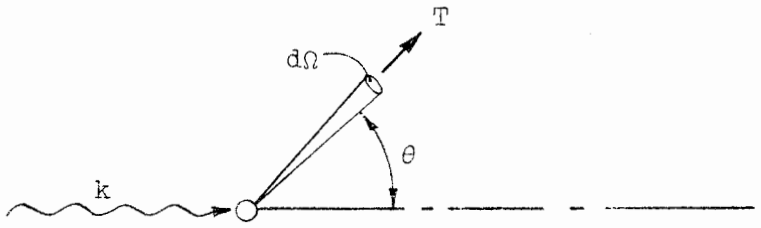

The yield of secondary neutrons per incident electron of energy E_o is

$$\frac{d^2n}{dTd\Omega} = \left(0.57 \frac{E_o X_o}{k^2}\right) \frac{N_o}{A} \left[KA \frac{d\sigma}{d\Omega^*}\right] \frac{\partial(k,\theta^*)}{\partial(T,\theta)}$$

Track length | Cross section per nucleus | Jacobian

where an asterisk denotes the center of mass, and where

$\frac{d^2n}{dTd\Omega}$	is the number of neutrons per (Mev-sr) per incident electron for the reaction indicated by σ.
N_o	is Avogadro's number.
σ	is the cross section per "effective target nucleon" in a copper nucleus.
KA	is the number of effective target particles per nucleus.
A	is the atomic weight of target.
K	is the number of effective target particles per nucleon (K depends on the reaction).
$\frac{\partial(k,\theta^*)}{\partial(T,\theta)}$	is the Jacobian which converts $d\Omega^* dk$ to $d\Omega dT$.

The following method of calculation is similar to that used by Olson, and we have leaned heavily on his work.[12] We consider five reactions which yield secondary neutrons. The first three are direct photoproduction:

$$\gamma + \text{nucleon} \rightarrow 1\pi + \text{recoil neutron} \quad (1)$$

$$\gamma + \text{nucleon} \rightarrow 2\pi + \text{recoil neutron} \quad (2)$$

$$\gamma + \text{nucleon pair} \rightarrow \text{nucleon} + \text{recoil neutron} \quad (3)$$

The other two are secondary reactions between a pion and a nucleus.

$$\text{(absorption)} \quad \pi + \text{nucleon pair} \rightarrow \text{nucleon} + \text{neutron} \quad (A)$$

$$\text{(scattering)} \quad \pi + \text{nucleon} \rightarrow \pi + \text{neutron} \quad (S)$$

---

[12] D. N. Olson, "Photoprotons from Nuclei Exposed to 1 Bev Bremsstrahlung Radiation," Thesis, Cornell University, Ithaca, New York, 1960 (unpublished). A. Silverman told me about this reference, and it has been very stimulating.

We suppose that these secondary reactions occur only in the same nucleus in which the pion is produced. (The neutral pions usually cross this nucleus but not many others.) The accelerator pipe itself is a small part of a nuclear mean free path thick, and we make a minor error in neglecting it. We do not take explicit account of the neutrons produced by pions in the shielding. We denote by G the probability that a pion gives rise to a neutron by reaction (A) or (S).

It will turn out that for our shield calculation reaction (1) followed by reaction (A) or (S) is the dominant source of neutrons ($\theta \approx 90^{\circ}$).

We proceed in two steps. First we estimate the elementary-particle cross section (σ). Then we estimate the number of effective target particles per nucleon (K) for each particular reaction.

We neglect the effects of the Pauli principle and also the quantitative effects of Fermi motion. Partly for these reasons and partly for the sake of simplicity we assume that the production reactions (1), (2), and (3) are isotropic in the center of mass, even though many of the free-particle reactions are known to be nonisotropic. We take

$$\frac{d\sigma}{d\Omega^*} = \frac{\sigma_{\text{total}}(k)}{4\pi}$$

For reaction (1) we use a cross section which is approximately the average of the measured cross sections for $\gamma + p \rightarrow p + \pi^{\circ}$ and $\gamma + p \rightarrow n + \pi^{+}$. (Roos and Peterson[13] have a nice summary of the data on total photo-pion cross sections, which we show in Fig. 4.)

There are four reactions under category (1):

$$\begin{aligned} \gamma + p &\rightarrow \pi^{\circ} + p \qquad (1a) \\ &\rightarrow \pi^{+} + n \qquad (1b) \\ \gamma + n &\rightarrow \pi^{\circ} + n \qquad (1c) \\ &\rightarrow \pi^{-} + p \qquad (1d) \end{aligned}$$

---

[13] C. E. Roos and V. Z. Peterson, Phys. Rev. 124 1610 (1961).

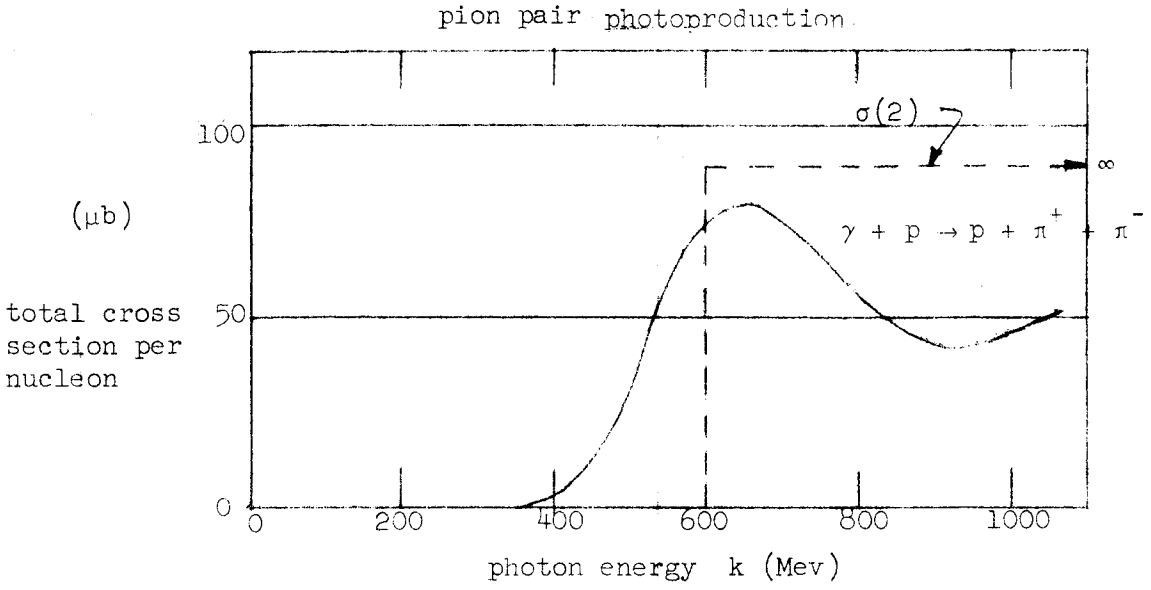

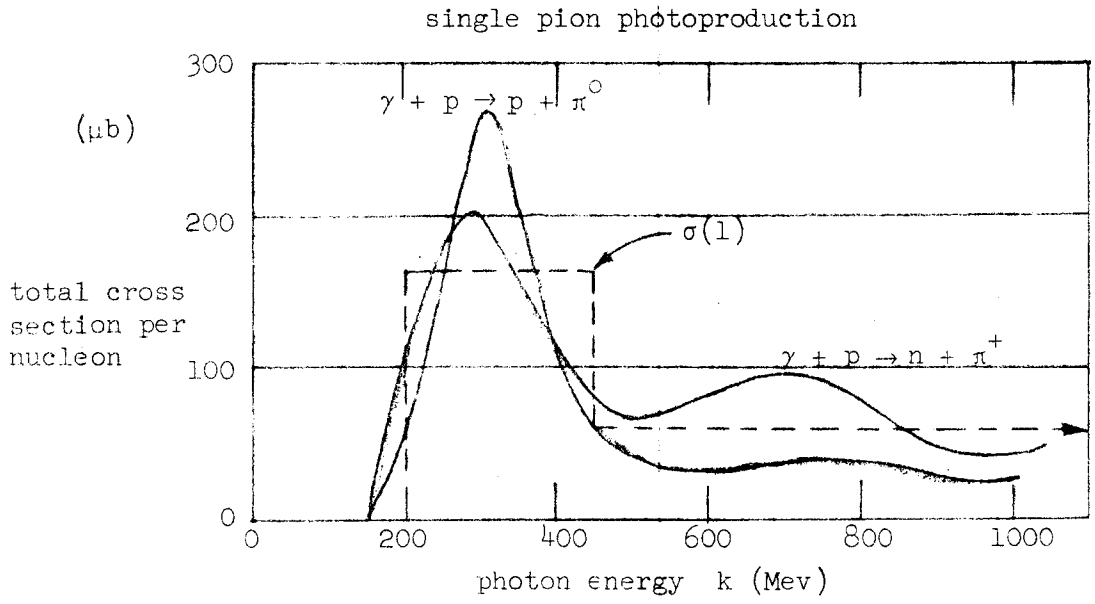

FIG. 4--Measured pion photo cross sections and our approximations vs photon energy.

Of these only (1b) and (1c) lead to final neutrons. We assume that all four cross sections are equal and take

$$\sigma(1) \approx \tfrac{1}{2}\left[\sigma_{exp}(1a) + \sigma_{exp}(1b)\right]$$

For neutron production each proton contributes once (1b) and each neutron contributes once (1c), so we assume that there is one effective target particle for each nucleon in the copper nucleus (K = 1).

For charged-pion production we also have K = 1, but for pion absorption we have K = 2 because here the neutral pions contribute. So we have

K (1) = 1	neutrons
K (1) = 1	charged pions
K (1) = 2	total pions

For reaction (2) we use a cross section which is approximately the same as that observed for $\gamma + p \rightarrow p + \pi^+ + \pi^-$ (see Fig. 4).

There are six reactions in category (2):

$$\begin{aligned}
\gamma + p &\rightarrow \pi^+ + \pi^- + p \qquad (2a)\\
&\rightarrow \pi^o + \pi^o + p \qquad (2b)\\
&\rightarrow \pi^+ + \pi^o + n \qquad (2c)\\
\gamma + n &\rightarrow \pi^+ + \pi^- + n \qquad (2d)\\
&\rightarrow \pi^o + \pi^o + n \qquad (2e)\\
&\rightarrow \pi^- + \pi^o + p \qquad (2f)
\end{aligned}$$

Three of these lead to recoil neutrons. We assume that all of these cross sections are equal,

$$\sigma(2) \approx \sigma_{exp}(2a)$$

For neutron production each target proton contributes once, and each target neutron contributes twice. Even though there are more neutrons than protons, we assume that on the average there are 3/2 effective target particles per nucleon. For charged pions, each neutron reaction and each

proton reaction contributes one charged pion on the average, and there are three reactions for each nucleon. Thus the effective number of nucleons per nucleon times the average yield of pions per interaction is 3, and we take $K = 3$. Again there are as many neutral pions as charged pions. We have

$K(2) = 1.5$	neutrons
$K(2) = 3$	charged pions
$K(2) = 6$	total pions

Reaction (3) has been measured up to $k = 900$ Mev on deuterium.[14] The cross section shows a slight peak at about $k = 250$ Mev and falls approximately as $1/k^3$ above $k = 300$ Mev. We approximate the deuteron cross section as follows:

$$\sigma(3) \approx \sigma_{exp}(3)$$

$$\sigma(3) = 60 \ \mu b \quad \text{for} \quad k < 300 \text{ Mev}$$

$$= 60 \left(\frac{300}{k}\right)^2 \mu b \quad \text{for} \quad k > 300 \text{ Mev}$$

This is the approximation introduced by Panofsky for the original Monster shielding calculations[1,15] and it is similar to the approximation used in some of the CEA calculations.[16]

There is some doubt about the proper value of K to use; however, we have already made rather violent approximations in the pion reactions which turn out to dominate the neutron yield, so it does not make sense to worry too much about the particular value of K.

Levinger[18] has interpreted the nuclear photo-effect by representing the nucleus as a group of pseudo-deuteron clusters. He derived the theoretical result

$$\sigma_{th}(\text{nucleus}) = \alpha' \frac{NZ}{A} \sigma_{th}(\text{deuteron})$$

---

[14] Myers, Gomez, Guinier, and Tellestrup, Phys. Rev. 121, 130 (1961).

[1] "Proposal for a Two-Mile Linear Electron Accelerator," Stanford University. (Stanford Linear Accelerator Center), Stanford, California, 1957.

[15] "Conference on Shielding of High-Energy Accelerators, New York, April 1957," TID-7545 Technical Information Service Extension, Oak Ridge, Tennessee.

[16] R. Wilson, "A Revision of Shielding Calculations," CEA-73, Cambridge Electron Accelerator, Harvard University, Cambridge, Massachusetts, May 1959.

[18] J. S. Levinger, Nuclear Photo-Disintegration (Oxford, London, 1960).

where both cross sections are theoretical, A is the atomic weight, Z the atomic number, N = A - Z, and α' is a numerical constant equal to about 6.4 to 8 (see References 17 and 18).

Experiments on the nuclear photo-effect with ≈ 300 Mev bremsstrahlung have been analyzed following the ideas of Levinger and R. R. Wilson (see, for example, reference 19).

$$\sigma_{exp}(\text{nucleus}) = \alpha \frac{NZ}{A} \sigma_{exp}(\text{deuteron})$$

The values of α range from about 1.5 to 3.0, as found by the MIT group.[19]

In our present notation,

$$\sigma\,(\text{nucleus}) = KA\ \sigma_{exp}(\text{deuteron})$$

So

$$K = \alpha \frac{NZ}{A^2}$$

For copper,

$$\frac{NZ}{A^2} = 0.248 \approx 1/4$$

In this report we use K = 1, which corresponds to α = 4.0.

We summarize the values of α used in various reports.

Report	Reference	α	K
Panofsky in Proposal	1	1.5	0.37
Dedrick in M-227	20	1.5	0.37
DeStaebler in M-262	2	3.0	0.75
Olson (thesis)	12	6.4	1.6
Wilson in CEA-73 (for iron)	16	0.85	0.21
This report		4.0	1.0

[19] Stein, Odian, Wattenberg and Weinstein, Phys. Rev. 119, 348 (1960).

Before considering the secondary reactions (A) and (S), in which a pion interacts inside its parent nucleus and a high-energy neutron is produced, we digress for a moment to discuss kinematics. For the production reactions (1), (2), and (3) we use two-body kinematics and assume that the initial nucleon is at rest (no Fermi motion). The final state of reaction (2) actually contains three particles. We force it into the two-body situation by assuming that the two pions always behave like a single particle of mass 474 Mev. (This is not supposed to represent an actual resonance; it is simply two pion masses plus a Q value of about 200 Mev.) We get pions from this fake "di-pion" by assuming that the di-pion decays at once and that each pion has half the total energy of the di-pion and that each pion moves in exactly the same direction as the di-pion did when it was produced. This is our most Procrustean application of the requirement of two-body kinematics. Schematically,

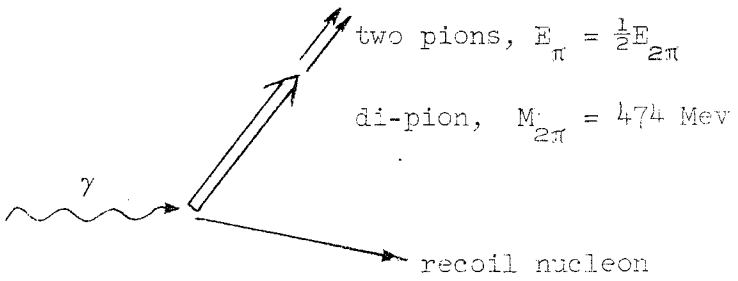

In our calculations we find that for copper and for angles $\theta \approx 80^\circ$ the dominant source of neutrons is from the interaction of single pions. Olson found at these angles from carbon that the contributions from the pseudo-deuteron photo-effect and from single pion absorption were roughly equal and together accounted for the observed proton yield.[12] So the pion interaction is important, and we describe the drastic approximations which are made in the kinematics to simplify the calculations. We do not describe Olson's approximations, but only the ones we have used.

---

[12] D. N. Olson, op. cit.

When a pion interacts inside the nucleus the kinematic situation gets very complicated. We use the same kinematic approximations for reactions (A) and (S), and they are indicated in the sketch.

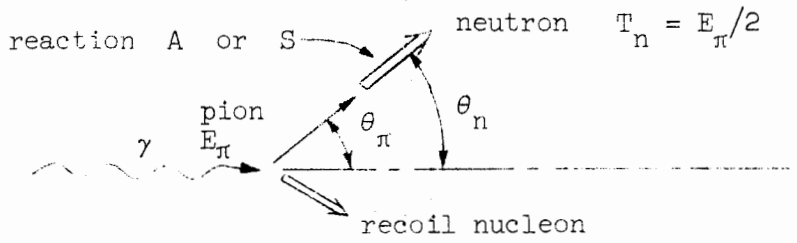

We assume that

$$T_n = \tfrac{1}{2}E_\pi$$
$$\theta_n = \theta_\pi$$
$$d\Omega_n = d\Omega_\pi$$

The obvious reason for making these assumptions is simplicity; the only justification for their use lies in the agreement with experiment they lead to, but we say a few words about the physics of these assumptions anyhow. The idea behind the angular assumption is that this is a bad-geometry situation. We are interested in neutrons at angle θ. A pion with initial angle θ rarely makes a neutron at angle θ; however, pions with angles greater or less than θ can make neutrons at θ. The energy assumption would seem to greatly overestimate the neutron energy for scattering (S), but in the case of absorption (A) it is true, on the average.

Now we consider the probability that a pion interacts before leaving the nucleus, and, following Olson, we use the optical model which relates the probability of interaction to the size of the nucleus and to the mean-free path for interaction in nuclear matter.

If pions are produced uniformly in a spherical nucleus of radius R.

the probability that they interact on the way out of the nucleus is

$$G = 1 - \frac{3}{2x}\left\{1 - \frac{2}{x^2}\left[1 - (1 + x)\, e^{-x}\right]\right\}$$

where

$$x = 2R/\lambda$$

and λ is the mean-free path in nuclear matter and in general is a function of the pion energy.[23] If the interaction cross section is σ (cm^2/nucleon), and the nucleon density is

$$\rho = \frac{A}{\frac{4}{3}\pi R^3} \qquad \text{(nucleon/cm}^3\text{)}$$

then

$$\lambda = \frac{1}{\rho\sigma} = \frac{\frac{4}{3}\pi R^3}{A\sigma} \qquad \text{(cm)}$$

and

$$x = \frac{2R}{\lambda} = \frac{3}{2}\frac{A\sigma}{\pi R^2}$$

Substituting

$$R = r_o A^{1/3}$$

gives

$$x = \frac{3}{2} A^{1/3}\left(\frac{\sigma}{\pi r_o^{\,2}}\right)$$

---

[23] Brueckner, Serber and Watson, Phys. Rev. 84, 258 (1951).

For copper we take $r_o = 1.2 \times 10^{-13}$ cm and $A = 64$, which gives

$$x = \frac{3 \times 4}{2} \frac{\sigma}{45 \text{ mb}} = \frac{\sigma(\text{mb})}{7.5}$$

where σ is the effective interaction cross section per nucleon.

To get σ we first consider reaction (A). Experimental data is available on $\pi^+ + d \rightarrow p + p$ and on the inverse reaction $p + p \rightarrow \pi^+ + d$.[24] There remains the question of the number Γ of deuteron-like clusters per nucleon in the nucleus. We take $\Gamma = 1$ rather arbitrarily (Olson used $\Gamma = 4Z/A = 1.8$). So we use

$$\sigma(A) = \sigma_{exp}(\pi^+ + d \rightarrow p + p)$$

and this is plotted in Fig. 5a.

For reaction (S) it does not seem appropriate to use the total scattering cross section, especially when we consider the drastic kinematic assumptions which we are making for reactions (A) and (S). For the sake of argument we arbitrarily say that the appropriate cross section is one-fifth of the average charged pion total cross section on protons.[24]

$$\sigma(S) = \frac{1}{5} \times \frac{1}{2} \left[\sigma_{exp}(\pi^+ + p) + \sigma_{exp}(\pi^- + p) \right]$$

This is plotted in Fig. 5a. In Fig. 5b we plot values of G derived using $\sigma = \sigma(A) + \sigma(S)$. In the following calculations we take G to be constant independent of pion energy. This is indicated by the dashed line at $\bar{G} = 0.40$.

Note that the neutron energy spectrum has an additional factor of 2 from changing energy variables:

$$\left(\frac{d^2N}{dT_n d\Omega} \right)_{\text{neutrons}} = KG \frac{d^2N}{dT_\pi d\Omega} \frac{dT_\pi}{dT_n}$$

$$T_n \equiv \frac{1}{2}\left(M_\pi + T_\pi \right)$$

$$\frac{dT_\pi}{dT_n} = 2$$

[24] See references cited in S. J. Lindenbaum, Ann. Rev. Nuclear Sci. 7, 317 (1957).

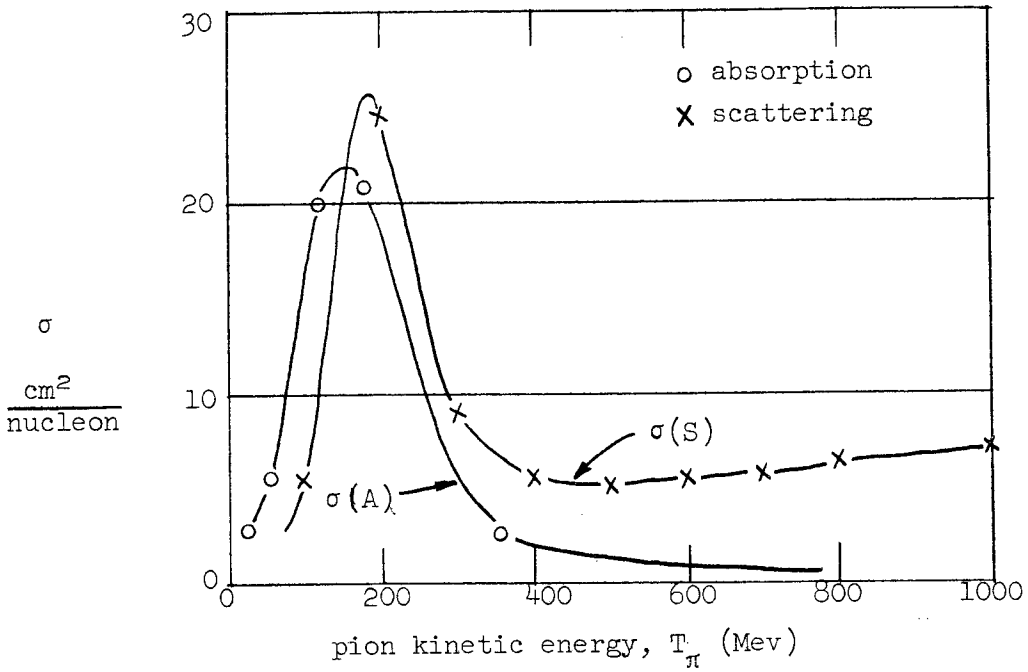

FIG. 5a--Cross sections for pion absorption and scattering vs pion kinetic energy.

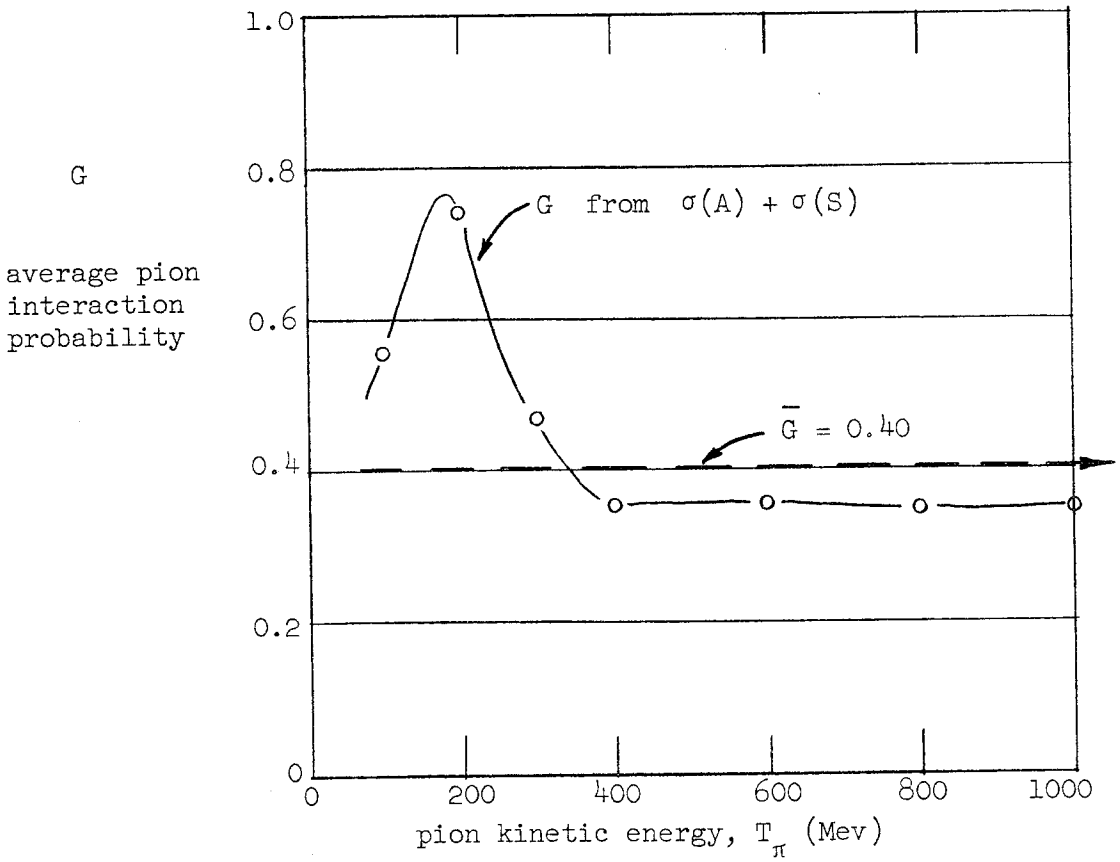

FIG. 5b--Average pion interaction probability vs pion kinetic energy.

We summarize the values of the numerical factors which govern the yield of neutrons and pions, and which multiply the direct production cross sections denoted earlier by $\sigma(1)$, $\sigma(2)$, and $\sigma(3)$:

Neutron Production

	Direct	Via Pion Interaction	
Reaction	K_n	$K_{all\ \pi}$	$\bar{G}K_{all\ \pi}$
1 (single π)	1.0	2	0.8
2 (di π)	1.5	6	2.4
3 (deuteron)	1.0	0	0

Charged Pion Production

	Direct	Reduced by Pion Interaction
Reaction	$K_{ch\ \pi}$	$(1-\bar{G})\ K_{ch\ \pi}$
1 (single π)	1	0.6
2 (di π)	3	1.8
3 (deuteron)	0	0

B. Experiment

At the Mark III accelerator at Stanford we measured the yield of protons from copper irradiated by 925 Mev thin-target bremsstrahlung. Considering the crudeness of the approximations which are made in the calculation and the symmetry between neutrons and protons, we take the yield of neutrons and protons to be the same; thus the measured proton yield will be used to check the calculated neutron yield. The protons were detected at angles with respect to the photon beam of $\theta = 50^\circ$, 65°, 80° and 94° (95° could not be reached for mechanical reasons) and over the momentum range 400 Mev/c $\leq p \leq$ 900 Mev/c, which corresponds to a kinetic energy range of 80 Mev $\leq T \leq$ 360 Mev. These energies and angles are important ones for the transverse shielding, and thus the measurement provides a significant test for our calculation.

The apparatus will be described very briefly. The analyzing magnet used was that developed by R. Hofstadter (180° bend angle, $n = 1/2$, double-focusing, 72-inch radius of curvature). The gamma-ray beam, the electronics, and the counters were developed by C. Schaerf to detect the recoil proton from the reaction $\gamma + p \rightarrow p + \pi^{\circ}$. The present measurement was made as an adjunct to Schaerf's experiment. Schematically we had the following arrangement:

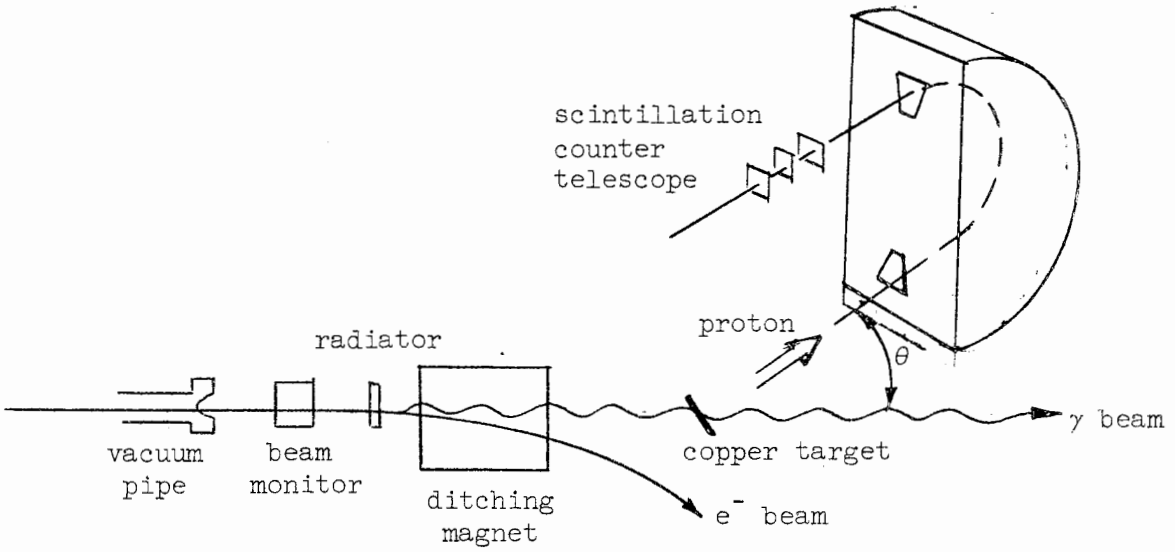

All of the equipment and techniques were standard. The telescope consisted of three plastic scintillators in prompt coincidence. This coincidence opened a gate which caused the pulse from the middle counter to be pulse-height analyzed. The final counting rate was derived from the analyzer data where the protons and (π^{+},e^{+}) were separated by pulse height. The momentum acceptance of the system was determined by the width of the first scintillation counter; the solid angle was fixed by a lead aperture ("baffle") 2-inches thick placed three-quarters of the way through the magnet.

We now calculate, as before, the expected number of proton counts per incident electron, N. The calculation involves two-body kinematics, so that for each reaction there is a unique relation between (k,θ^{*}) and

it would put a sharp peak at about 500 Mev/c, which seems "intuitively" unreasonable. The results at the other three angles are similar to those at 65°. Most of the protons come from the interaction (scattering or absorption) of pions produced singly. In all cases we smooth off the yield from this reaction around k = 800 Mev so that the total yield curve drops fairly smoothly as the proton momentum rises. The pseudo-deuteron model contributes significantly only at the largest momenta. At 50° recoil protons from single-pion production are significant, but at larger angles these protons have momenta which are too low.

In the following four figures (Fig. 7 through Fig. 10) we compare the measured points with 0.60 times the total calculated yield (again excluding the contribution of protons from di-pion absorption). The factor 0.60 is in no sense a best fit; it is used only to make a visual comparison easier. Each point is corrected for counting losses ($\lesssim 5\%$) and for chance coincidences (a few percent at low momenta and up to 30% at high momenta)* and has a background of 1.0 ± 0.2 count/volt subtracted. Some typical error bars are shown (counting statistics only).

C. Recapitulation

The justification of our calculated yields lies in the "agreement" with the measured yields. In the succeeding calculations we make use of the yields as calculated in Section IV.A (including the di-pion reactions), and we ascribe to them an uncertainty of a factor of 2.

*The singles rates were almost independent of the true signal rate, so the chance rates were independent of the signal. But the signal decreased as the momentum increased, so the correction increased with momentum. Delayed coincidences were continuously measured, and these were used to make the correction. Any systematic uncertainties in this correction were ignored.

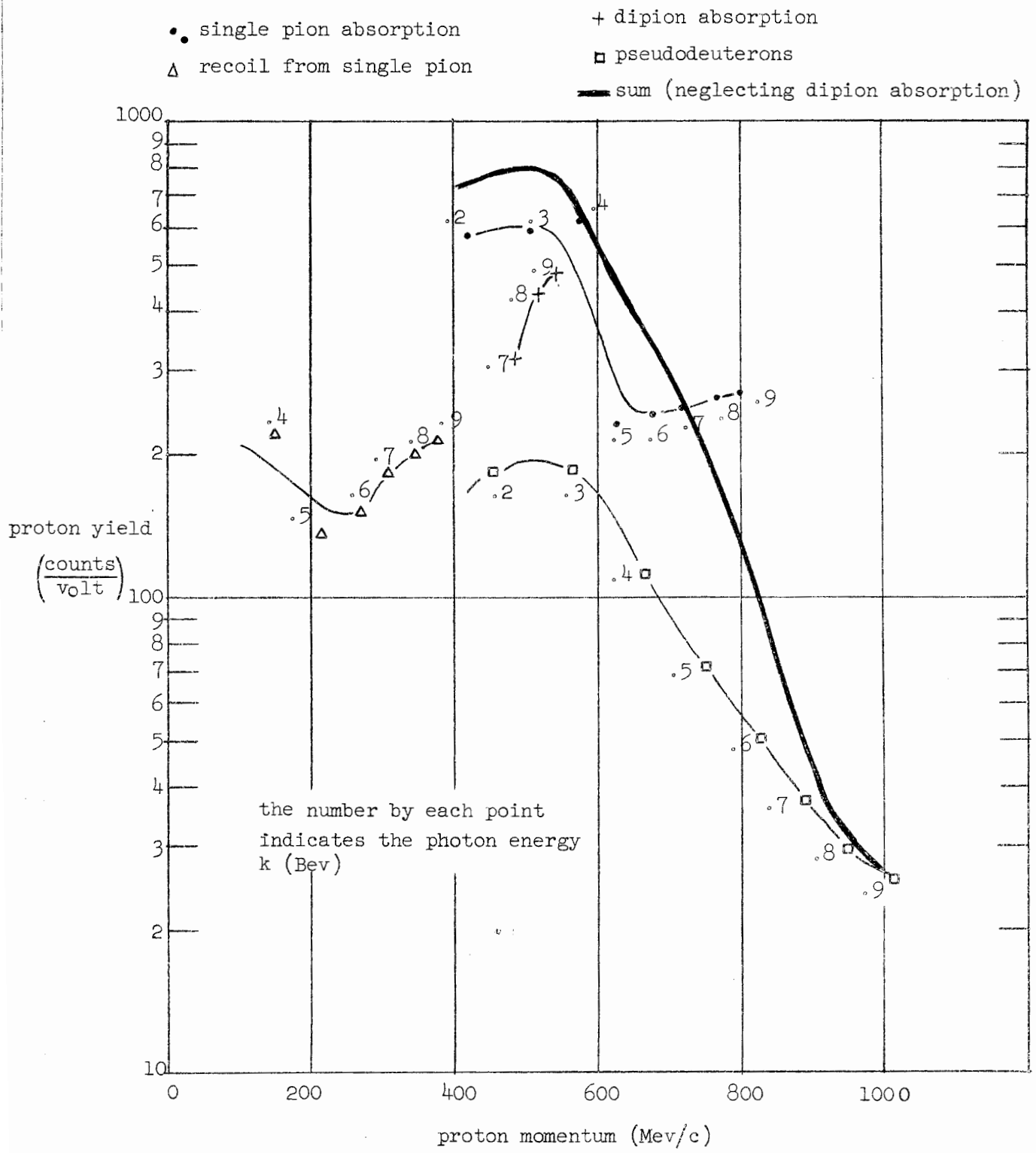

FIG. 6--Calculated yields of photo-protons from copper at $\theta = 65^{\circ}$.

where C is the value of the integrating capacitor, and (ϵe) is the effective charge collected per beam electron.

The radiator consists of a piece of copper, a piece of aluminum and some junk (mostly aluminum foils and air). We use a total radiator thickness of $t = .057$ radiation lengths apportioned as follows.

	Thickness (inches)	Density* ($g\text{-}cm^{-3}$)	Radiation** lengths ($g\text{-}cm^{-2}$)	Thickness (r.l.)
Copper	0.0202	8.90	12.8	3.56×10^{-2}
Aluminum	0.0620	2.70	23.9	1.77×10^{-2}
Junk				0.40×10^{-2} (estimated) $(.42 \pm .05) \times 10^{-2}$ (measured)

*Handbook of Chemistry and Physics

**UCRL 2426 (rev.)

The target consisted of a piece of copper 0.0404 inches thick rotated vertically by $45^\circ \pm 2^\circ$ with respect to the beam direction in such a way that the protons had less copper to go through to get to the analyzing magnet. The target thickness was

$$\rho\ell = 8.90 \left(\frac{.0404 \times 2.54}{.707}\right) = 1.29 \text{ g-cm}^{-2}$$

Air at STP surrounded the copper, but in 3 inches, which was approximately the width seen by the magnet, the air amounted only to about .01 $g\text{-}cm^{-2}$ and it is neglected.

Using the method of calculation described in the first part of Section IV (but with a thin-target bremsstrahlung spectrum) and using the numerical values just given, we calculate the expected yield of protons. Fig. 6 shows the result for $\theta = 65^\circ$. We neglect the contribution from di-pion absorption because its calculation is most uncertain and because

Ray-tracing for a point source shows that the limiting aperture is the upper baffle, which has a trapezoidal hole with

$$A = 12.94 \times \frac{3.13 + 2.44}{2} = 36.0 \text{ in.}^2$$

We use $r_o = 72$ inches and $d_o = 50.6$ inches and get

$$\Delta\Omega = \frac{36.0}{72^2 + 50.6^2} = 4.6 \times 10^{-3} \text{ sr}$$

This value of $\Delta\Omega$ is consistent (within uncertainties estimated as ± 30%) with that derived from electron scattering peaks taken by Schaerf. (These peaks depend on the absolute value of the electron scattering cross sections, and also on the efficiency of the telescopes which we take here as unity.) Finally we have

$$\int\int_{\text{Magnet}} \frac{dp}{p} d\Omega = \frac{\Delta p}{p} \Delta\Omega = 6.9 \times 10^{-3} \; (4.6 \times 10^{-3}) = 3.2 \times 10^{-5} \text{ sr}$$

The main electron beam is monitored by a secondary-emission monitor (SEM) in which one low-energy secondary electron is collected for about every 10 primary beam electrons which pass through. The efficiency of the SEM, ϵ, is determined by comparing the ratio of charge collected by the SEM to that collected by a large Faraday cup which absorbs all of the charge in the main beam. We use $\epsilon = .045$. This value is probably accurate to a few percent.

The experimental counting rate is not protons/electron but rather protons/volt of integrated beam current. The number of electrons per integrated volt, n, is given by

$$n(\epsilon e) = C \times 1 \text{ volt}$$

$$n = \frac{1.06 \times 10^{-7}}{.045 \times 1.60 \times 10^{-19}} = 1.47 \times 10^{13} \text{ electron/volt}$$

calculation; we take $f(k) = 1$ for all k.

$$N_{(p^+/e^-)} \cong t(\rho\ell) \frac{N_o K\sigma(k)}{4\pi} \frac{p}{k} \frac{\partial(k,\theta^*)}{\partial(p,\theta)} \iint \frac{dp}{p} d\Omega$$

The last factor is the magnet acceptance. The p in the denominator is put in to make this factor more nearly constant. We evaluate the acceptance according to the first-order optical equation of Judd.[21] The momentum acceptance $\Delta p/p$ for a counter width Δx is

$$\frac{\Delta p}{p} = \frac{1}{D} \frac{\Delta x}{r_o}$$

where r_o is the central radius of curvature, and D is the dispersion.

$$D = \frac{1 + M}{1 - n}$$

For our case the magnification $M = 1$ and $n = 1/2$, so $D = 4$.[22] We have $\Delta x = 2$ inches, so

$$\frac{\Delta p}{p} = \frac{1}{4} \frac{2}{72} = 0.693\%$$

The solid angle is given by[21]

$$\Delta\Omega = \frac{A}{d_o^2 + r_o^2}$$

where A is the area of the limiting aperture, and d_o is the object distance.

---

[21] D. L. Judd, Rev. Sci. Instr. 21, 213 (1950).

[22] Values of D measured by F. Bumiller are within about 5% of the theoretical values.

(p,θ). In terms of the production variables,

$$N_{(p^+/e^-)} = \iint \left(\frac{dn}{dk}\,dk\right) \left(\frac{N_o}{A}\,\frac{KA\sigma(k)}{4\pi}\,d\Omega^*\right) (\rho\ell)$$

Magnet acceptance; Photon spectrum; Cross section; Target thickness

In terms of magnet variables,[25]

$$N = \iint \left[\frac{tf(k)}{k}\right] \frac{N_o K\sigma(k)}{4\pi} \cdot (\rho\ell)\, \frac{\partial(k,\theta^*)}{\partial(p,\theta)}\, dp d\Omega$$

A sketch can define some of the symbols:

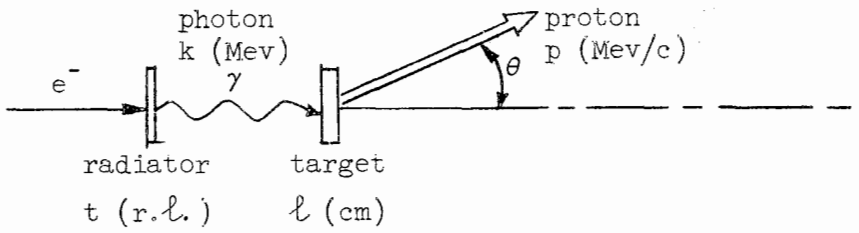

As before, more than one reaction can contribute, and the total rate is a sum over all reactions. The factor $f(k)$ gives the detailed shape of the bremsstrahlung spectrum and would vary from about 1.1 to 0.9 in this

[25]For the Jacobian we used Hand, Kendall, and Schaerf, "Relativistic Two-Body Kinematics," HEPL-236, High-Energy Physics Laboratory, Stanford University, Stanford, California, April 1961.

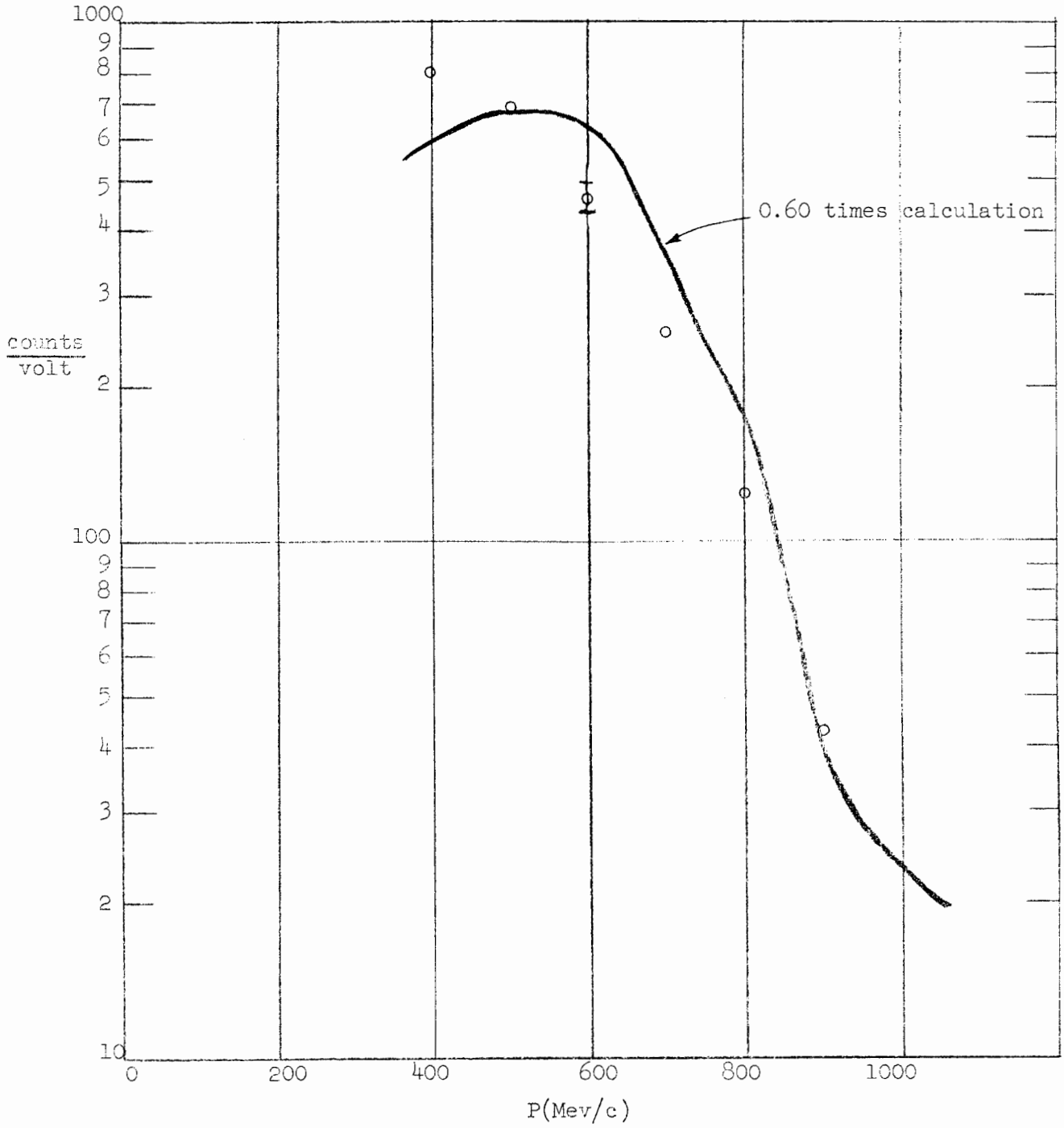

FIG. 7--Comparison of calculation and experiment at $\theta = 50^{\circ}$.

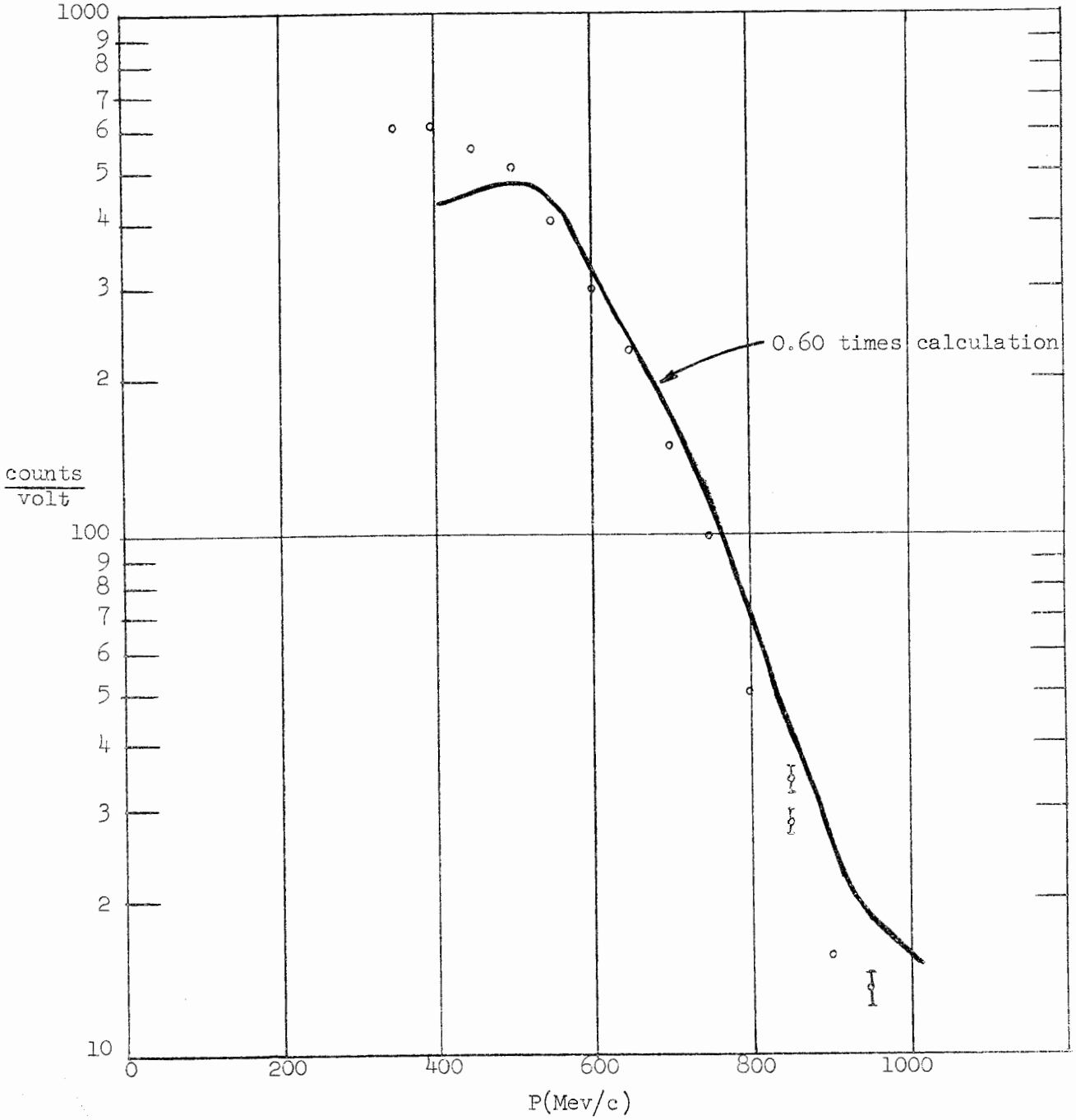

FIG. 8--Comparison of calculation and experiment at $\theta = 65^{\circ}$.

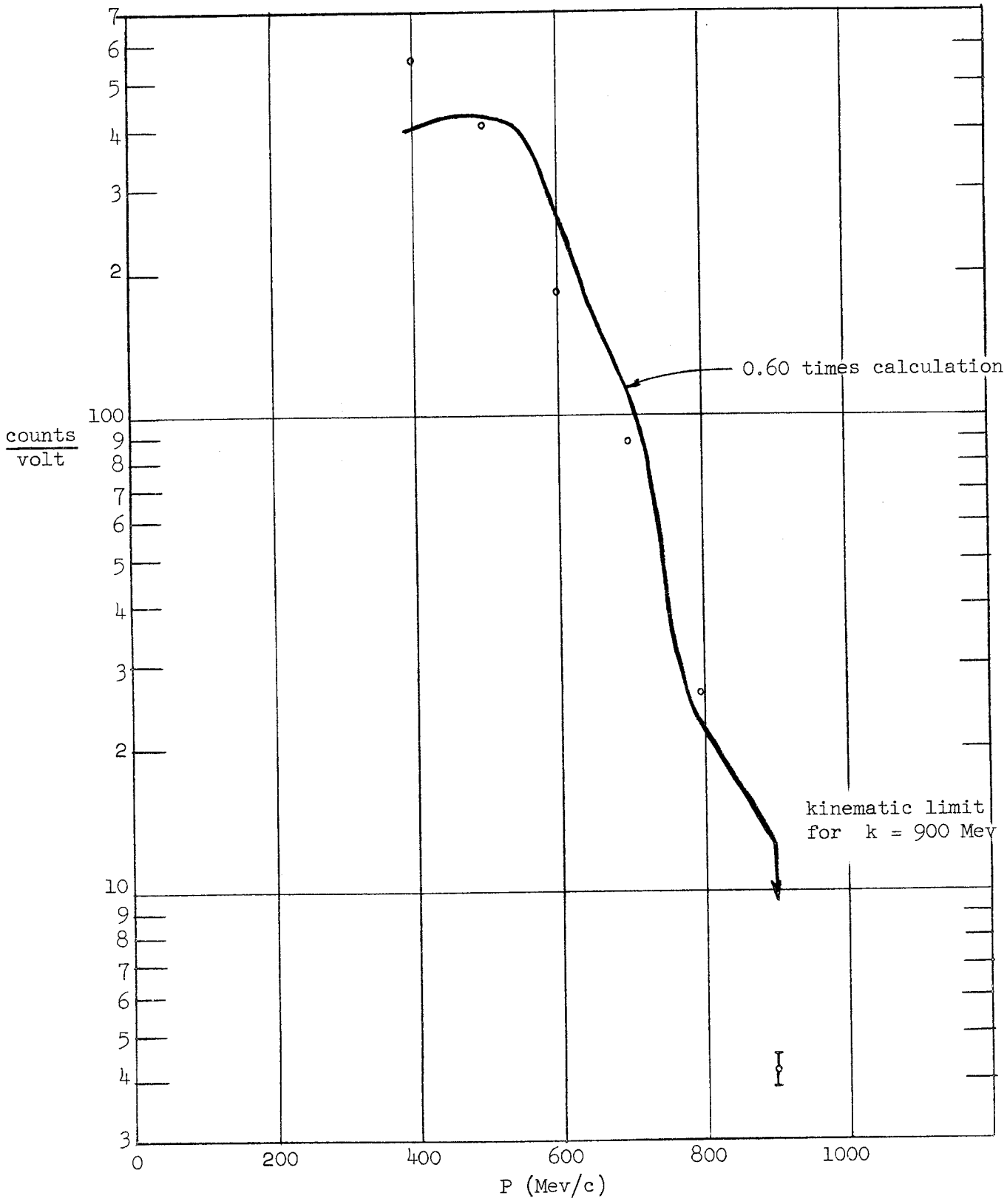

FIG. 9--Comparison of calculation and experiment at $\theta = 80^{\circ}$.

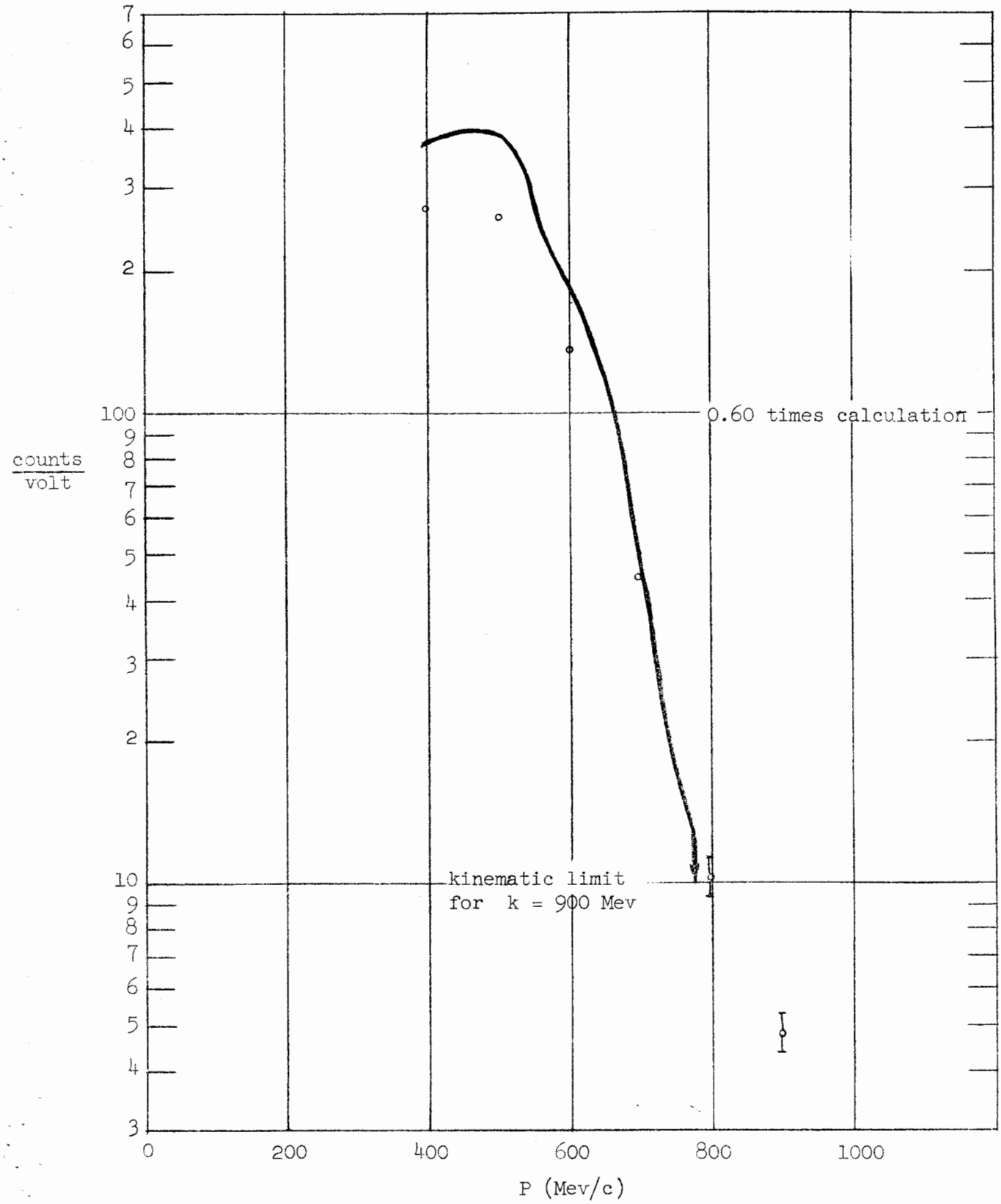

FIG. 10--Comparison of calculation and experiment at $\theta = 95^{\circ}$.

V. PENETRATION THROUGH THE SHIELD AND THE RADIATION LEVEL AT THE OUTER SURFACE OF THE SHIELD

In this section we describe two calculations of the penetration of neutrons through the shield. We refer to the first calculation as the Method of Moyer, since it is basically an application to our conditions of a technique developed by B. J. Moyer at the Lawrence Radiation Laboratory, Berkeley.* The second calculation is one performed at the Oak Ridge National Laboratory in which three coupled integro-differential equations describing the transport through the shield of neutrons, protons and charged pions are solved numerically on a computer. The two calculations differ in many ways, but they give similar answers. One common feature is that each treats the nuclear cascade in one dimension only. All of the spreading in angle and space comes only from the spreading of the initial neutrons coming from the machine, as calculated in the preceding section. At the end of this section we estimate the consequences of this one-dimensional approximation.

A. Method of Moyer

Consideration of the following simple experiment, which is typical of most shielding experiments, will elucidate the important features of penetration of particles through a thick shield. A beam of particles of energy E_o is incident on a shield of thickness H behind which there is a detector whose threshold energy E_d is usually much smaller than E_o.

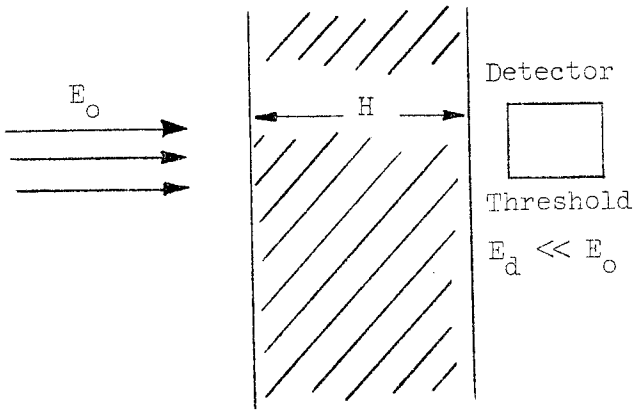

*Our name for this method and our description of it have not been sanctioned by Prof. Moyer, and we apologize if we have said anything which embarrasses him.

In general the response of the detector as the thickness is changed looks like this (semi-log plot):

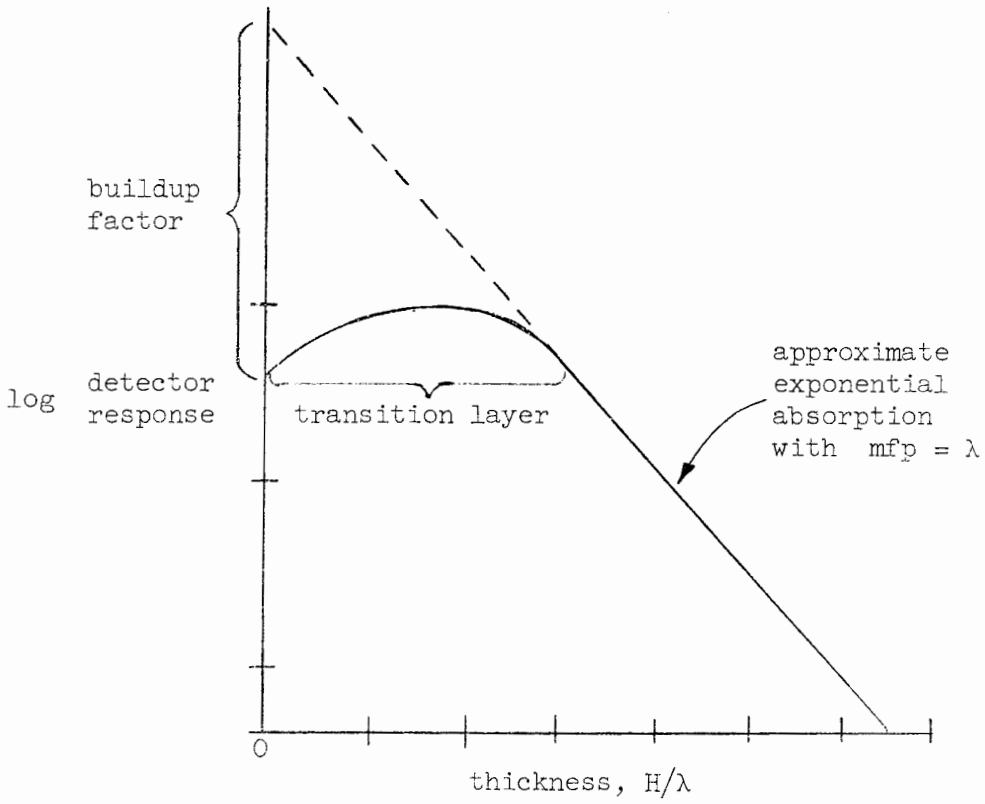

and can be represented at large depths as

$$\text{response} = Be^{-H/\lambda} \qquad (H \gtrsim \text{few } \lambda)$$

In general B is a function of E_o and E_d, and λ is a function of E_o but is independent of E_d. This last observation is very important. The transition region is about 2λ wide. The response curve is simply explained if the cross section as a function of energy decreases or remains constant as the energy increases, as is the case for nuclear particles over a wide energy range. For $H < \lambda$ there are few interactions, and the response is constant. For $H \approx \lambda$ one or two interactions occur, each secondary has enough energy to activate the detector, and the response increases. For $H >$ few λ some of the secondaries have low enough energies so they do not trigger the detector, and the response starts to decrease. For $H \gg$ few λ the primaries, which are the most penetrating, are in

equilibrium with the secondaries, tertiaries, etc., and the observed exponential absorption arises from the interaction of the primaries and the rapid absorption of the secondaries. In the following calculations we treat B approximately and λ more exactly.

The experimental knowledge of λ as a function of incident energy is meager. Many of the measurements were made in the course of designing a needed shield and are not published, and the errors are poorly known. A bias which affects some measurements concerns the apparent attenuation resulting from scattering out of the beam rather than true absorption. There are two approaches: one is to use very bad geometry, with the incident beam very wide and with large angular divergences and assume that as much scatters in as scatters out; the other approach is to use a narrow, parallel, incident beam and use a wide detector so that all of the scattered particles are counted. Most experimental geometries lie in between these two extreme cases by some more or less unknown amount. Table I summarizes some of the measurements.

The Berkeley and Brookhaven measurements all have fairly poor geometry, and the effect of apparent attenuation caused by scattering-out should be f irly small. In the CERN experiments the scattering-out is serious, so these values of λ are lower limits. The particular Princeton calculation we refer to is one dimensional so it is completely free of scattering effects. A calculation done at Oak Ridge will be described extensively in the next section and is not discussed here.

In Table II we list some properties of various materials. Under heavy aggregates we show the chemical composition of the principal constituent. For earth and ordinary concrete, SiO_2 is the main constituent; and for attenuation purposes this is probably a satisfactory approximation except for neutron energies below about 1 Mev where the interactions with hydrogen in the water become important. The last column shows the nuclear mean free path relative to SiO_2. For a single element we have (λ in g-cm^{-2})

$$\frac{1}{\lambda} = \frac{N_o}{A}\sigma \qquad (N_o \text{ is Avogadro's number})$$

With

$$\sigma = \pi R^2 = \pi\left(r_o A^{\frac{1}{3}}\right)^2$$

we have

$$\frac{1}{\lambda} = \frac{N_o \pi r_o^2}{A^{\frac{1}{3}}} \approx \frac{1}{A^{\frac{1}{3}}}$$

For a mixture of elements we have

$$\frac{1}{\lambda} \propto \sum \frac{f_i}{A_i^{\frac{1}{3}}}$$

where f_i is fractional abundance by weight of the i'th element. Earth and concrete always contain some water, but this has not been included in the calculation. The proper conclusion from this simple calculation is probably that the mean free path ($g\text{-}cm^{-2}$) in heavy concrete is about 15% longer than in earth or ordinary concrete, and that it is appreciably longer in iron, copper, or lead.

In order to summarize the data from Table I we divide the measured values of λ by the calculated mean free path relative to SiO_2 and plot the points in Fig. 11 (log-log plot). This procedure is supposed to give λ in $g\text{-}cm^{-2}$ of earth equivalent. We also show the mean free paths derived from the total cross section for neutrons on aluminum (taken as a representative nucleus for comparison). Generally the removal mean free path is about two times larger than the mean free path from the total cross section. In order to get the removal mean free path as a function of neutron energy we follow Moyer and co-workers and use the general shape of the aluminum mean free path to connect the three measured Berkeley points. It is tempting to look for some physics in this relationship, which shows that the effective removal mean free path is about twice the total mean free path over a wide energy range. One might expect that the removal mean free path should roughly equal the inelastic mean free path, since at high energies the backward elastic cross section is small. However, below about 150 Mev the effective removal mean free path in concrete is smaller than the inelastic mean free path in aluminum. Our approach is to use the variation of the aluminum total mean free path to guide the eye in drawing a smooth curve through the three Berkeley points.

TABLE I

Laboratory	Incident Beam		Shield Material		Detector	λ	References
	Particle	Energy	Kind	Density ($g\text{-}cm^{-3}$)		($g\text{-}cm^{-2}$)	
Berkeley	n	90 Mev	Ordinary	2.3	Bi fission	97	26,27,31,32
		270 Mev	Concrete			152	26,32
		4.5 Bev			Chamber	172	27,32
Brookhaven	n	1.5 Bev	Heavy	4.0 - 4.5	Scint.Ctr.& ionization ch.	130^{+16}_{-9}	26
		2.5 Bev	Concrete			169± 32	26
	π	4.5 Bev	Ordinary	2.3	Scintillation counter	118± 8*	28
		69 Bev	Concrete			121± 8*	28
		9 Bev				129± 9*	
	π	4.5 Bev	Iron	7.8	Scintillation counter	155± 11*	28
		6				155± 11*	
		9				179± 12*	
CERN	p	24 Bev	Earth,light & heavy concrete		Emulsion	145± 10	29
	p	20 Bev	Heavy concrete	3.6	Emulsion	115± 15	29
Princeton	n	300 Mev	Heavy concrete	3.85	Monte Carlo calculation	145± 10*	30

*My error estimate

NOTE: All references are given at the end of the report.

TABLE II

Properties of Materials

Material	Approximate Constitution	Density ($g\text{-}cm^{-3}$)	Density ($Lb\text{-}Ft^{-3}$)	Radiation Length ($g\text{-}cm^{-2}$)	λ Relative to SiO_2 ($g\text{-}cm^{-2}$)
Earth	SiO_2	1.8	112	28	1.00
Ordinary Concrete	SiO_2	2.3	144	28	1.00
Heavy Aggregates					
Barite	$BaSO_4$			11	1.38
Chromite	$FeO\ Cr_2O_3$			17	1.20
Geothite	$Fe_2O_3 \cdot H_2O$			18	1.14
Hematite	Fe_2O_3			17	1.20
Ilmenite	$FeO\ TiO_2$			18	1.18
Limonite	$2Fe_2O_3 \cdot 3H_2O$			18	1.11
Magnetite	Fe_3O_4			17	1.21
Iron	Fe	7.8	487	13.9	1.41
Copper	Cu	8.9	550	13.0	1.46
Lead	Pb	11.3	705	5.8	2.27

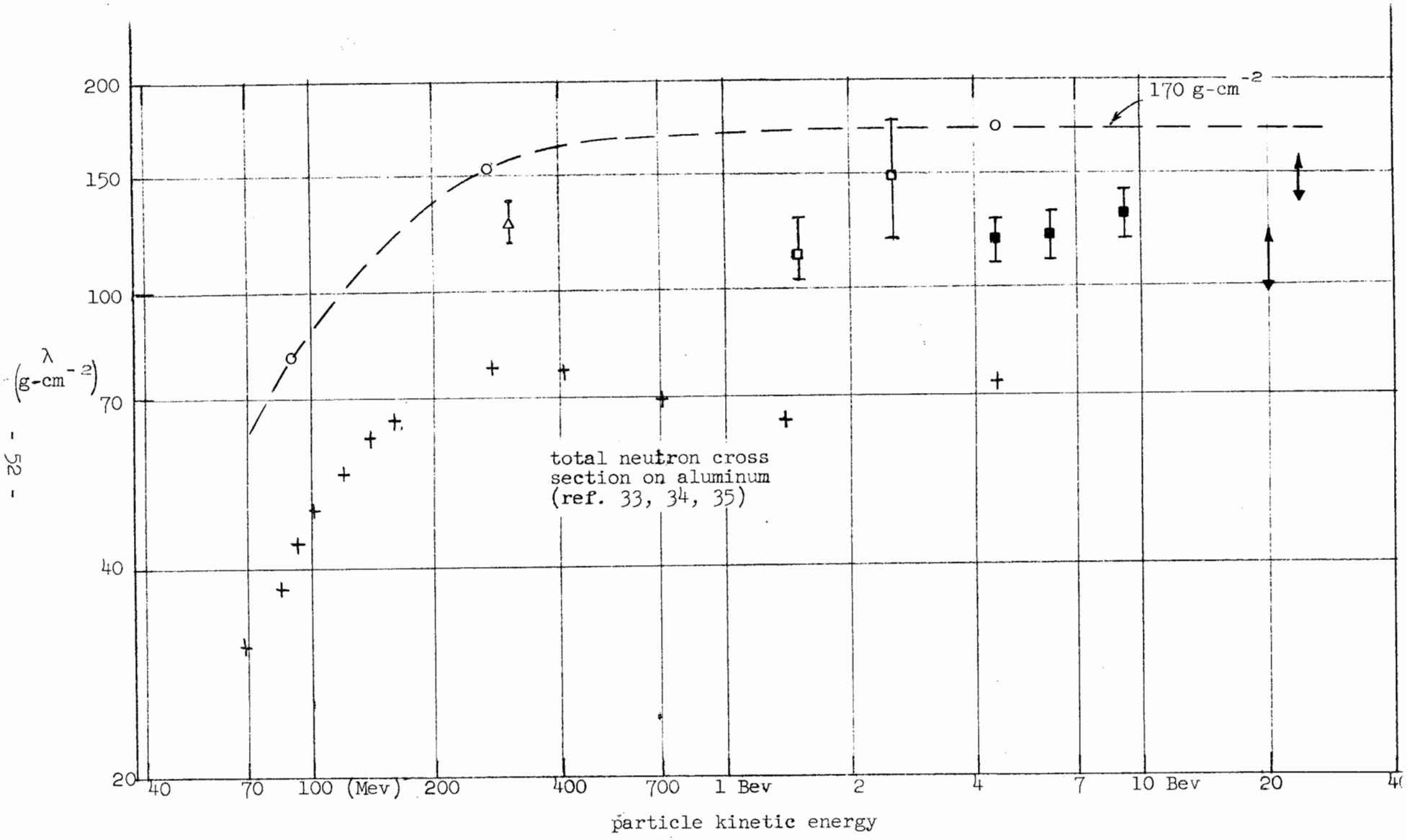

FIG. 11--Removal mean-free paths (earth equivalent).

The resulting curve (shown dashed in Fig. 11) is what we use in the subsequent calculations for $\lambda(T)$; over much of the range of interest λ is almost the same as its high-energy value of 170 g-cm^{-2}. It may appear that we are being unnecessarily conservative in taking the largest values of λ which have been measured, but the specter which haunts us in this connection is the unknown contribution to the attenuation from scattering out. For use in a one-dimensional calculation, λ should be obtained by measuring the total detector response throughout the whole transverse plane at a particular depth, and it is not clear to what extent this was done in the various experiments. The differences between incident neutrons and protons or pions should be small at high energies after a few mean free paths. At lower energies ionization losses in the incident beam could make important differences, especially for protons.

In the following we use $\lambda(T_n)$ so determined in a one-dimensional absorption calculation. An important result is the decrease in λ below about 300 Mev, which means that the lower energy particles are very strongly attenuated. (We note that Moyer has approximated this behavior by taking λ constant at the high-energy value of 170 g-cm^{-2} down to 150 Mev and neglecting all neutrons below this energy--in effect making the approximation $\lambda = 170$ g-cm^{-2} above 150 Mev and $\lambda = 0$ below 150 Mev.) Since the thick-target bremsstrahlung spectrum is rich in low-energy photons, the lower energy neutrons are especially abundant. The lack of high-energy photons and the strong attenuation of the low-energy neutrons have the result that the most troublesome neutron energy is around 300 Mev.

Next we consider the geometry and define a number of symbols. We approximate our conditions by a cylindrical shield of thickness H surrounding a uniform line source, and we wish to calculate the radiation level at the surface as a function of H.

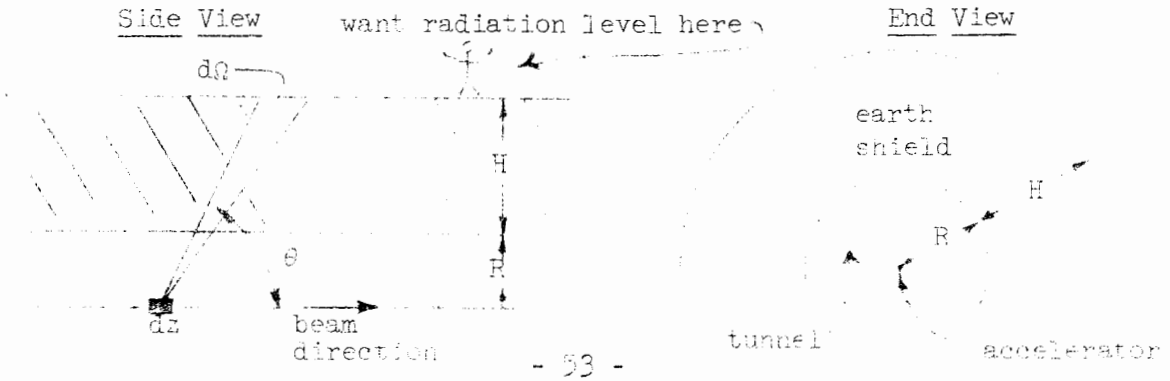

When one electron of energy E_o hits the machine, the yield of neutrons (calculated in Section IV) is a function of E_o, T and θ which we call

$$\frac{d^2n}{dTd\Omega}$$

For each neutron incident on the inside of the shield the number of particles emerging is

$$B(T) \exp - H/[\lambda(T) \sin \theta]$$

where B is the buildup factor, and λ is the removal mean free path, each a function of the neutron energy. To find the flux at the surface of the shield we have a choice of whether the unit of area through which we count the particles is to be parallel to the surface of the shield or perpendicular to the direction of motion of the particles. We choose the one perpendicular to the direction of motion because the radiation is quite penetrating. At any rate, the choice is of small consequence because most of the radiation comes out (in the one-dimensional approximation) at about 90^o where there is slight difference between the two fluxes. This means that to find the total yield through the shield it is a good approximation to multiply the flux at any point by the total outside area of the shield. If dI/dz is the rate at which electrons of energy E_o hit the accelerator at a distance z down the machine (number of beam electrons per cm-sec), the flux (differential in neutron energy) at the surface of the shield is

$$\frac{d\Phi}{dT} = \int_{z=0}^{L} dz E_o \frac{dI}{dz} \frac{1}{\epsilon} \frac{d^2n}{d\Omega dT} B(T) \exp[- H/(\lambda \sin \theta)] \left| \frac{\sin \theta}{H + R} \right|^2$$

where L is the length of the machine. In our calculations of $d^2n/dTd\Omega$ we use an incident electron energy of $\epsilon = 45$ Bev. We change from an integration over z to an integration over θ for a fixed point P

$$\tan \theta = \frac{R + H}{z}$$

$$dz = - (R + H) \frac{d\theta}{\sin^2 \theta}$$

We have

$$\frac{d\varphi}{dT} = \int_{-\pi/2}^{\pi/2} d\theta \, \frac{dI}{dz} \frac{E_o(z)}{\epsilon} \left(\frac{d^2n}{dT d\Omega} \right) B(T) \exp[-H/(\lambda \sin\theta)] \left(\frac{1}{H + R} \right)$$

We take the product $E_o(z)(dI/dz)$ to be constant and equal to $f(I_f E_f)/L$, where $I_f E_f$ is the final beam power of the machine (2.4 Mw = 60 μa at 40 Bev), f is the total fraction of the beam power absorbed in the walls of the machine (f = 3%), and L is the total length of the machine ($L = 10^4$ ft).

$$\frac{d\varphi}{dT} = \frac{f(I_f E_f)}{L} \frac{B(T)}{R + H} \int_{-\pi/2}^{\pi/2} d\theta \, \frac{1}{\epsilon} \frac{d^2n}{dT d\Omega} \exp\{-H/[\lambda(T) \sin\theta]\}$$

To get the radiation level (mrem/hr) we multiply the flux by F(T), the number of rem/n-cm^{-2} (taking proper account of the difference in time units) and integrate over the neutron energy:

$$D(\text{mrem/hr}) = \int_0^\infty F(T) \frac{d\varphi}{dT} dT$$

$$= f \frac{I_f E_f}{L} \frac{1}{R + H} \int_{-\pi/2}^{\pi/2} d\theta \int_0^\infty dT \, B(T)F(T) \left\{ \frac{1}{\epsilon} \frac{d^2n}{dT d\Omega} \exp\{-H/[\lambda(T)\sin\theta]\} \right\}$$

An approximation made by Moyer is to extract the product B(T)F(T) from under the integral and to replace it by a constant $< BF >$. This approximation is made plausible by consideration of the radiation which one would expect to be in equilibrium with a high-energy particle.[38] This radiation consists mostly of low-energy, short-range nucleons with some electrons and gammas arising mainly from π^o decay. The composition of this radiation would be expected to change somewhat as the energy of the primary neutron changes, and there is some effective factor F'(T)(rem/n-cm^{-2}) which would convert the neutron flux to a biological dose. This factor

[38] B. J. Moyer in "Conference on Shielding of High Energy Accelerators" (Ref. 15). See also S. J. Lindenbaum, Ann. Rev. Nuclear Sci. 11, 229 (1961).

is primed to differentiate it from the $F(T)$ defined in Section II, for which there are calculated values. F' is an effective value of F averaged over the actual spectrum of secondaries, tertiaries, etc. which accompany each surviving neutron. The biological dose, D (mrem/hr), is

$$D = \int_0^\infty F'(T) \frac{d\varphi}{dT} dT$$

$$D = f \frac{I_f E_f}{L} \frac{1}{R + H} \int_{-\pi/2}^{\pi/2} d\theta \int_0^\infty dT\, F'(T) B(T) \frac{1}{\epsilon} \frac{d^2 n}{dT d\Omega} \exp - H/[\lambda(T) \sin \theta]$$

In line with the simplifications which have already been made, Moyer takes the product $F'(T)B(T)$ as a constant $< F'B >$ equal to 1.25×10^{-7} rem/n-cm^{-2}, which he believes to be conservative (i.e., larger than the true but unknown value).[39] From Fig. 1 in Section II we see that this is the value which Neary calculated for 150 Mev neutrons accompanied by their equilibrium radiation. This seems like reasonable agreement. In the following we use $< F'B > = 1.25 \times 10^{-7}$ rem/n-cm^{-2}. The final formula for the radiation level is

$$D = 3.6 \times 10^6 \, f \frac{I_f E_f}{L} \frac{< F'B >}{R + H} \int_{-\pi/2}^{\pi/2} d\theta \int_0^\infty dT \frac{1}{\epsilon} \frac{d^2 n}{dT d\Omega} \exp - H/[\lambda(T) \sin \theta]$$

---

[39] B. J. Moyer, "Evaluation of Shielding Required for the Improved Bevatron," UCRL-9769, Lawrence Radiation Laboratory, Berkeley, California, June 1961.

where

D is the radiation level (mrem/hr).

3.6×10^6 is the numerical factor which changes rem/sec to mrem/hr.

$I_f E_f$ is the power in the beam as it emerges from the machine (3.75×10^{14} $e^-/s \times 40$ Bev = 60 μa $\times 40$ Bev = 2.4 Mw).

f is the fraction of the beam power absorbed in the machine (3%).

L is the length of the machine (3.05×10^5 cm = 10^4 ft).

$< F'B >$ is the effective biological effect per neutron (1.25×10^{-7} rem/n-cm^{-2}).

R is the radius of the tunnel which contains the machine (152.5 cm = 5 ft).

H is the thickness of the cylindrical earth shield (ρ = 1.8 g-cm^{-3}) which surrounds the machine (H in centimeters).

θ is the angle of emission of the neutrons with respect to the beam direction (in radians).

T is the energy of the neutrons emitted from the machine (in Mev).

$\frac{d^2n}{dTd\Omega}$ is the neutron yield per absorbed beam electron of energy ϵ (neut/Mev-sr).

ϵ = 45 Bev.

$\lambda(T)$ is the removal mean free path of neutrons of energy T; at large energies λ is approximately constant at 170 g-cm^{-2} = 94.5 cm = 3.10 ft.

So we have

$$D = \frac{3.6 \times 10^6 \times 3 \times 10^{-2} \times 3.75 \times 10^{14} \times 40 \times 1.25 \times 10^{-7}}{30.5 \times 10^4 \times 45}$$

$$\cdot \frac{1}{152.5 + H} \int_{-\pi/2}^{\pi/2} d\theta \int_0^\infty dT \left[\frac{d^2n}{dTd\Omega}\right] \exp - H/[\lambda(T) \sin \theta]$$

$$D(\text{mrem/hr}) = \frac{1.47 \times 10^7}{152.5 + H} \int_{-\pi/2}^{\pi/2} d\theta \int_0^\infty dT \, \frac{d^2n}{dTd\Omega} \exp - H/[\lambda(T) \sin \theta]$$

The quantity $d^2n/dTd\Omega$ is calculated for neutrons as described in the previous Section.*

Fig. 12 shows the neutron yield $d^2n/dTd\Omega$ for $\theta = 30^\circ$, which is near the angle of peak neutron flux. Fig. 13 shows the product $(d^2n/dTd\Omega)\exp[-H/\lambda(T)\sin\theta]$ for $H = 26.9$ ft, which is near the 25-foot thickness we eventually choose for the shield. Fig. 14 shows the integral

$$\int_0^\infty dT \left\{\frac{d^2n}{dTd\Omega}\right\} \exp\left\{-H/[\lambda(T)\sin\theta]\right\}$$

for $H = 26.9$ ft and for various values of θ. Fig. 15 shows the radiation level as a function of shield thickness. For reference the dashed line shows our radiation worker tolerance, 0.75 mrem/hr.

B. Comparison of the Princeton Monte Carlo Calculation and the Method of Moyer

One of the calculations of the Princeton group is the penetration of 300 Mev neutrons in heavy concrete using a numerical Monte Carlo procedure.[30] They give the total number of particles, mostly neutrons, with energies greater than about 5 Mev as a function of depth, and the energy spectrum at a depth of 170 inches (about 30 ft earth equivalent). There are statistical errors inherent in the Monte Carlo procedure, as well as errors arising from the input data and various approximations. The overall error is not known explicitly.

The number of particles at depth x can be represented by

$$N(x) = Be^{-x/\lambda}$$

$$B = 5.2$$

$$\lambda = 145 \text{ g-cm}^{-2} \text{ heavy concrete}$$

The energy spectrum is

$$\frac{dN}{dT} \approx 1/T^n \quad (5 \text{ Mev} \approx T_1 < T < T_2 \approx 300 \text{ Mev})$$

$$n \approx 0.5 \text{ to } 0.7$$

---

*I am indebted to Charles H. Moore for the machine computation of this quantity and the integrals.

[30] C. J. Tsao, "Monte Carlo Shield Calculations for 3 Bev Protons," Princeton-Pennsylvania Accelerator, Princeton, New Jersey, ca 1959. (Unpublished.) I am indebted to G. K. O'Neill for sending me a copy of this report.

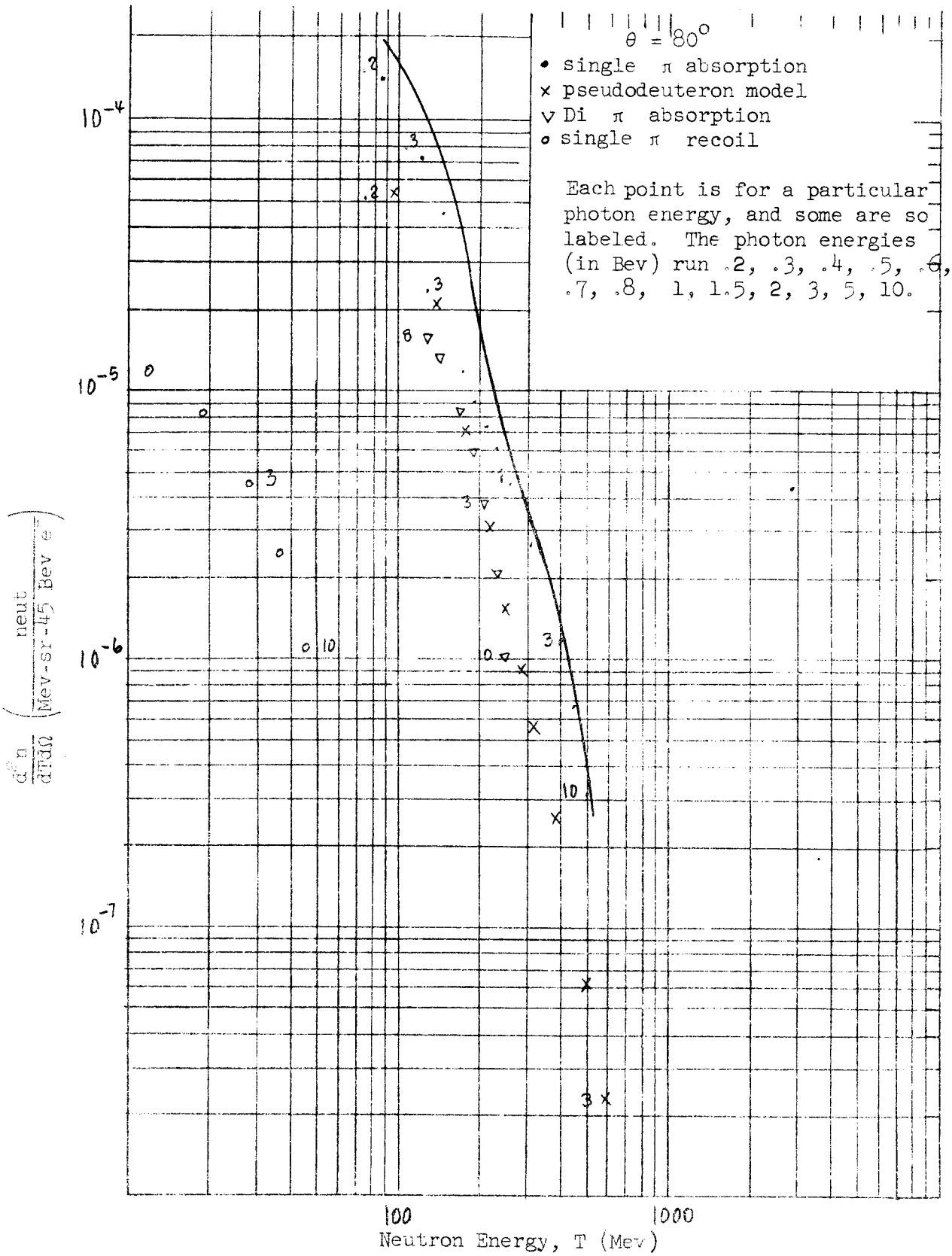

FIG. 12--Neutron yield vs neutron energy

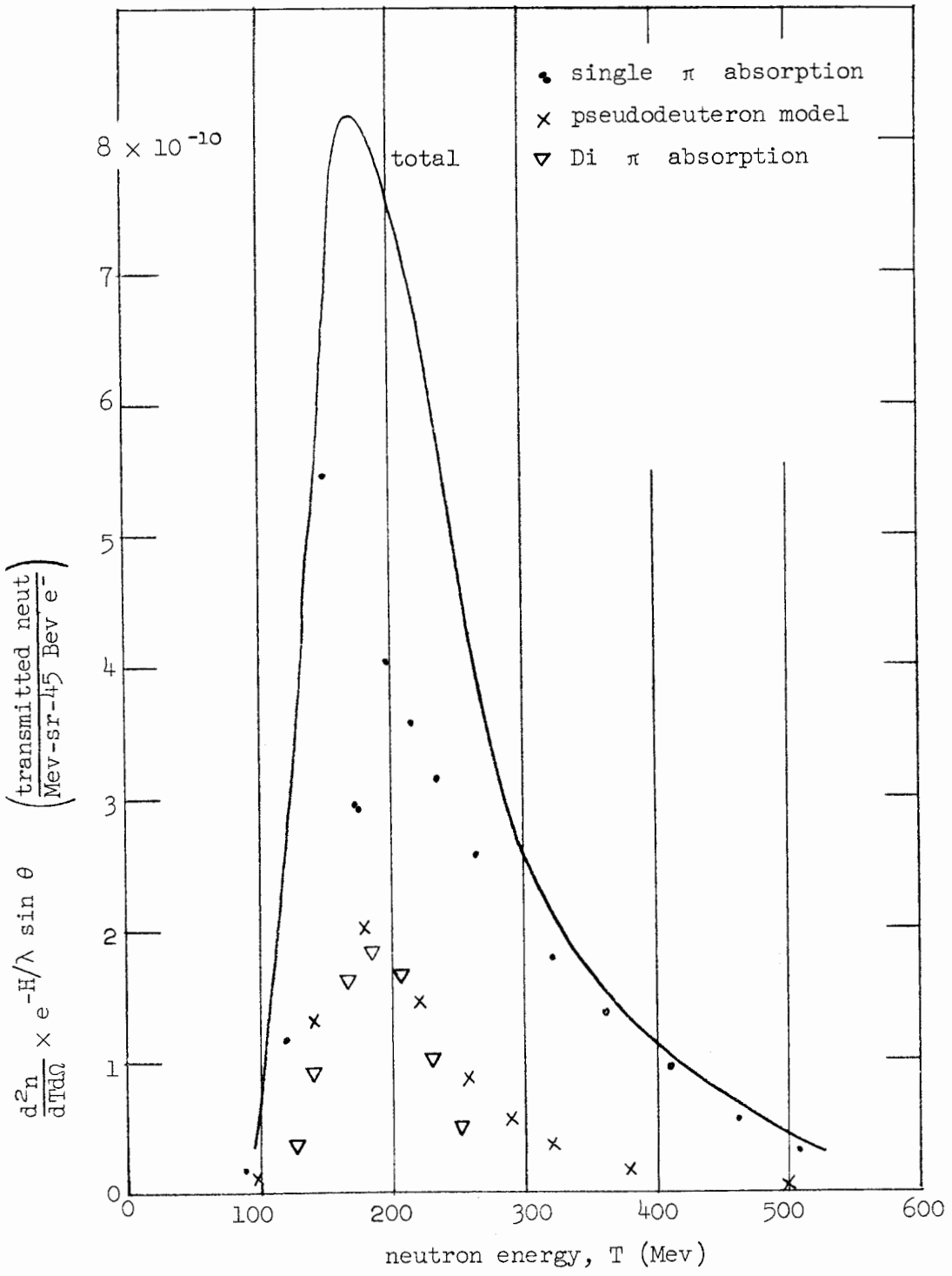

FIG. 13--Transmitted neutron spectrum vs neutron energy at $\theta = 80^{\circ}$, H = 26.9 ft.

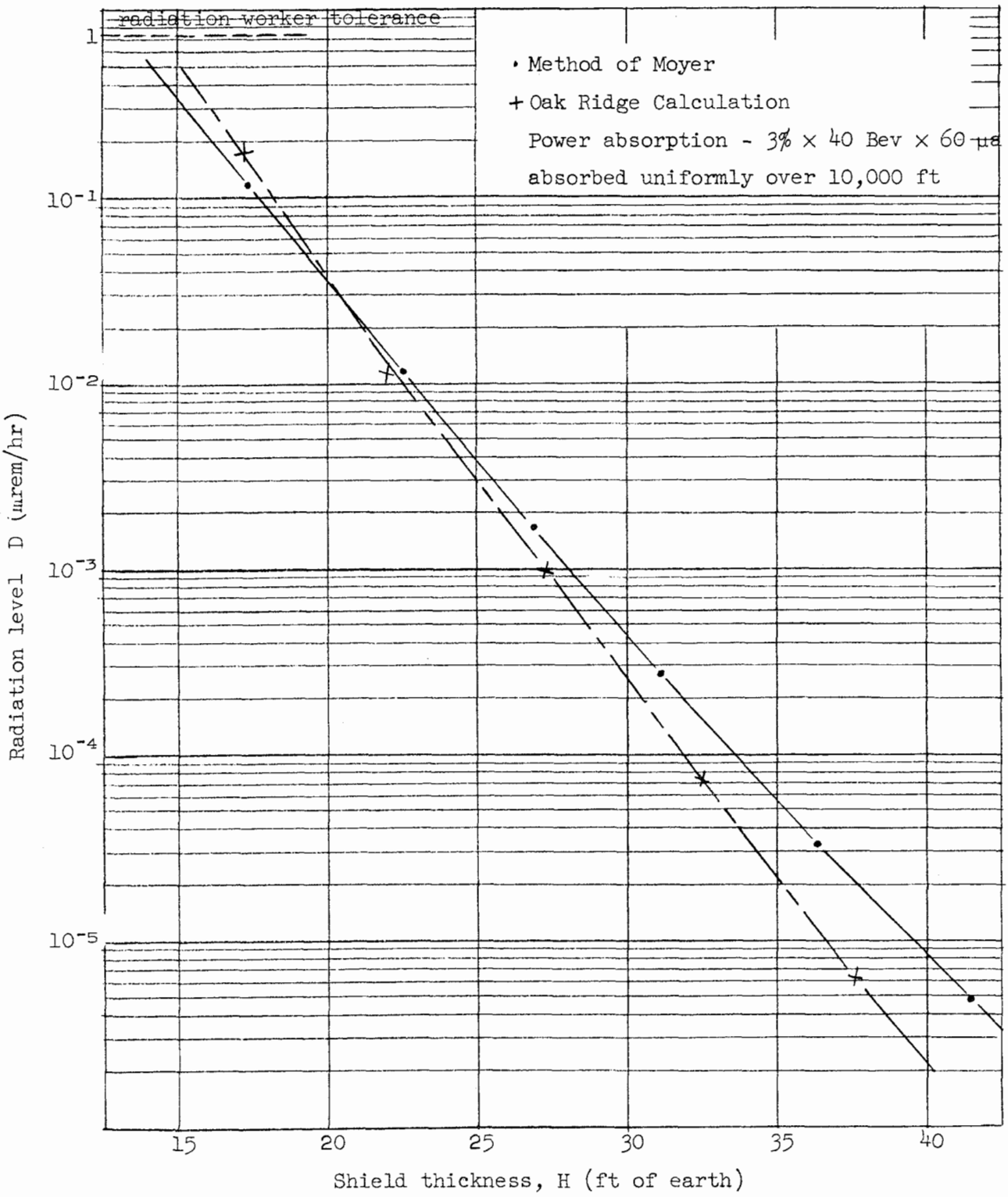

FIG. 15--Radiation level at the surface of the shield vs shield thickness.

H = 26.9 ft
Limits of integration are 100 Mev and T corresponding to a gamma ray energy of 10 Bev.

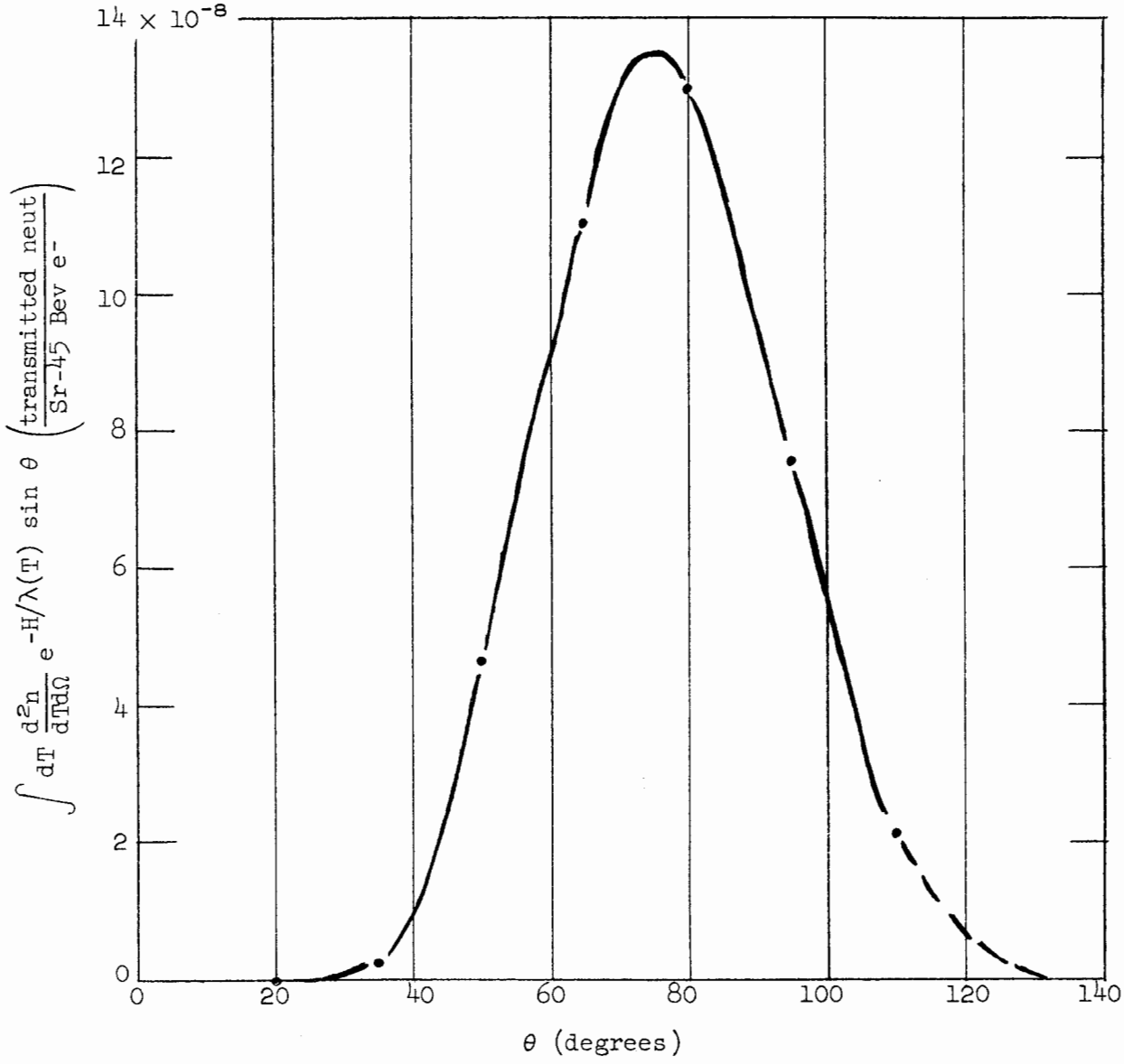

FIG. 14--Total neutron transmission vs angle.

optical model with an absorption probability of about 1/2, it would seem reasonable to suppose that the effective incident flux used in the Oak Ridge calculations is about twice as great as we used in Section V.A in applying Moyer's method. The second piece of input information concerns the cross sections and energy distributions used in the transport equations, and the third input concerns calculation of the dose. We discuss these two aspects further.

In the cascade the general process consists of a particle of kind i with energy E_o interacting with a nucleus of kind j and creating particles of kind k with energies E. The process is specified by the interaction cross section, the multiplicity of secondaries of each kind (n, p, π^+) and their energy distributions. Since this is a one-dimensional calculation, the angular distribution of the secondaries does not appear; they all go straight ahead. The Oak Ridge calculation makes the approximation that earth is aluminum. The neglect of any hydrogen seems to be the most serious shortcoming, but it is only important for neutrons with energies less than a few Mev. Since the calculation follows the cascade particles down only to about 30 Mev, this is all right. Figures 16, 17 and 18 show the numerical values of the input data used. Figure 16 shows the interaction (inelastic only) mean free paths for the various kinds of incident particles as a function of energy. The neutron data is measured; the proton data is measured and deduced from Monte Carlo calculation; pions are assumed to be the same as protons. Figure 17 shows multiplicities, ν, of the various kinds of secondary particles as a function of the energy of the incident particles. They assume that $\nu_n = \nu_p$, and that all of the multiplicities are independent of the kind of incident particle. The multiplicity data are derived from stars in nuclear emulsions, and no corrections are made for any differences in atomic weight between emulsion and aluminum. Figure 18 shows the energy distributions of the secondary particles. These are shown independent of incident energy, but they go to zero for energies greater than allowed by energy conservation. These are also derived from cosmic ray and Monte Carlo data.

The dose in rads at a particular thickness of shield is calculated by letting the energy spectra of protons, neutrons, charged pions and muons interact with water. For the transverse shielding the secondary neutrons predominate, and we only discuss the energy deposited by them.

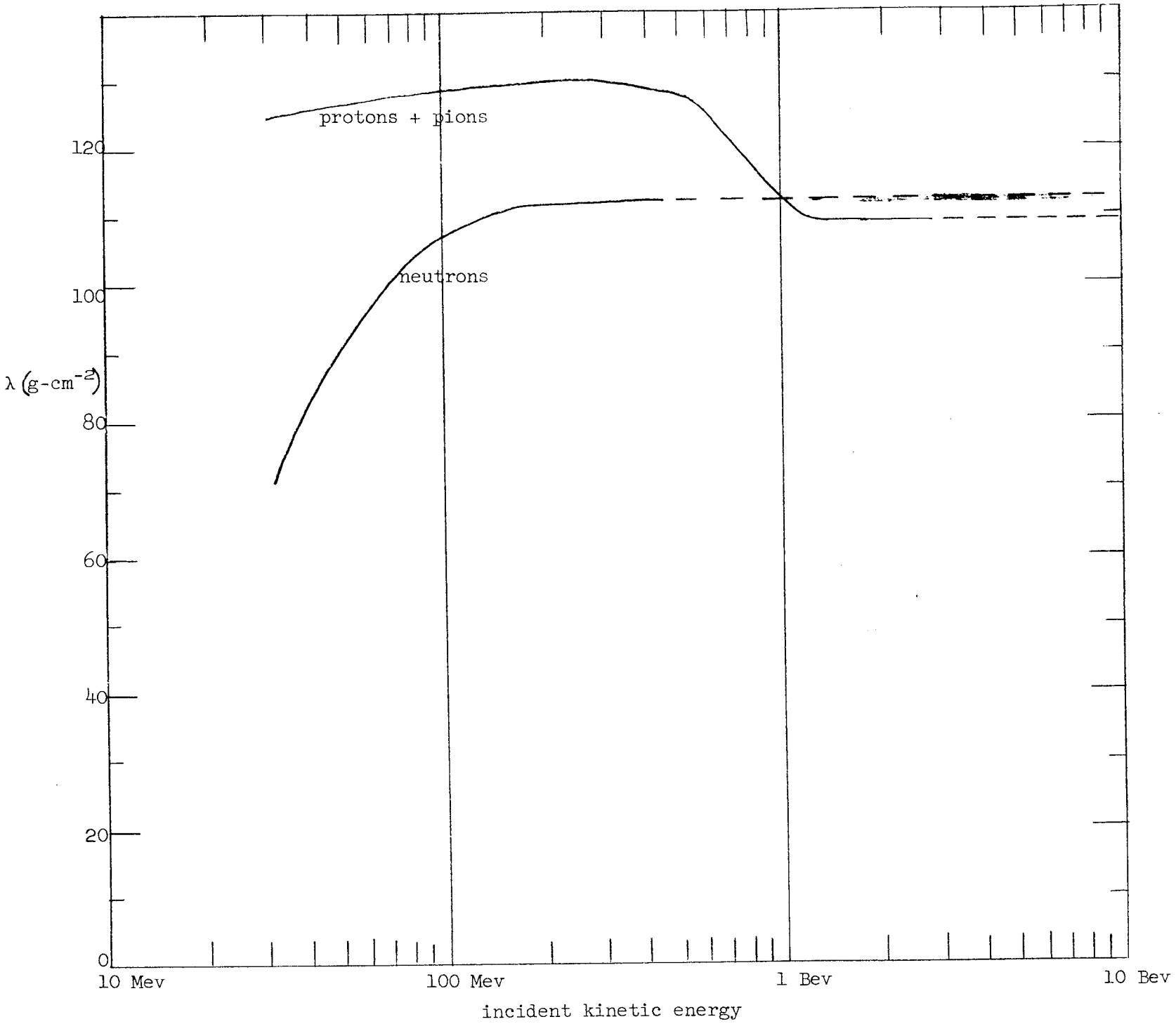

FIG. 16--Inelastic interaction mean free path vs energy.

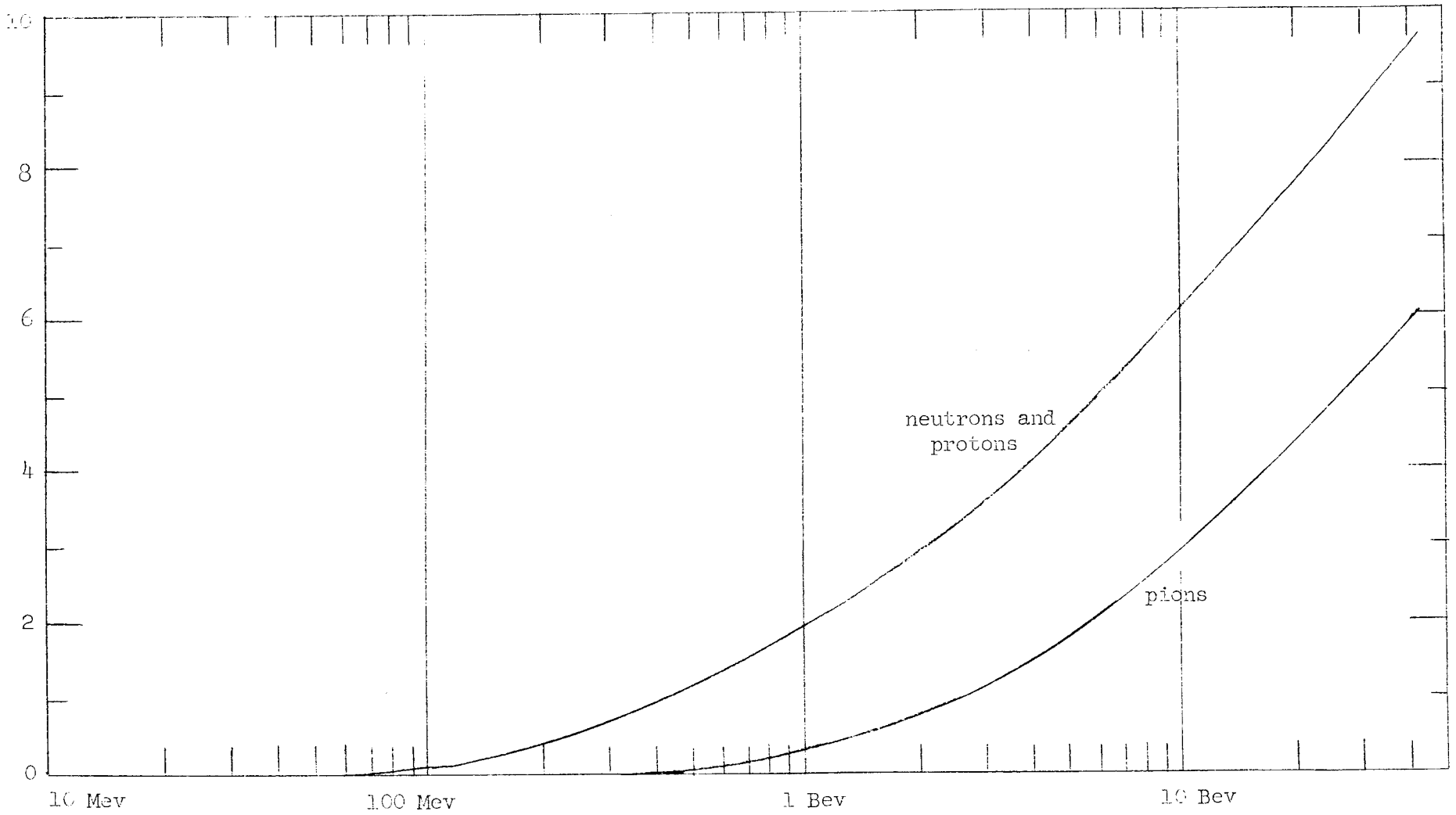

FIG. 17--Secondary multiplicity vs primary energy (independent of type of primary particle).

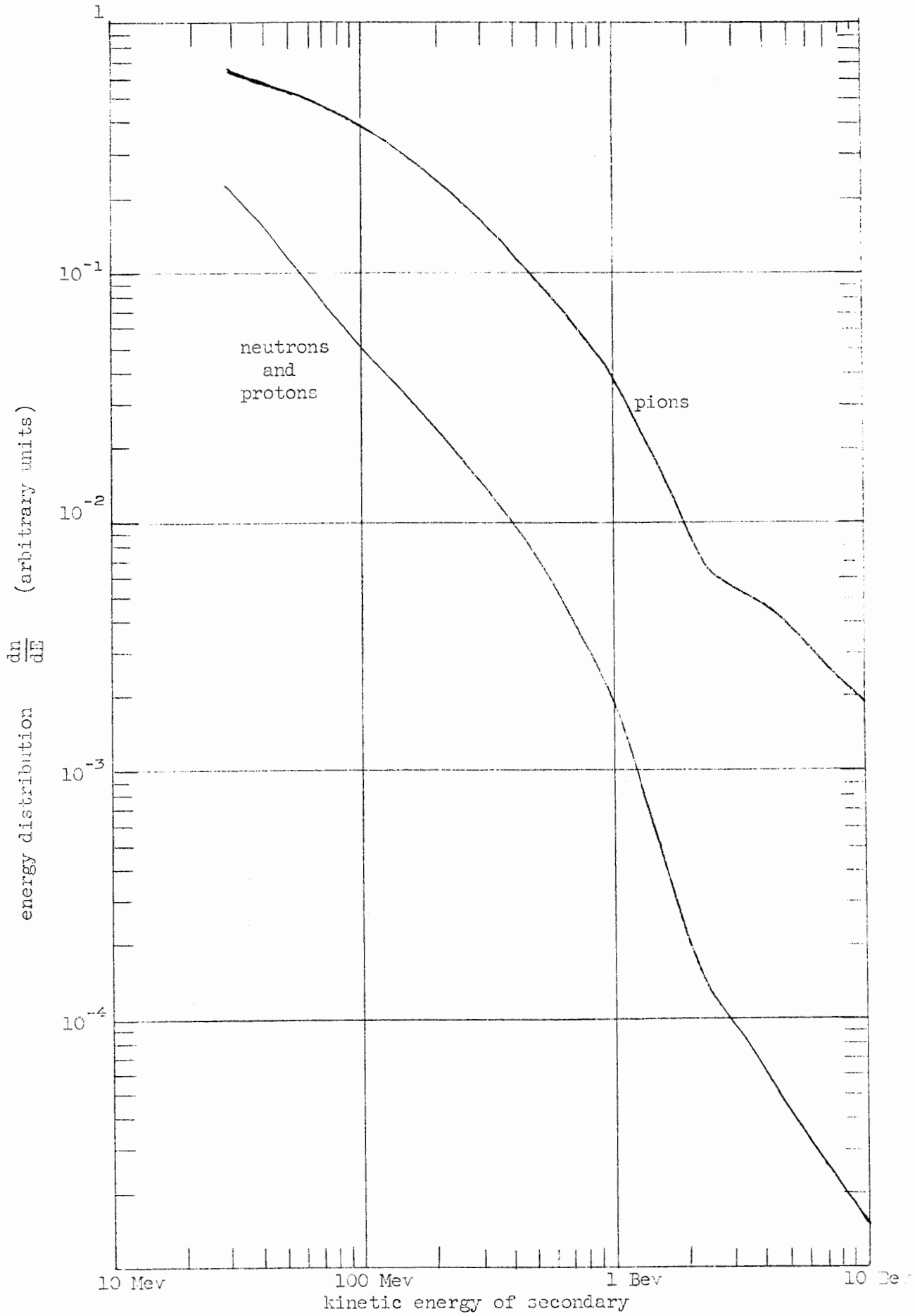

FIG. 18--Secondary energy distribution vs secondary energy.

The neutron spectrum is divided into three energy ranges. Above some cut-off energy Γ the neutron spectrum is given by the Oak Ridge calculation; the neutrons interact in water by elastic scattering from hydrogen or by non-elastic interaction with oxygen; at each interaction half of the neutron energy is absorbed locally. Between Γ and 10 Mev the neutron spectrum varies as $1/E$ (a variation suggested by the cosmic-ray neutron spectrum in the atmosphere) and is joined smoothly to the calculation at Γ; again half of the neutron energy is absorbed locally at the site of an interaction. From 0 to 10 Mev the $1/E$ spectrum is used, but a different method of calculating the absorbed energy as a function of neutron energy is used and is not described explicitly.[41]

For Γ = 109 Mev about 80% of the absorbed dose (rad) comes from neutrons with energies less than Γ. It is not clear how sensitive the dose calculation is to the choice of Γ, or how much of the dose comes from interactions in hydrogen and how much from interactions in oxygen. It seems possible that the assumption that half of the energy is absorbed locally is generous and that perhaps less than this is actually absorbed. However, the actual situation is complicated.

The result of the Oak Ridge calculation is the dose in rad as a function of shield thickness and angle for one 45-Bev electron absorbed in the machine. We use the same geometrical considerations and beam loss as we used for the Moyer calculation, and we arbitrarily use an RBE of 3 to convert the dose in rad to a dose in rem. As before the radiation level is a maximum around 80°. Figure 15 shows the radiation level at the surface of the shield as a function of shield thickness. This calculation is about the same as the Moyer calculation. It would be comforting to think that the differences between them are indicative of the errors inherent in each, but such an inference is probably unwarranted.

---

[41] In the Oak Ridge Calculation the reference for this subsidiary method is to C. D. Zerby "A Monte Carlo Calculation of Air-Scattered Neutrons," ORNL-2227, Oak Ridge National Laboratory, Oak Ridge, Tennessee, 1957.

D. Effects of Angular Spread in the Nuclear Cascade

In the calculations so far the geometry is very bad, and so we might expect the scattering-in to cancel the scattering-out. The source of penetrating particles in the machine is long, and their angular distribution is broad. However, the most serious effect of spreading in the nuclear cascade itself occurs because particles that scatter to greater angles see a thinner shield and experience less nuclear absorption.

The amount of spreading that actually occurs in a nuclear cascade is not especially well known. An early version of the Princeton Monte Carlo calculation indicated that the root-mean-square angle between the shower particles and the beam direction was around 15° at depths of 2 to 3 mean free paths.[43] In a shielding experiment at the Cosmotron with 3-Bev protons the lateral width of the cascade was ± (1 to 2) ft at a depth of 13 feet in heavy concrete.[44] This corresponds to an angle from the point of incidence of the beam ± $(5 \text{ to } 10)^{\circ}$.

We estimate the effect of spreading in the cascade by changing the angular distribution of the neutrons leaving the machine by $(10 \text{ to } 15)^{\circ}$. Since the significant angles for the neutrons are around 90°, changing these by 15° does not change the effective shield thickness very much. For example if an angle is changed from 65° to 80° the effective thickness increases by $\sin 80^{\circ}/\sin 65^{\circ} = 1.09$. If we take 10^{-6} as the effective attenuation in this region, the exponent increases by $6(.09) = .54$, and the transmission decreases by about a factor of 3. This probably overestimates the average effect of spreading on the radiation level at the surface.

Dedrick has done a calculation which is an extreme case of spreading of the cascade.[45] He makes the assumption that, no matter what angle θ

---

[43] G. K. O'Neill in "Conference on Shielding of High-Energy Accelerators" New York, April, 1957, TID-7545, Technical Information Service Extension, Oak Ridge, Tennessee.

[44] L. Beebe, J. Cumming, W. Moore, and C. Swartz, "Shielding Measurements" Cosmotron Internal Report, 10/1/56, Brookhaven National Laboratory, Upton, New York.

[45] K. G. Dedrick and H. H. Clark, "Elementary Calculation of the Transverse Shielding," M-296, Stanford Linear Accelerator Center, Stanford, California, February 1962.

a neutron has when it leaves the machine, as soon as it hits the shield it turns and penetrates into the shield with $\theta = 90^{\circ}$. This is indicated in the sketch.

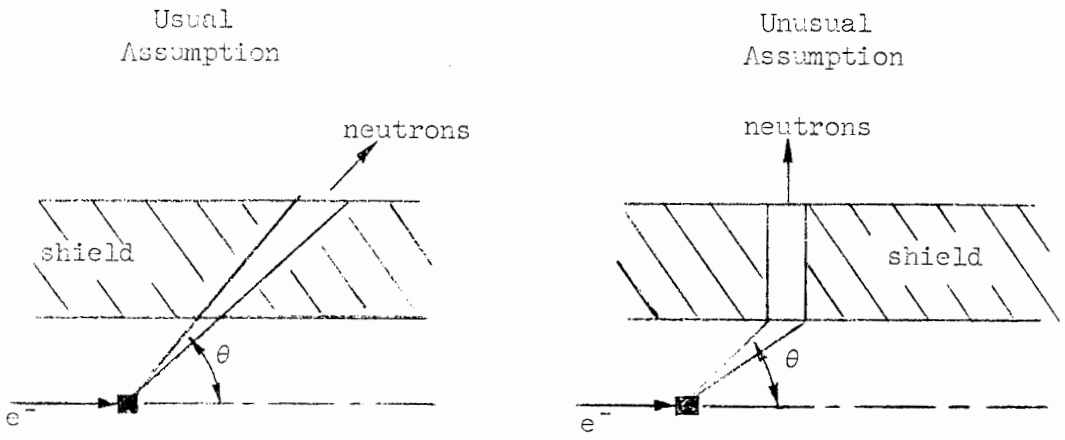

For a shield thickness of 25 ft of earth about 6 times more neutrons are transmitted under the extreme assumption than under the usual assumption.

In view of these considerations, in our final selection of the shield thickness we increase the radiation levels in Fig. 15 by a factor of 2 to take account of the spreading.

E. Hazard from μ Mesons

Muray has shown,[36] using pion yields calculated by Dedrick from a statistical model,[37] that μ mesons are not a problem for the SLAC transverse shielding. (However, they are a serious problem for the straight-ahead shielding, which we do not consider in this report.) We now give the results of a calculation based on the pion yields calculated from Section IV and also repeat approximately part of Muray's calculation.

---

[36] J. J. Muray, "Muon Yields from Pion Decay and Electromagnetic Pair Production," M-267, Stanford Linear Accelerator Center, Stanford, California, May 1961.

[37] K. G. Dedrick, "Calculation of Pion Photoproduction from Electron Accelerators According to the Statistical Model," M-228, and "More Calculation of Photopion Yields," M-229, Stanford Linear Accelerator Center, Stanford, California, October 1960.

In the Oak Ridge calculation almost all of the dose arises from the neutrons; the dose from the muons is less than 10^{-4} of the neutron dose. This is mainly because their calculations were carried out at large angles ($\approx 80^{\circ}$) where the neutron levels were expected to be largest, and not at small angles ($\approx 10^{\circ}$) where the muon level is greatest.

The geometry appears in the following sketch.

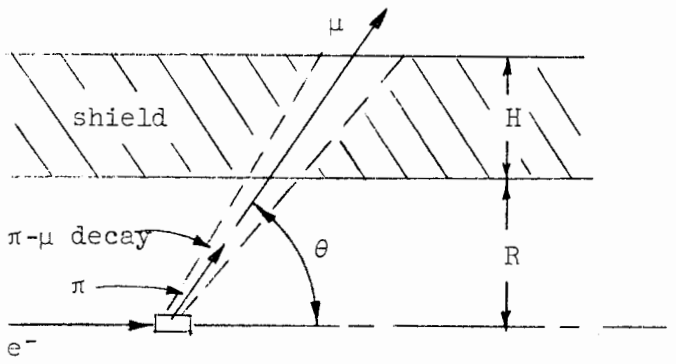

We use the pion spectra calculated in Section IV. The mean free path for decay of a pion of momentum p is $c\tau(p/mc)$ where τ is the mean lifetime, and m is the mass of the pion. At an angle θ the probability that a π decays before entering the shield is

$$1 - \exp\left[- \frac{R}{\sin\theta \; c\tau} \left(\frac{mc}{p}\right)\right] \approx \frac{R}{c\tau \sin\theta} \frac{mc}{p}$$

We make the generous assumption that the kinetic energy of the resulting μ is the same as the kinetic energy of the π, and we assume that $\theta_{\mu} = \theta_{\pi}$. If the residual range of the μ is greater than $H/\sin\theta$, the μ penetrates the shield and contributes to the radiation hazard outside the shield. If not, the μ is absorbed and we forget it. We neglect π decay inside the shielding, but we overestimate the μ energy, because we take $T_{\mu} = T_{\pi}$ whereas on the average $< E_{\mu} > = 0.79 < E_{\pi} >$.

We write down equations similar to those used for the neutron penetration

We compare the doses calculated by the method of Moyer and by the Princeton group. We average the product $B(T)F(T)$ over the Princeton spectrum using the approximation from Fig. 1 in Section II, namely, $F(T) = aT^b$ with $b \approx 0.3$ to 0.5.

$$< BF > = \frac{\int_{E_1}^{E_2} BF \frac{dN}{dT} dT}{\int_{E_1}^{E_2} \frac{dN}{dT} dT} = Ba \frac{\int T^{-n+b} dT}{\int T^{-n} dT}$$

$$= BaT_2^b \left(\frac{-n+1}{-n+b+1} \right) \left[\frac{1 - \left(T_1/T_2\right)^{-n+b+1}}{1 - \left(T_1/T_2\right)^{-n+1}} \right]$$

We evaluate this for $B = 5.2$, $a = 1.93 \times 10^{-8}$, $b = 0.39$, $n = 0.60$, $T_1 = 5$ Mev, $T_2 = 300$ Mev:

$$< BF >_P = 5.5 \times 10^{-7} \text{ rem/n-cm}^{-2}$$

The value used by Moyer, including a 25% contribution from photons, is

$$< BF >_M = 1.25 \times 10^{-7} \text{ rem/n-cm}^{-2}$$

The Princeton calculation does not include photons, so in the comparison we use

$$< BF >_M = 1 \times 10^{-7} \text{ rem/n-cm}^{-2}$$

We calculate the dose at a shield thickness of 25 ft of earth (at $\rho = 1.8$ this is 1370 g-cm^{-2}) and summarize the results in the following table.

	λ (g-cm^{-2} earth equivalent)	$< BF >$ (rem/n-cm^{-2})	$< BF > e^{-x/\lambda}$ (rem/n-cm^{-2})
Princeton	126	5.5×10^{-7}	0.94×10^{-11}
Moyer	155	1.0×10^{-7}	1.40×10^{-11}

Although the factors $< BF >$ and the values of λ are rather different, they tend to cancel in the dose values, which differ by about 50% at a thickness of 25 ft. A 5% change in either of the values of λ would cause about a 50% change in the corresponding dose value. This comparison does not prove anything, but it shows that two completely different methods of calculation give dose values which are rather similar.

Most of the results of the Princeton calculation are concerned with their particular conditions. Since their primary beam consists of protons and ours consists of electrons, the spectra of particles incident on the shield are quite different; therefore, it is not possible to apply most of the Princeton results directly to our shielding calculations.

C. Oak Ridge Calculation

This calculation involves the numerical solution (on an IBM 7090) of three coupled integro-differential equations, one each for neutrons, protons, and charged pions, which describe the interaction and regeneration of particles in a nuclear cascade.[40] The problem was set up in complete analogy with the electromagnetic cascade, in which there are only two transport equations, one for photons and one for electrons and positrons. The Oak Ridge calculation takes account of ionization loss of the protons and charged pions; it neglects the effects of neutral pions because the decay γ rays are absorbed quickly relative to the rate of absorption of the nuclear particles; it includes μ mesons from π-μ decay, but these are negligible for the present purpose (see Section V.E) and we do not discuss them here; pions are removed by decay as well as by nuclear interaction.

There are three separate pieces of physical input information. The first is the energy distribution of the particles leaving the machine which impinge on the inside surface of the shield. The Oak Ridge calculation uses the spectra calculated here in Section IV. They include the neutrons and the pions; the calculation was not done separately for the neutrons and pions, so the relative contributions are not known. However, since most of the neutrons arise from pion reabsorption via the

---

[40] R. G. Alsmiller, F. S. Alsmiller, J. E. Murphy, "Transverse Shielding for a 45 Gev Electron Accelerator," ORNL-3289, Oak Ridge National Laboratory Oak Ridge, Tennessee, 1962.

in the method of Moyer. The μ spectrum is

$$\frac{d^2n_\pi}{dTd\Omega} \frac{R}{c\tau \sin\theta} \frac{mc}{p}$$

and the differential flux at the surface of the shield is

$$\frac{d\varphi}{dT} = f \frac{I_f E_f}{L} \frac{1}{R+H} \int_{-\pi/2}^{\pi/2} d\theta \frac{1}{\epsilon} \frac{d^2n_\pi}{dTd\Omega} \frac{R}{c\tau \sin\theta} \frac{mc}{p}$$

Note that the flux is across an area perpendicular to the direction θ and not across the surface of the shield. This makes a big difference at small θ. The flux is

$$\Phi = f \frac{I_f E_f}{\epsilon L c\tau} \frac{R}{R+H} \int_{-\pi/2}^{\pi/2} \frac{d\theta}{\sin\theta} \int_{T_o}^{\infty} dT \frac{d^2n_\pi}{dTd\Omega} \frac{mc}{p}$$

where T_o is the kinetic energy of a μ with residual range equal to $H/\sin\theta$. Again we convert to dose level by multiplying by 3.6×10^6 and using a dose conversion factor of $F = 3.2 \times 10^{-8}$ rem/μ-cm^{-2}.

$$D = 3.6 \times 10^6 \, fF \frac{I_f E_f}{\epsilon} \frac{1}{Lc\tau} \frac{R}{R+H} \int_{-\pi/2}^{\pi/2} \frac{d\theta}{\sin\theta} \int_{T_o}^{E_o} dT \frac{d^2n_\pi}{dTd\Omega} \frac{mc}{p}$$

where

- D is the radiation level at the surface of the shield (mrem/hr).
- f is the fraction of beam power loss (3%).
- F is the dose conversion factor (3.2×10^{-8} rem/μ-cm^{-2}).
- I_f is the final beam current (3.75×10^{14} e^-/s = 60 μa).
- E_f is the final beam energy (40 Bev).
- ϵ is the energy for which pion yield was calculated (45 Bev).

L is the length of the machine (3.05×10^5 cm = 10^4 ft).

$c\tau$ is the proper decay distance of pion ($3 \times 10^{10} \times 2.5 \times 10^{-8} = 750$ cm).

R is the radius of the tunnel (5 ft).

H is the thickness of the shield (25 ft).

θ is the angle of emission of the π with respect to the direction of travel of the electron beam.

T is the kinetic energy of pion (or muon).

$\frac{d^2n}{dTd\Omega}$ is the yield of pions per 45-Bev electron hitting the machine (π/Mev-sr-e^-).

m is the mass of pion (140 Mev).

p is the momentum of pion (Mev/c).

$$D = 840 \int_{-\pi/2}^{\pi/2} \frac{d\theta}{\sin\theta} \int_{T_o}^{E_o} dT \, \frac{d^2n}{dTd\Omega} \frac{m}{p}$$

To evaluate the integrals we make some approximations which overestimate the flux of penetrating muons. We take $p = T$, $E_o = E_f$, and $T_o \ll E_f$.

We evaluate the energy integral for two different calculations of the pion spectra: that calculated here in Section IV, and that calculated by Dedrick in M-229. For the spectra in Section IV we observe that they always drop faster than $1/T_\nu$, where ν is a function of θ which increases from 1 at 5^o to 3 at 30^o; so we make the approximation

$$\frac{d^2n}{dTd\Omega} \leq \left(\frac{d^2n}{dTd\Omega}\right)_{T_o} \left(\frac{T_o}{T}\right)^\nu , \qquad T \geq T_o$$

Then

$$\int_{T_o}^{E_o} dT \, \frac{d^2n}{dTd\Omega} \frac{mc}{p} \lesssim \int_{T_o}^{E_f} dT \left(\frac{d^2n}{dTd\Omega}\right) \left(\frac{T_o}{T}\right)^\nu \frac{mc^2}{T} \approx \left(\frac{d^2n}{dTd\Omega}\right)_{T_o} \frac{mc^2}{\nu} \left(\frac{T_o}{T}\right)^\nu \Bigg|_{E_f}^{T_o}$$

$$\lesssim \left(\frac{d^2n}{dTd\Omega}\right)_{T_o} \frac{mc^2}{\nu}, \qquad \text{for } T_o \ll E_f.$$

The calculations of Dedrick, based on a statistical model, give spectra which drop faster than exponentially at high energies, so we make the approximation

$$\frac{d^2n}{dTd\Omega} \lesssim \left(\frac{d^2n}{dTd\Omega}\right)_{T_o} e^{-\left(T-T_o\right)/T_i}, \qquad T_o \leq T$$

Then

$$\int_{T_o}^{E_o} dT \, \frac{d^2n}{dTd\Omega} \, \frac{mc}{p} \lesssim \left(\frac{d^2n}{dTd\Omega}\right)_{T_o} mc^2 \int_{T_o}^{E_f} e^{-T/T_i} \left(\frac{dT}{T}\right)$$

We simplify and overestimate the integral by holding T in the denominator constant at T_o and assuming $T_o \ll E_f$. Then

$$\int_{T_o}^{E_o} dT \, \frac{d^2n}{dTd\Omega} \, \frac{mc}{p} < mc^2 \left(\frac{d^2n}{dTd\Omega}\right)_{T_o} \frac{T_i}{T_o}$$

We evaluate these integrals by making the approximate analytical fits to the calculated pion spectra. We take $H = 25$ ft, $E_f = 40$ Bev, and 2.2 Mev/g-cm^{-2} for the energy loss of the muons[46] (for example, at $\theta = 90^\circ$ this gives $T_o = 3.0$ Bev). The values of the approximate integral over energy are shown in Fig. 19. The statistical model gives yields that are about 1000 times smaller than the yields from single photoproduction ("dipion" production, as described in Section IV, does not give any muons which penetrate the shield). This probably arises because in the statistical model very few pions have large energies. To see why this is so we summarize briefly the assumptions behind these two calculations. In the statistical model (a) the cross section is 100 μb/nucleon independent of photon energy, (b) the average pion multiplicity increases with energy and the actual multiplicity has a Poisson distribution, and (c) in the final state center of mass the nucleon is at rest and the created pions are isotropic and equally share the

[46] This is the plateau value of the ionization loss in a hypothetical medium with $Z = 10$ and $A = 20$. E. P. George in Progress in Cosmic Ray Physics Vol. I (North Holland Pub. Co., Amsterdam, 1952).

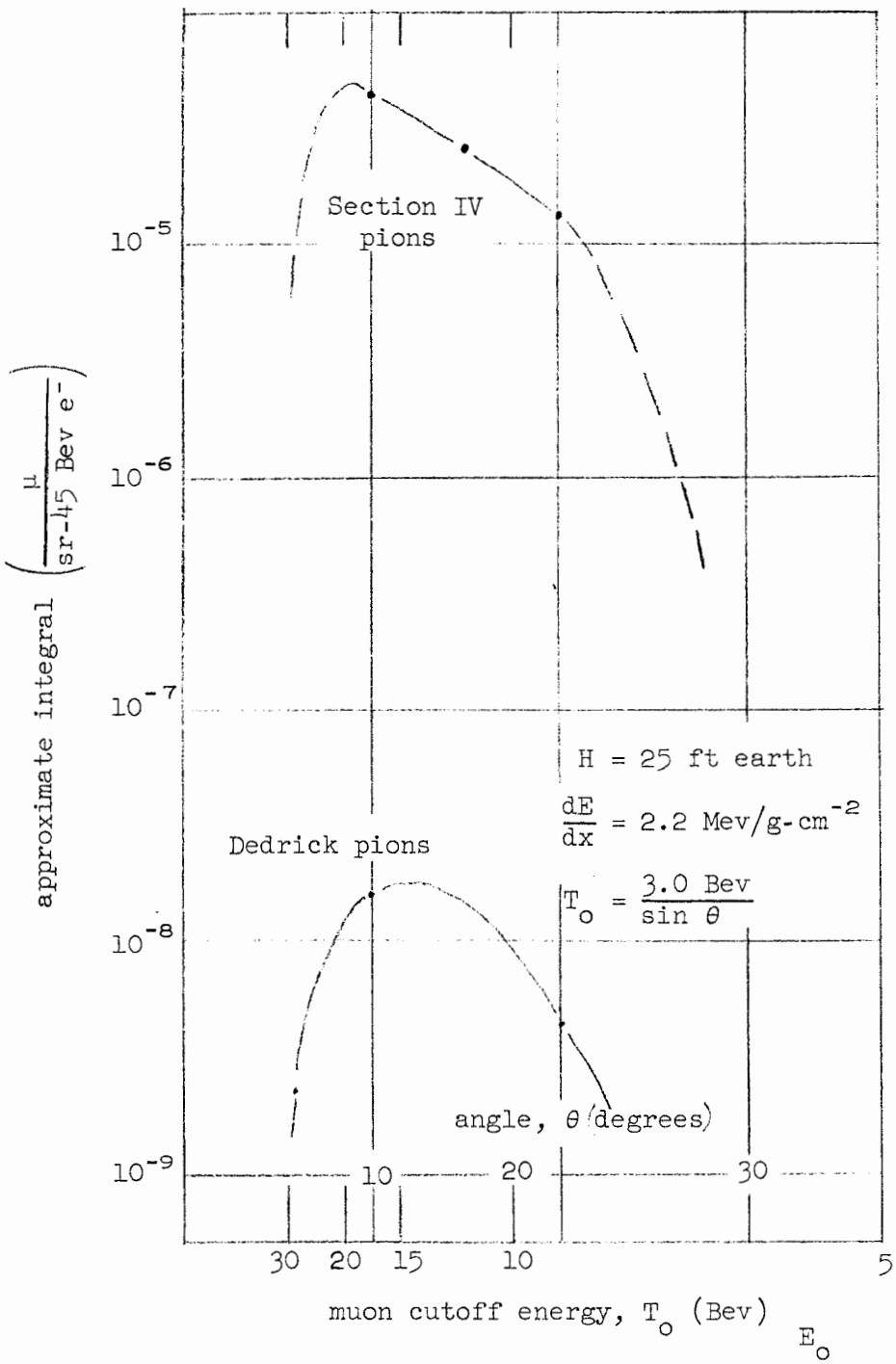

FIG. 19--Approximate values of $\frac{1}{\sin \theta} \int_{T_o}^{E_o} dT \left(\frac{d^2n}{dTd\Omega}\right)\frac{m}{\rho}$

available energy . In contrast, the assumptions in Section IV were that (a) the cross section is isotropic in the center of mass and equal to 60 μb/nucleon independent of photon energy, (b) a single pion is created, and (c) two-body kinematics prevail with the initial nucleon at rest in the laboratory system.

We integrate numerically over angle and find a radiation level of 7.2×10^{-3} mrem/hr for the Section IV pions, which is about 100 times below tolerance (the Dedrick pions give a level about 1000 times smaller, and we neglect them in the following). The radiation level from the neutrons is also about 100 times below tolerance, so the accuracy of the muon calculation is of interest.

All of the approximations we have made overestimate the muon level except perhaps the neglect of angular divergence arising from scattering and π-μ decay. However, because of the bad geometry most of the muons which scatter toward less shielding are compensated by those which scatter into more shielding. In addition, the assumption that the muon energy equals the pion energy overestimates the muon energy; and since only the highest energy muons penetrate, this approximation tends to compensate for any increased yield arising from scattering. In our calculation the muon radiation level arises only from photons with energies greater than 20 Bev, where the pion production has not been investigated experimentally.

The pion yields from the statistical model at energy T_o are about 30 times smaller than those calculated in Section IV at large pion energies. The integrals over the pion spectrum are about 200 times smaller for the statistical model because the yield falls so rapidly as the pion energy increases.

Just for fun we calculated the radiation level which would arise from μ mesons which are pair-produced electromagnetically (we used a "Bethe-Heitler" pair formula derived by Drell[42]), and which subsequently Rutherford-scatter with form factor equal to unity. This level turned out to be about 10 times less than the level arrived at using Dedrick's pion calculation, so we neglect it.

---

[42]S. D. Drell in "Some Aspects of Target Area Design for the Proposed Stanford Two-Mile Linear Electron Accelerator," M-200, Stanford Linear Accelerator Center, Stanford, California, Summer 1960. Also Phys. Rev. Letters 5 278(1960).

F. Effects of Different Geometry and Different Beam Loss

We briefly consider the effects on the radiation level caused by neutrons at the surface of the shielding as we decrease the distance over which the beam is absorbed. As shown in Fig. 14 most of the radiation at a point S comes from the accelerator at angles between 40° and 110°. As long as the primary electron beam is absorbed over a distance ℓ which includes the length subtended between 40° and 110° (ℓ_o), then the radiation level will be proportional to $1/\ell$ (always assuming that the beam power is absorbed uniformly over the length ℓ).

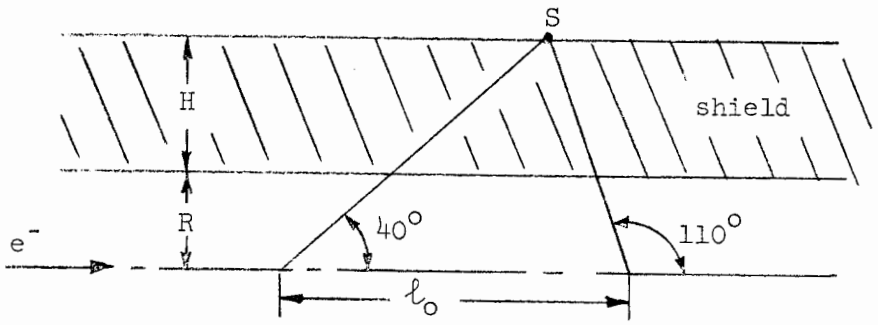

$$\ell_o = (R + H)[\cot 40^\circ + \cot(180^\circ - 110^\circ)] = 30 \times 1.55 = 47 \text{ ft}$$

For the limiting case in which the beam is absorbed at one point the radiation level as a function of angle is given by

$$D_S = f \left(I_f E_f\right) \frac{\langle F'B \rangle \sin^2\theta}{(R + H)^2} \int_0^\infty dT \, \frac{1}{\epsilon} \left(\frac{d^2n}{dT d\Omega}\right) \exp[- H/\lambda(T) \sin\theta]$$

with the same notation as before. The integral is shown in Fig. 14 for $H = 26.9$ ft as a function of angle and it has a maximum at about 75°.

$$\left(D_S\right)_{max} = f \frac{\left(I_f E_f\right)}{\epsilon} \frac{< F'B >}{(R + H)^2} \left\{ \sin^2 \theta \int_0^{\infty} dT \left(\frac{d^2 n}{dT d\Omega} \right) \exp[- H/\lambda(T) \sin \theta] \right\}_{max}$$

where

f is the fractional beam power loss (3%)

I_f is the final electron beam current (3.75×10^{14} e^-/s = 60 μa).

E_f is the final beam energy (40 Bev).

ϵ is the computational energy (45 Bev).

$< F'B >$ is the biological effect (1.25×10^{-7} rem/n-cm^{-2}).

R is the radius of tunnel (5 ft).

H is the thickness of shield (25 ft).

$\int_0^{\infty} dT \left(\right)_{max}$ is plotted in Fig. 14.

$$D_S(\text{mrem/hr}) = 5.38 \times 10^{-6} \left\{ \sin^2 \theta \int_0^{\infty} dT \frac{d^2 n}{dT d\Omega} \exp[- H/\lambda(T) \sin \theta] \right\}$$

where the brackets have units (neutron/sr-45 Bev e^-). From Fig. 14 (adjusting to $H = 25$ ft) we see that the brackets have a maximum value of about 3.3×10^{-7}, so the maximum radiation level at the surface from a point source is

$$\left(D_S\right)_{max} = 5.38 \times 10^{-6} \times 3.3 \times 10^{-7} = 1.8 \text{ mrem/hr}$$

The radiation levels are clearly proportional to the total amount of beam power absorbed. In Fig. 20 we show the radiation level at S for $H = 25$ ft (calculated with the method of Moyer) as a function of the

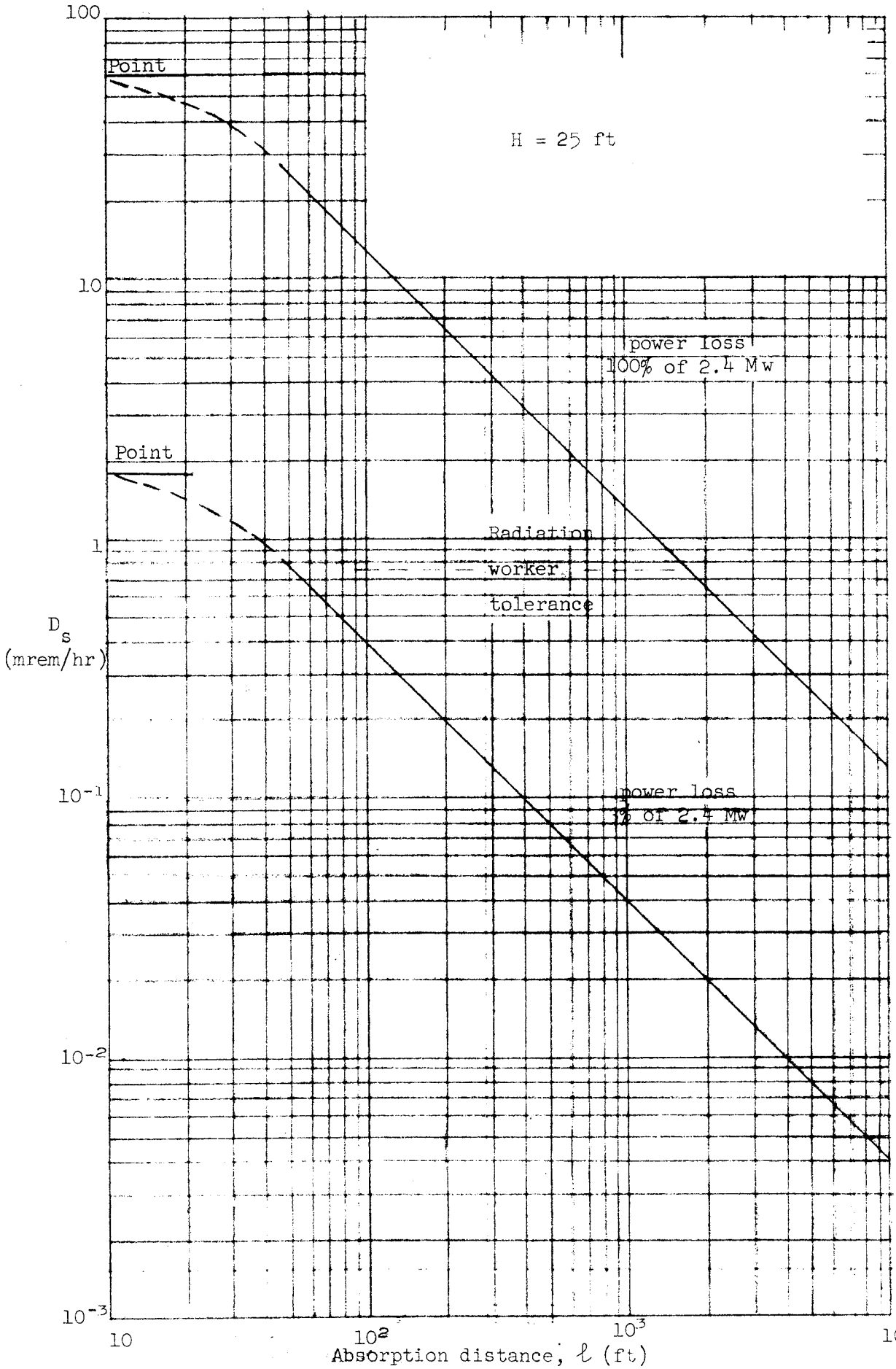

FIG. 20--Maximum radiation level at surface of shield vs the length over which the power is uniformly absorbed.

distance over which the beam power is absorbed ℓ for a 3% loss and for a 100% loss with a beam power of 60 μa at 40 Bev. For any ℓ we assume that S is located so that it has the highest radiation level anywhere along the surface of the shield. At ℓ = 10 ft we show the limiting level for a point source, which is 60 mrem/hr for the full 2.4 Mw power loss.

As an example, we estimate the increased shielding needed near a positron radiator. Positron beams are made by first accelerating electrons; the electron beam hits a thick, high-Z radiator inside the machine, and the emerging, low-energy positrons are accelerated in the remainder of the machine by shifting the rf phase by 180°. The design of the lateral extent of the extra shielding is complicated, but the extra thickness is simply estimated.

For the sake of argument we assume that 500 kw of beam power is absorbed at one point. From Fig. 20 we see that the radiation level at the surface is

$$\frac{500 \text{ kw}}{2.4 \text{ Mw}} 60 = 12.5 \text{ mrem/hr}$$

which is 17 times the radiation worker tolerance of 0.75 mrem/hr.

Assume that a safety factor of 30 is desirable; then the shield must transmit 16.7 × 30 = 500 times less. We achieve this by replacing some of the earth shield near the accelerator by a dense material of thickness h. For ease of operation and construction, it is desirable to keep a constant separation between the machine and the klystron gallery (on the surface).

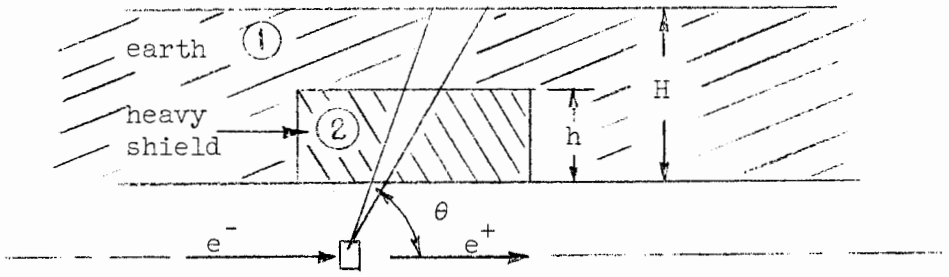

From Fig. 14 we see that the most critical angle is $\theta \approx 75^{\circ}$. If A_o is the additional required attenuation factor $\left(A_o = 1/500\right)$, then

$$e^{-\left(h/\Lambda_2 \cos\theta\right)} e^{-\left(H-h\right)/\Lambda_1 \cos\theta} = A_o\, e^{-H/\Lambda_1 \cos\theta}$$

where Λ_1 is the attenuation length in earth, and Λ_2 is the attenuation length in the dense material (both in feet); the requirement is

$$h = \frac{\Lambda_2/\Lambda_1}{1 - \Lambda_2/\Lambda_1}\, \Lambda_1 \cos\theta \ln 1/A_o$$

We use notation with Λ measured in feet and λ measured in g-cm^{-2}, so $\Lambda \propto \lambda/\rho$. The ratio $\left(\Lambda_2/\Lambda_1\right)$ depends on the density as well as the atomic weight. Since Λ is energy dependent, we use an average value derived from Fig. 15 after removing the inverse distance factor and find

$$\lambda_1 = 138 \text{ g-cm}^{-2} \text{ earth}$$

With $\rho = 1.8$ g-cm^{-3}, this gives

$$\Lambda_1 = 2.52 \text{ ft earth}$$

For $\theta = 75^{\circ}$ and $A_o = 1/500$,

$$\Lambda_1 \cos\theta \ln 1/A_o = 2.52\ (0.906)\ 6.22 = 14.2 \text{ ft}$$

Using values from Table II we have

	Material	ρ	ρ_1/ρ_2	λ_2/λ_1	Λ_2/Λ_1	h(feet)
(1)	Earth	1.8				
(2)	Light concrete	2.3	0.78	1.00	0.78	50
(2)	Heavy concrete Heavy aggregate	$\approx$ 3.7	0.49	$\approx$ 1.15	0.56	18.1
(2)	Iron	7.8	0.23	1.41	0.32	6.7

Light concrete is not dense enough to achieve the required extra shielding in 25 ft.

VI. RADIATION LEVELS FAR FROM THE MACHINE

In this chapter we estimate the radiation levels at the project boundary using several different models. We conclude that the shielding thickness required by consideration of radiation-worker tolerances at the surface of the shield is about the same as the shielding thickness required by consideration of general-population tolerance at the boundary of the project.

A. One-Dimensional Calculation

1. Application

We apply the spirit and model of the previous chapter in order to estimate the radiation level far from the machine. The main point is that we assume that the one-dimensional model of the nuclear cascade is a valid approximation. We have the following geometry:

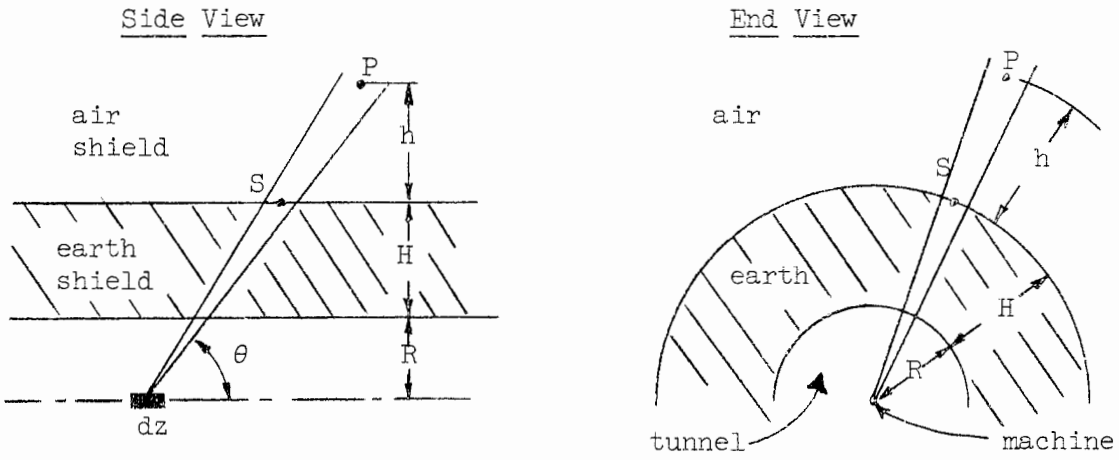

and we integrate over all values of z just as before.

We estimate the radiation level at a distance of h = 500 ft from the machine, which is the minimum distance to the project boundary. We shall conclude that, to within a factor of 2 or 3, the general-population tolerance level exists at the boundary if the radiation-worker tolerance exists at the surface of the shielding. This is true for a line source of radiation which is long compared to 500 ft. If the source is short compared to 500 ft, then the relative radiation level at the boundary will

be even lower because the radiation level will decrease more like $1/r^2$ than like $1/r$. To our degree of approximation there is no significant difference in nuclear properties between air and earth (again with the possible exception of hydrogen content). The radiation level at P is less than the radiation level at the surface, S, because of an inverse r factor and because of the slightly increased nuclear absorption:

$$D_P = D_S \left(\frac{R + H}{R + H + h} \right) e^{-h/\lambda}$$

Here λ is the effective absorption length averaged over energy; to be conservative we use $\lambda_o = 170$ g-cm^{-2}. For $h = 500$ ft we have $h = 500 \times 30.5 \times 1.3 \times 10^{-3} = 20$ g-cm^{-2}. With $R = 5$ ft and $H = 25$ ft,

$$D_P = D_S \left(\frac{5 + 25}{5 + 25 + 500} \right) e^{-20/170} = D_S \frac{0.89}{1 + 16.7}$$

$$D_P = \frac{D_S}{20}$$

So the radiation level at the boundary is 20 times less than the radiation level at the surface of the machine. In the strict one-dimensional approximation, in which all particles move in a straight line away from the machine, there is very little uncertainty in the ratio. If we can believe one level, we can believe the other. The ratio of the recommended tolerance levels for radiation workers (40 hr/week occupancy) and for the general population (continuous occupancy) is 65. On the basis of this calculation the requirements of the general population set the required attenuation by about a factor of 3. That is, the requirements of the two groups are about equal. In a previous calculation we concluded that the requirements of the general population might require an attenation 20 to 50 times more than the requirements of radiation workers.[2] However, the previous calculation had large uncertainties, and it now seems that we greatly overestimated the radiation levels far from the machine.

---

[2]H. DeStaebler, "A Review of Transverse Shielding Requirements for the Stanford Two-Mile Accelerator," M-262, Stanford Linear Accelerator Center, Stanford, California, April, 1961.

Still in the spirit of the one-dimensional approximation with cylindrical symmetry we can easily calculate the radiation levels at the boundary in the same way as we did in Section V.E for the case in which the beam power is not absorbed over the full 10,000 feet of accelerator. The absorption distance in the machine for which the radiation level ceases to be proportional to $1/\ell$ is

$$\ell_o = (R + H + h)\,[\cot 40^\circ + \cot (180^\circ - 110^\circ)]$$
$$= 530 \times 1.55 = 810 \text{ ft}$$

When the beam is absorbed at a point, the maximum level is $(30/530)^2$ times less than at the surface:

$$(D_P)_{max} = (D_S)_{max} \left(\frac{R + H}{R + H + h}\right)^2$$
$$= 1.8 \times 3.2 \times 10^{-3} = 5.8 \times 10^{-3} \text{ mrem/hr.}$$

The variation of radiation level with ℓ and fractional power loss is shown in Fig. 21.

2. Discussion and qualification

We now consider the adequacy of the one-dimensional approximation for a truly three-dimensional problem. For simplicity we first consider the case in which the source and the observation point P are imbedded in a homogeneous shield, and we want to obtain the radiation level at P (that is, the rate of energy loss per gram in tissue) as a function of the geometry and density of the shield. It is important to recognize that the geometry and density of the detector at P (a person, for example) do not change as we change the characteristics of the shield. The quantity which counts is the flux of particles at P (particles/cm^2-sec) where we assume that the introduction of a person at P does not seriously modify the fluxes near P. We consider the omni-directional flux, that is, the total path length of particles across a small sphere, divided by the volume of the sphere.

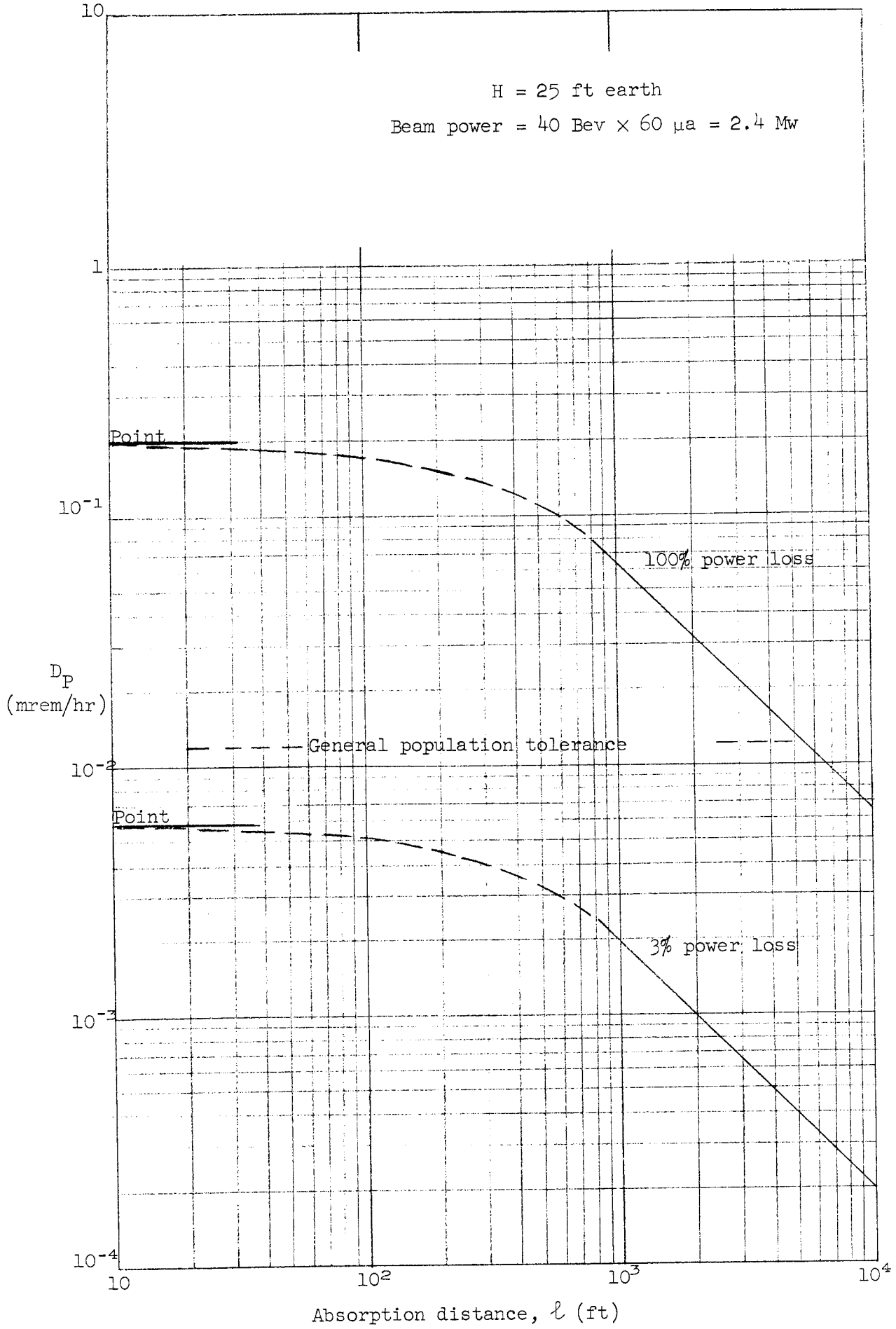

FIG. 21--Maximum radiation level 500 ft from shield vs the length over which power is uniformly absorbed.

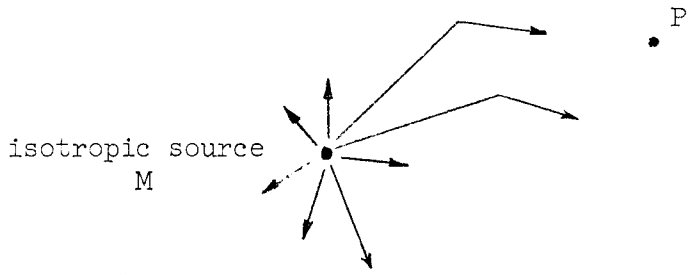

In the sketch it is clear that the geometry is bad, and for every particle originally heading for P which scatters away, there will be another particle originally bending away from P which scatters toward it. However, there will be some particles which go past P and then are scattered back through P.

If the radiation at P is well diffused, then we would expect that about half of the radiation is composed of forward-going particles and about half of backward-going particles. However, if the level is composed mainly of high-energy particles, these probably move preferentially away from the source. So if we know the flux of forward-going particles at P, the total flux is about a factor of 1 to 2 times larger.

We now change the density of the medium by keeping constant the number of atoms and by expanding all dimensions except those of the detector and the source.

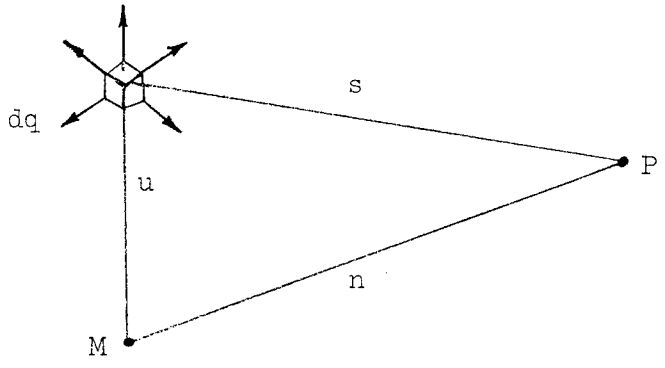

Suppose that the flux at P can be written as a volume integral over the whole medium where the effective secondary-source strength of any volume element depends on the number of nuclear interactions in it, i.e., it is proportional to the number of atoms in the volume element times the flux from the source. We take

$$dq \approx (\rho\, dv)\ \frac{e^{-u/\Lambda}}{u^2}$$

where Λ is some effective nuclear absorption length and is measured in g-cm^{-2}. We assume that the differential flux at P from dq also decreases as the square of the distance with a similar exponential attenuation

$$d\Phi \approx \frac{dq}{s^2}\ e^{-s/\Lambda}$$

Then

$$\varphi \approx \frac{\rho}{\Lambda} \int_{\substack{\text{all}\\ \text{space}}} \frac{dv}{\Lambda^3} \left(\frac{\Lambda}{u}\right)^2 \left(\frac{\Lambda}{s}\right)^2\ e^{-u/\Lambda}\ e^{-s/\Lambda}$$

The integral is independent of the density if the limits of integration expand as we change the density; Λ is independent of density because it is related to the nuclear cross sections of the medium. So Φ is proportional to ρ when P is imbedded in a uniform thick shield and the geometry changes with the density.

For the case at hand, we first consider the radiation level at the surface of the shield. What is the effect of being at the interface between two media of similar nuclear properties but very different densities? Since the density of the air is low, the fraction of the flux at the surface coming from the air is less than if the air were compressed overhead to the density of the earth. For P located in the air well away from the shield it seems that the flux should be similar to that calculated from the one-dimensional model.

Now we relax the assumption of cylindrical symmetry. A typical cross section will look something like these, the following sketches, depending

upon whether the tunnel is in a cut or a fill.

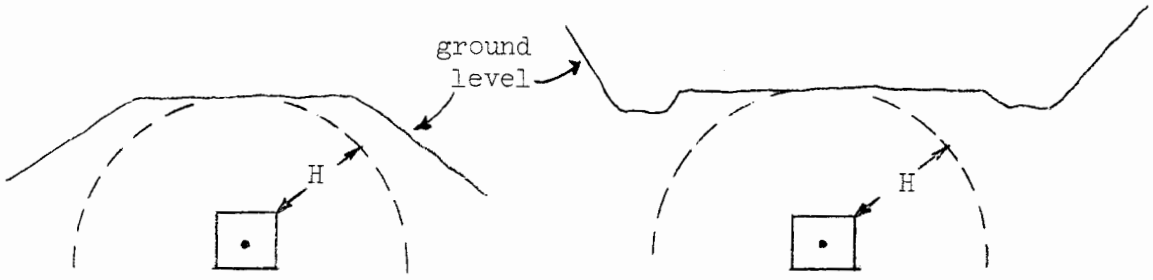

tunnel in cut tunnel in fill

In either case the radiation level on the surface of the ground at the boundary would be less than calculated on the basis of cylindrical symmetry, and it is possible that the increased attenuation could be significant.

B. Skyshine

Skyshine is a concept which is particularly appropriate to a shield which has two distinct parts of different thickness but not to a shield such as ours which is substantially uniform. A typical situation is depicted below in which a radiation source is shielded by thick walls and a thin roof. Then most of the radiation level can arise not from penetration of the walls, but from penetration of the roof followed by subsequent scattering in the air; hence the name "skyshine".

Measurements of the neutron flux at ground level and at distances of about 200 ft to 1000 ft from the Mark III machine at Stanford[46a] and at the Bevatron[47] show that the flux decreases approximately as $1/r^2$.

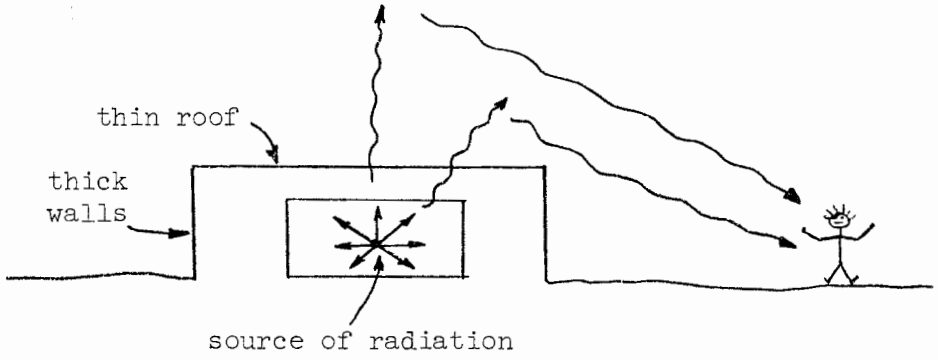

[46a] C. W. Olson, Private Communication, 1962.

[47] For example, R. W. Wallace and B. J. Mayer, "Shielding and Activation Considerations for a Meson Factory", UCRL-10086, Lawrence Radiation Laboratory, Berkeley, California, April 1962.

Lindenbaum applied the results of three-dimensional diffusion plus absorption in a homogeneous medium to the problem of skyshine.[26] For a unit source the flux $\varphi(r)$ at a distance r is approximately

$$\varphi(r) \approx \frac{e^{-r/\lambda_t}}{4\pi r^2} + \frac{e^{-r/\lambda_o}}{4\pi D r}$$

where

λ_t = total mean free path $\approx$ 450 ft in air

$D \approx \lambda_t/3$

λ_a = absorption mean free path $\approx 10\ \lambda_t$ (in air $\lambda_a > 10\ \lambda_t$, but it is made shorter to take account somewhat of the effect of the dense earth)

$$\lambda_o = \sqrt{\frac{\lambda_t\ \lambda_a}{3}}$$

The first term is the flux which has not interacted, and the second term contains all scattered particles. It is sometimes argued that at large distances the second term dominates and makes φ vary as $1/r$. The quantity $4\pi r^2\varphi(r)$ is plotted in Fig. 22, and it is apparent that for $r < 2000$ ft the predicted variation of φ is about as $1/r^2$. Apparently the exponential numerator in the second term looks like about $1/r$.

We make a rough estimate of the radiation level to be expected at the SLAC project boundary by assuming that the surface of the shield is a line source each element of which propagates according to Lindenbaum's recipe for neutrons. The basic assumption is that the radiation propagates in the same way as the fast neutron flux. For a line source of length L and total strength Q, the omni-directional flux at a distance r is, for $r \ll L$,

---

[26] S. J. Lindenbaum, Ann. Rev. Nuclear Sci. 11,213 (1961).

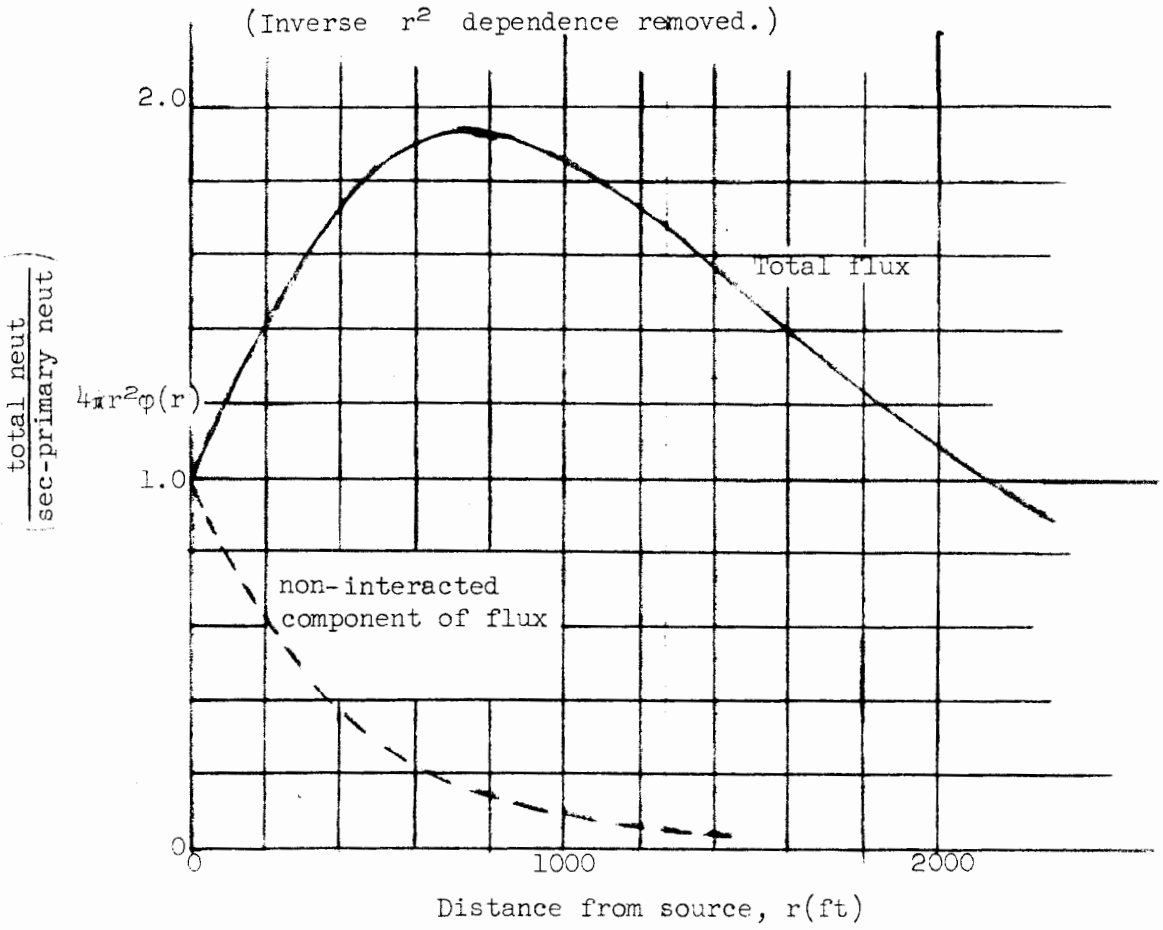

FIG. 22--Variation of neutron flux with distance in air.

$$\varphi(r) \approx \int_{-\infty}^{\infty} \frac{Q dz}{L} \frac{\sin^2\theta}{4\pi r^2}$$

$$z = r \cot \theta$$

$$\varphi(r) \approx 2 \frac{Q}{L} \int_{0}^{\pi/2} \frac{r d\theta}{4\pi r^2} = \frac{Q}{4Lr}$$

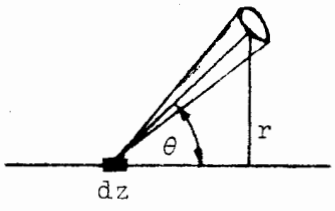

To get the relative dose levels at the surface of the shield and at $h = 500$ ft we approximate Q, the total strength, by the level at the surface D_S times the area $\pi L(R + H)$. Using the same notation as before, $r \approx h$, and

$$D_P \approx \frac{D_S \pi L(R + H)}{4Lh} = D_S \frac{\pi}{4} \frac{R + H}{h}$$

This is essentially the same as we calculated in Section VI.A on the basis of the one-dimensional approximation.

A very careful experiment was done at the Rutherford Laboratory in which the neutron fluxes from aluminum and beryllium targets bombarded by 32 Mev protons were measured as a function of distance from about 30 to 900 ft.[48] Up to 100 - 200 ft there was good absolute (± 30%) agreement with Lindenbaum's calculation. From about 200 ft to 900 ft the experimental points dropped below Lindenbaum's curve until at 900 ft the curve was about a factor of 3 high. This may indicate the influence of the nearby, dense ground.

A Monte Carlo calculation of neutron scattering was carried out at Oak Ridge in which the earth was included in an approximate way.[49] The source energies varied from 1 to 10 Mev. Inelastic scattering was

---

[48]R. H. Thomas, "First International Conference on Shielding Around High Energy Accelerators", Orsay and Saclay, France, February 1962.

[49]W. E. Kinney, "A Monte Carlo Calculation of Scattered Neutron Fluxes at an Air-Ground Interface Due to Point Isotopic Sources on the Interface," ORNL-3287, Oak Ridge National Laboratory, Oak Ridge, Tennessee, July 1962.

treated as elastic; neutrons disappeared only through (n,p) and (n,α) reactions. The air was taken as 79% N_2 and 21% O_2 with a density of 1.2×10^{-3} g-cm^{-3}, and the ground was taken as SiO_2 with a density of 1.8 g-cm^{-3}. The calculation yielded the neutron flux at the air-ground interface as a function of neutron energy, and these fluxes were compared with those developing in an infinite air medium. For $0 < r < 100$ meters the fluxes were higher with the ground included, presumably because the increased density accelerated the diffusion. For $100 < r < 200$ meters the fluxes were about equal in the two cases. For $r > 200$ meters the fluxes with the ground included were about 2 times smaller than the fluxes with air alone.

We estimate the effect of neglecting the hydrogen content of the ground by finding the relative energy loss in oxygen and in hydrogen as a function of neutron energy. The total energy loss per unit of path is

$$\Delta E = \sum \frac{w_i}{\lambda_i} \Delta E_i \approx \sum w_i \frac{\sigma_i}{A_i} \Delta E_i$$

where λ_i is the mean free path for the i'th kind of interaction, w_i is the weight percent of the i'th kind of nucleus with atomic weight A_i, and ΔE_i is the energy loss in the i'th interaction. We take as materials O_2 with 1% and 10% H_2O by weight. The first corresponds to air with 65% relative humidity at 20° C, and the second is a typical water content in the ground. These give the following values:

	1% H_2O		10% H_2O	
	w_i wt%	w_i/A_i atom %	w_i wt%	w_i/A_i atom %
H	0.11	1.7	1.1	15
O	99.9	98.3	98.9	85

In hydrogen on the average the neutron loses half its energy in each collision (elastic scattering only). In oxygen on the average the neutron loses $2/A = 1/8$ of its energy in each elastic scattering; and in inelastic scattering the neutron loses 6 Mev, which is approximately the first energy level in oxygen. For neutron energies less than 6 Mev only elastic scattering is possible. Figure 23 shows the cross sections; from about 0.5 to 2 Mev the resonances in the oxygen elastic cross section are completely smoothed over. The following table gives the proportions of the energy lost in H and O interactions as a function of neutron energy.

Neutron Energy (Mev)	1% H_2O		10% H_2O	
	% E loss in H	% E loss in O	% E loss in H	% E loss in O
10	2	98	17	83
1	8	92	46	54
.1	20	80	73	27
.01	27	73	79	21

It would thus appear that neglecting the energy loss in water is not a bad approximation in air, but that it is a poor approximation in earth below about 0.5 Mev. So the Oak Ridge skyshine calculations are probably slightly distorted.

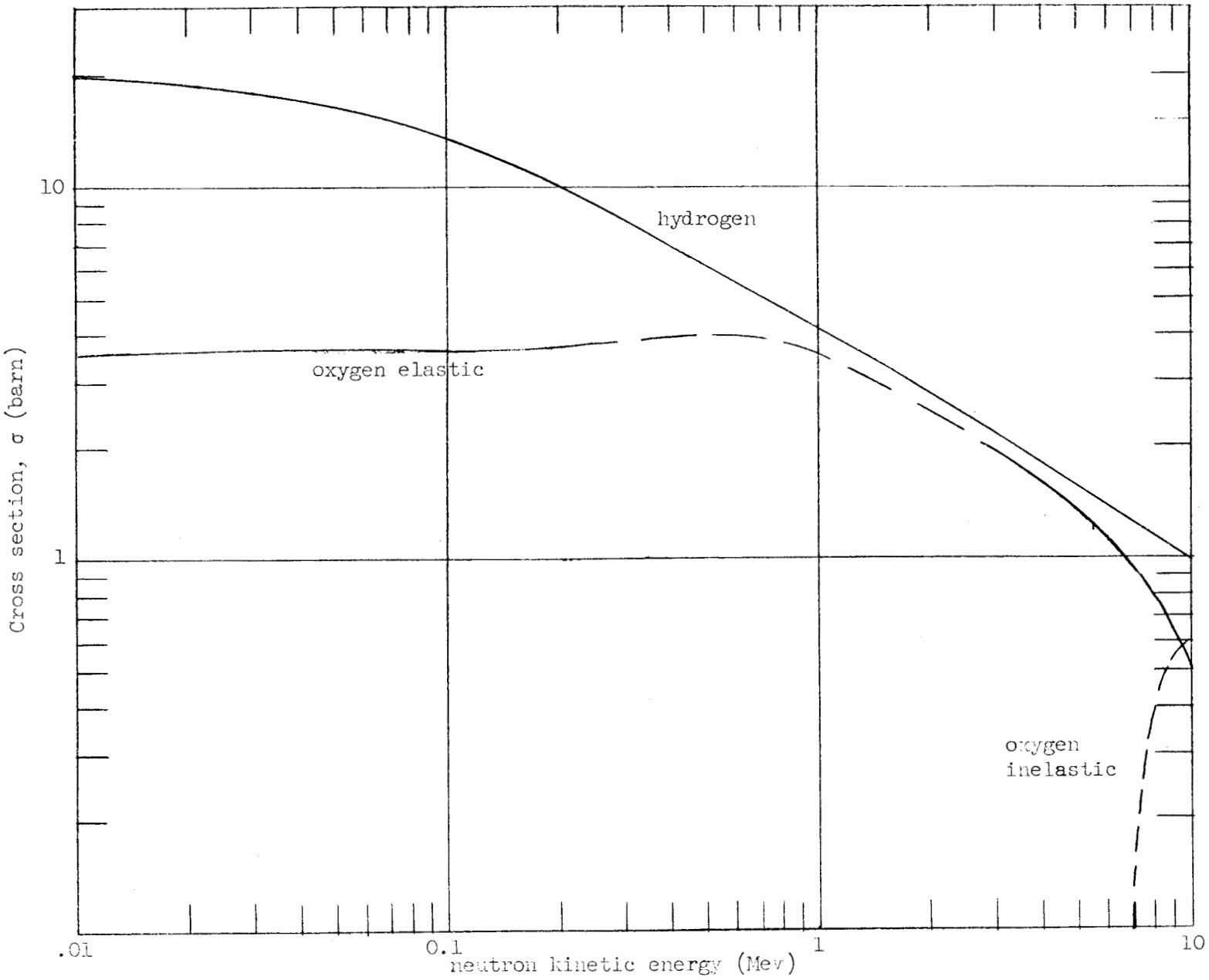

FIG. 23--Neutron cross sections in hydrogen and oxygen as functions of neutron energy.

VII. CONCLUSIONS

A. Along the Machine

The determination of the appropriate shield thickness depends on many physical facts, some of which are poorly known. It also depends on operational and economic considerations, and on the probable consequences of making the shield too thin.

In this report we are mainly interested in the earth shielding between the accelerator and the above-ground klystron gallery. It is anticipated (hoped) that the accelerator will run continuously and that the radiation level in the gallery will be less than radiation worker tolerance. Since the klystrons, vacuum pumps, and cooling system are in the klystron gallery, it would be very costly in time and money if it became necessary to increase the shielding thickness between the machine and the gallery. Therefore, we have significant incentive to be conservative in selecting this thickness. Even though this conservatism costs some money,* it represents insurance against the catastrophe of having large radiation levels in the klystron gallery and the accompanying large radiation levels at the boundary, which could lead to (a) an extensive, expensive shut down to add shielding; (b) machine operation at reduced current; or (c) severely restricted access to the gallery, modified operational procedures, and controlled access for the general population near the project boundary.

Calculation of the radiation level at the surface of the shield relative to tolerance involves a number of steps which we recapitulate in Table III. For each we estimate an uncertainty factor f_i, and we find the combined uncertainty factor F, by

$$(\ell nF)^2 = \sum \left(\ell nf_i\right)^2$$

which gives $F = 6.5$.**

---

*The cost as a function of shielding thickness is complicated by a number of factors stemming from all of the pipes, wires, waveguides, etc., which go from the gallery into the tunnel.

**This corresponds roughly to combining the squares of random errors. The product of the errors, $\pi f_i = 51$, corresponds roughly to adding the magnitudes of the errors.

TABLE III

SUMMARY OF FACTORS AFFECTING SELECTION OF SHIELD THICKNESS

Item	Estimated uncertainty factor	Comments
Tolerance	1	We use 1/3 of the current AEC recommendation.
Beam loss	3	We use 3% power loss uniformly absorbed. Extra shielding above localized sources is feasible.
Electromagnetic cascade	1	Monte Carlo calculations verify Approximation A except at high energies where it overestimates the track length.
Neutron production	2	Experiment checks the calculation.
Neutron attenuation	3	We take about ± 10% in the mean free path.
Lateral spread	2	We increase the 1-dimensional yield by a factor of 2.
Biological hazard	2	We depend on empirical measurements.

The radiation level at large distances is uncertain by an additional factor of 3, which yields $F = 8.7$.

From Fig. 15 in Section V, after multiplying by 2 for lateral spread, we see that the radiation level is about 100 times below tolerance for $H = 25$ ft. To get a feeling for whether this is a comfortable safety factor we note that $100 \approx F^2$ to $F^{2.5}$. We interpret F as a kind of standard deviation in a Gaussian sense, in which case there is roughly a probability of 1% of finding a fluctuation greater than 2 to 2.5 standard deviations. The error estimates are rough at best, and their interpretation is terribly imprecise, but it is supposed to support our conclusion that a 25 ft earth shield along the machine is probably adequate and that it is not excessively thick.

From Fig. 20 in Section V we see that the radiation level is 150 times tolerance (including the extra factor of 2 for spreading) if all of the beam is absorbed in a single point. This is not a serious level for short occupancy.

B. Above Beam Switchyard

In the beam switchyard we expect that the average beam loss will be very different than in the accelerator for several reasons. In the switchyard large magnets bend the beam through angles like 10° to 20°, and if there is a maladjustment or failure in the magnets, generators, or control equipment the whole beam can be dumped inside the tunnel. Energy slits define the energy spread in the beam by absorbing particles whose energies lie outside prescribed limits. These absorbers are strong localized radiation sources, and it is feasible to have special shielding around them, although simply thickening an earth shield may be cheaper.

Tentatively we estimate that the switchyard tunnels are 500 ft long, and that a uniform beam loss of 25% in this distance is a reasonable guess at average operating conditions. Using the procedure in Section V such a source would yield radiation levels

$$\left(\frac{10{,}000}{500}\right)\left(\frac{25}{3}\right) = 167$$

times larger than calculated for the klystron gallery-accelerator tunnel shielding. Figure 15 in Section V indicates that increasing the shielding

thickness from 25 ft to 37 ft decreases the radiation level by the same factor. Such a thickness would yield a radiation level about 100 times less than tolerance at the surface of the shield. In the extreme case in which 100% of the beam is absorbed at a point where there is no special, local shielding, the radiation level outside of a 37 ft shield is about equal to tolerance instead of 100 times below tolerance.

We chose a thickness of 40 ft of earth for the beam switchyard shielding because this conservatism is not very expensive. We note that the final design of this shielding does not need to be made at this time, and that refined calculations may suggest that a slightly different thickness is better.

APPENDIX A

COMPARISON OF PREVIOUS CALCULATIONS

In Table A-1 we give approximate relative values of some of the factors entering the shielding calculations used in three previous reports. In Table A-2 we summarize the conclusions of these three reports. There has been a shift in general design criteria from the 1957 Proposal in which the shield was to be adequate even if all of the beam (only 3 μa then) was stopped at any point. Now the shield is designed for average operating conditions.

TABLE A-1

SUMMARY OF SHIELDING CONSIDERATIONS

IN THREE REPORTS

Item	Relative Value: Proposal 1957	M-262 1961	This Report 1962	Comments
Tolerance	1	1	1	All calculations used the same radiation policies.
Absorbed Beam Power	1.7	1	1	In the Proposal the full current of 3 μa was stopped to give a point source.
Neutron Yield Per Electron	1	2	12	The two earlier reports considered only the deuteron photo-effect.
Source Geometry	Point	Line	Line	
Shield Geometry	Sphere	Cylinder	Cylinder	
Biological Hazard/Neutron	1	10	2	In M-262 the effect of high-energy neutrons was over-estimated.
Removal Mean Free Path	$\leqslant 1$	$\leqslant 1$	1	The earlier reports approximated $\lambda(T)$ at low energies to give larger transmission for the same thickness.

TABLE A-2

CONCLUSIONS FROM THREE REPORTS

Conclusion	Proposal 1957	M-262 1961	This Report 1962	
Shield Thickness (ft of earth)	35	35	25	
Controlling Human Group	Radiation Worker	General Population	Both the same	
"Safety Factor"	10	≈ 100	100	This is the tolerance level divided by the calculated radiation level. In the Proposal the assumed geometry was a worst case.
Uncertainty Factor	-	≈ 50	≈ 10	

APPENDIX B

PROPOSED RADIATION POLICIES FOR PROJECT M

This Appendix is a report written two years ago by Panofsky, and it describes the reasoning behind the selection of our tolerance radiation levels.

Since it was written, the concept of higher permissible exposures for individual, non-radiation workers has been abandoned, as was foreseen by Panofsky.

High-Energy Physics Laboratory
Stanford University

M-234
1 December 1960
W.K.H. Panofsky

PROPOSED RADIATION POLICIES FOR PROJECT M

In our proposal for the construction of a two-mile linear accelerator at Stanford (April 1957), we stated the following policy regarding radiation tolerances:

> "Since the general tendency has been toward more conservative radiation tolerances, we are adopting here for design purposes the following tolerances:
> 1) 30 mr/40-hr working week for 'radiation workers';
> 2) A level equal to natural background radiation (or 0.002 r per elapsed week) for all areas outside the project boundaries will be maintained. This is about a third of the 'doubling dose.'"

Since that time, the AEC has adopted specific regulations (given in AEC 0524-02-F) which essentially adopt the recommendations of the National Committee on Radiation Protection ("Maximum Permissible Radiation Exposures to Man," 8 January 1957). In addition, the Federal Radiation Council was established during the last year, and has issued its first report, "Background Material for the Development of Radiation Protection Standards" (13 May 1960).

Clearly, the radiation standards adopted in connection with the design of the two-mile accelerator should meet the AEC regulations, but in addition, considering the long-range nature of the project, a more conservative approach is indicated for the following reasons:

1) Past experience has been that radiation doses considered reasonable have decreased. For example, the average population exposure recommended as a guide for radiation protection standards by the FRC for large populations is half that given in the AEC Manual and in the recommendations of the NCRP.
2) The intensity estimates provided by accelerator designers at the inception of projects have been realistic; in some cases, in fact, intensities of the completed machines have exceeded the original estimates.

3) It is recognized that there is no level of exposure below which the expected statistical genetic effects will be zero, and therefore any exposure must be justified in terms of the benefits derived; in the words of the FRC report,

> "Under the working assumptions used, there can be no single 'permissible' or 'acceptable' level of exposure, without regard to the reasons for permitting the exposure. The radiation dose to the population which is appropriate to the benefits derived will vary widely depending upon the importance of the reason for exposing the population to a radiation dose."

For this reason, the FRC concludes, "...all exposures should be kept as far below any arbitrarily selected levels as practicable."

For these reasons, the policies adopted in designing the accelerator will under any circumstance rely on our best judgment, and will also be affected by the problem of relations between the project and the neighboring communities.

In connection with this project, we are concerned almost entirely with the control of penetrating whole-body radiations. There will be some problems with the handling of irradiated targets and other materials involving short-range radiations, and also with inhalation of short-lived radioactive gaseous isotopes which would be produced in closed target areas [for example, N^{13} formed by the reaction $N^{14}(\gamma,n)N^{13}$]. We believe that these can be controlled quite readily by appropriate handling procedures in the first case and ventilation in the second.

A summary of various whole-body exposures to penetrating radiations and recommended levels is given in the following table:

RECOMMENDATIONS ON MAXIMUM ANNUAL EXPOSURE TO WHOIE-BODY PENETRATING RADIATION

	Occupational	Non-occupational Individual	Non-occupational General population (30-yr average)
AEC Manual 0524-02-F	5 rem	0.5 rem	0.33 rem
Federal Radiation Council, Report 1 (13 May 1960)	5 rem	0.5 rem	0.167 rem
Stanford Project M Proposal, April 1957	1.5 rem	0.1 rem	0.1 rem

For comparison:

U.S. genetically significant per capita average exposure from natural sources	0.08-0.170 rem[1]
U.S. genetically significant per capita average exposure from man-made sources (mainly medical)	0.08-0.280 rem[1]

Our recommendation therefore proposes to limit radiation exposures to persons not directly involved in the project to levels below the average per capita level to which the population in the U.S. is now exposed. We do not consider it advisable to adopt a different standard for persons in the neighborhood of but not directly involved in the project from the standard for the general population. Apart from the great difficulty of justifying any other position to neighboring communities, we believe that giving substantial radiation exposures to persons not directly concerned with the project is not in accordance with the general guide-lines of the FRC quoted above. In addition, considering the general downward trend of occupational maximum permissible radiation exposures, we should like to retain as an objective the design figure of 30 mrem/week as given in our original proposal, which is a third of that allowed by the AEC.

The technical problems of radiation control of the project are such that our ability to meet the tolerances specified depends both on initial design of the shielding, target area arrangements, etc., and on the actual procedures used during machine operation. It is not feasible to design the target area so that it is absolutely impossible to cause excessive radiation levels arising from human error or equipment malfunction. The

---

[1] Summaries of Federal Radiation Council, Background Material for the Development of Radiation Protection Standards, Tables 3.1 and 3.2 (13 May 1960); see that report for discussion.

target area facilities must therefore include radiation detection devices and monitors which will automatically shut off the beam in a short time so that the accidentally high radiation levels will not contribute significantly to the long-time average exposure of the population. In addition, physical barriers must be provided so that even in the very short time before the beam can be shut off excessive exposures are prohibited for the most unlikely and extreme condition in which the entire beam is made to miss the shielding arrangements within the target area.

LIST OF REFERENCES

1. "Proposal for a Two-Mile Linear Electron Accelerator," Stanford University, Stanford, California, April, 1957.

2. H. DeStaebler, "A Review of Transverse Shielding Requirements for the Stanford Two-Mile Accelerator," M-262, Stanford Linear Accelerator Center, Stanford, California, April, 1961.

3. National Bureau of Standards Handbook 63, "Protection Against Neutron Radiation Up to 30 Mev," November, 1957, Superintendent of Documents, Washington 25, D. C.

4. G. J. Neary in unpublished reports of the Medical Research Council, Radiobiological Research Unit. AERE, Harwell. It is my understanding that these calculations will be included in a volume of Committee IV of the International Commission on Radiological Protection (probable title, "Protection Against X-Rays Above Three Million Volts and Heavy Particles Including Neutrons and Protons") to be published by Pergamon Press probably in 1963.

5. See a summary in Radiation Hygiene Handbook, Ed. H. Blatz (McGraw-Hill, New York, 1959).

6. "Background Material for the Development of Radiation Protection Standards," Staff Report No. 1 of the Federal Radiation Council, May 13, 1960, Government Printing Office, Washington 25, D. C.

7. "Measurement of Absorbed Dose of Neutrons and of Mixtures of Neutrons and Gamma Rays," National Bureau of Standards Handbook 75, February, 1961, Superintendent of Documents, Washington 25, D. C.

8. See, for example, Chodorow, Ginzton, Hansen, Kyhl, Neal, Panofsky, et al., Rev. Sci. Instr. 26, 134 (1955).

9. H. DeStaebler, "Scattering of Beam Electrons by the Residual Gas in the Accelerator," M-281, Stanford Linear Accelerator Center, Stanford, California, October 1961.

10. B. Rossi, High Energy Particles (Prentice-Hall, 1952), Chap. 5.

11. C. D. Zerby and H. S. Moran, "Studies of the Longitudinal Development of High-Energy Electron-Photon Cascades in Copper," ORNL-3329, Oak Ridge National Lab., Oak Ridge, Tenn., 1962.

12. D. N. Olson, "Photoprotons from Nuclei Exposed to 1 Bev Bremsstrahlung Radiation," Thesis, Cornell University, Ithaca, New York, 1960 (Unpublished). A. Silverman told me about this reference, and it has been very stimulating.

13. C. E. Roos and V. Z. Peterson, Phys. Rev. 124 1610 (1961).

14. Myers, Gomez, Guinier, and Tollestrup, Phys. Rev. 121, 130 (1961).

"Proposal for a Two-Mile Linear Electron Accelerator," Stanford University (Stanford Linear Accelerator Center), Stanford, California, April, 1957.

15. "Conference on Shielding of High-Energy Accelerators, New York, April, 1957," TID-7545 Technical Information Service Extension, Oak Ridge, Tenn.

16. R. Wilson, "A Revision of Shielding Calculations," CEA-73, Cambridge Electron Accelerator, Harvard University, Cambridge, Mass., May 1959.

17. J. S. Levinger, Phys. Rev. 84, 43 (1951).

18. J. S. Levinger, Nuclear Photo-Disintegration (Oxford, London, 1960).

19. Stein, Odian, Wattenberg and Weinstein, Phys. Rev. 119, 348 (1960).

20. K. G. Dedrick, "Deuteron Model Calculation of Photonucleon Yields," M-227, Stanford Linear Accelerator Center, Stanford, California, October, 1960.

H. DeStaebler, "A Review of Transverse Shielding Requirements for the Stanford Two-Mile Accelerator," M-262, Stanford Linear Accelerator Center, Stanford, California, April, 1961.

21. D. L. Judd, Rev. Sci. Instr. 21, 213 (1950).

22. Values of D Measured by F. Bumiller are within about 5% of the theoretical values.

23. Brueckner, Serber and Watson, Phys. Rev. 84, 258 (1951).

24. See references cited in S. J. Lindenbaum, Ann. Rev. Nuclear Sci. 7, 317 (1957).

25. For the Jacobian we used Hand, Kendall, and Schaerf, "Relativistic Two-Body Kinematics," HEPL-236, High-Energy Physics Laboratory, Stanford, California, April 1961.

26. S. J. Lindenbaum, Ann. Rev. Nuclear Sci. 11 213 (1961).

"Conference on Shielding of High Energy Accelerators, New York, April 1957," TID-7545, Technical Information Service Extension, Oak Ridge, Tennessee.

27. Private communication from Wade Patterson, 1961. See also R. W. Wallace and B. J. Moyer, "Shielding and Activation Consideration for a Meson Factory," UCRL-10086, 1962.

28. Private communication, J. Tinlot (Rochester U.) 1962. These measurements were made in connection with a proposed μ scattering experiment at the AGS.

29. Citron, Hoffmann and Passow, Nuc. Instr. and Meth. 14, 97 (1961).

30. C. J. Tsao, "Monte Carlo Shield Calculations for 3 Bev Protons," Princeton-Pennsylvania Accelerator, Princeton, New Jersey, ca 1958. (Unpublished). I am indebted to G. K. O'Neill for sending me a copy of this report.

31. H. Wade Patterson, "The Effect of Shielding on Radiation Produced by the 730 Mev Synchrocylotron and the 6.3 Bev Proton Synchroton at the Lawrence Radiation Laboratory," UCRL-10061, January, 1962, Unpublished.

32. B. J. Moyer, R. Hildebrand, N. Knoble, T. J. Parmley, and H. York, USAEC Document, AECD-2149 (1947).

33. A. Wattenberg in Encyclopedia of Physics, Vol. 50 (Springer-Verlag, Berlin, 1957).

34. F. F. Chen, C. Leavitt, A. M. Shapiro, Phys. Rev. 99, 857 (1955).

35. J. H. Atkinson, W. N. Hess, V. Perez-Mendez, R. W. Wallace, Phys. Rev. Lett. 2, 168 (1959).

36. J. J. Muray, "Muon Yields from Pion Decay and Electromagnetic Pair Production," M-267, Stanford Linear Accelerator Center, Stanford, California, May 1961.

37. K. G. Dedrick, "Calculation of Pion Photoproduction from Electron Accelerators According to the Statistical Model," M-228, and "More Calculation of Photopion Yields," M-229, Stanford Linear Accelerator Center, Stanford, California, October 1960.

38. B. J. Moyer in "Conference on Shielding of High Energy Accelerator," (Ref. 15). See also S. J. Lindenbaum, Ann. Rev. Nuclear Sci. 11, 229 (1961).

39. B. J. Moyer, "Evaluation of Shielding Required for the Improved Bevatron," UCRL-9769, Lawrence Radiation Laboratory, Berkeley, California, June 1961.

40. R. G. Alsmiller, F. S. Alsmiller, J. E. Murphy, "Transverse Shielding for a 45 Gev Electron Accelerator" ORNL-3289, Oak Ridge National Laboratory, Oak Ridge, Tennessee, 1962.

41. In the Oak Ridge calculation the reference for this subsidiary method is to C. D. Zerby "A Monte Carlo Calculation of Air-Scattered Neutrons," ORNL-2227, Oak Ridge National Laboratory, Oak Ridge, Tennessee, 1957.

42. S. D. Drell in "Some Aspects of Target Area Design for the Proposed Stanford Two-Mile Linear Electron Accelerator," M-200, Stanford Linear Accelerator Center, Stanford, California, Summer 1960. Also Phys. Rev. Letters 5, 278 (1960).

43. G. K. O'Neill in "Conference on Shielding of High-Energy Accelerators" (Ref. 15).

44. L. Beebe, J. Cumming, W. Moore, and C. Swartz, "Shielding Measurements," Cosmotron Internal Report, 10/1/56, Brookhaven National Laboratory, Upton, New York.

45. K. G. Dedrick and H. H. Clark, "Elementary Calculation of the Transverse Shielding," M-296, Stanford Linear Accelerator Center, Stanford, California, February 1962.

46. This is the plateau value of the ionization loss in a hypothetical medium with Z = 10 and A = 20. E. P. George in Progress in Cosmic Ray Physics Vol. I (North Holland Pub. Co., Amsterdam, 1952).

H. DeStaebler, M-262.

46a. C. W. Olson, Private Communication, 1962.

47. For example, R. W. Wallace and B. J. Mayer, "Shielding and Activation Considerations for a Meson Factory," UCRL-10086, Lawrence Radiation Laboratory, Berkeley, California, April 1962.

S. J. Lindenbaum, Ann. Rev. Nuclear Sci. 11, 213 (1961).

48. R. H. Thomas, First International Conference on Shielding Around High Energy Accelerators, Orsay and Saclay, France, February 1962.

49. W. E. Kinney, "A Monte Carlo Calculation of Scattered Neutron Fluxes at an Air-Ground Interface Due to Point Isotopic Sources on the Interface," ORNL-3287, Oak Ridge National Laboratory, Oak Ridge, Tennessee, July 1962.